



Characterizing the Phenotypic Plasticity of Uveal Melanoma

Hee Jin Hayley Shin

Faculty of Medicine, Department of Experimental Medicine

McGill University

April 2023.

A thesis submitted to McGill University in partial fulfillment of the requirements of the degree of

Master of Science (M.Sc.) in Experimental Medicine

©Hee Jin Hayley Shin – 2023

Table of Contents

ABSTRACT (ENGLISH)	5
ABSTRACT (FRENCH)	6
ACKNOWLEDGEMENTS	7
CONTRIBUTION OF AUTHORS	9
LIST OF FIGURES AND TABLES	10
LIST OF ABBREVIATIONS	12
LITERATURE REVIEW AND INTRODUCTION	15
1.1 The Physiology of the Eye	15
1.2 Uveal Melanoma	16
1.2.1 Disease Epidemiology.....	16
1.2.2 Cutaneous Melanoma versus Uveal Melanoma.....	18
1.2.3 Treatment Options for Uveal Melanoma.....	19
1.3 Phenotype Plasticity	25
1.3.1 Definition of Phenotypic Plasticity.....	25
1.3.2 Phenotypic Plasticity in other Heterogeneous Cancer Types.....	27
1.3.3 Introduction to Cell State Markers.....	29
1.4 CD36 in Cancer Progression	35
1.4.1 CD36 in Cells and Various Roles.....	35
1.4.2 CD36 in Cancer.....	37
1.4.3 CD36 Inhibitors.....	38
1.5 Rationale, Objectives, and General Introduction to the Project	40
METHODS	41

2.1 Cells and Reagents.....	41
2.2 RNA interference.....	42
2.2.1 siRNA mediated CD36 knockdown.....	42
2.2.2 shRNA mediated CD36 knockdown.....	42
2.3 Immunoblotting.....	43
2.4 Flow Cytometry.....	44
2.4.1 Staining.....	44
2.4.2 Antibody Titration.....	44
2.4.3 Flow Cytometry Assays.....	45
2.5 Wound Healing Migration Assay.....	46
2.6 Invasion Assay.....	47
2.7 Proliferation Assay.....	47
2.8 RNA extraction and Quantitative real-time PCR.....	48
2.9 Splenic Injections.....	48
2.10 Kinetic curves for IVIS Imaging.....	49
2.11 Immunohistochemistry (IHC) Staining.....	49
2.12 Statistical Analysis.....	50
RESULTS.....	52
3.1 Characterization of Uveal Melanoma Cell Lines.....	51
3.1.1 Flow Cytometry Using a Novel “UMarkit” Panel shows High Heterogeneity Amongst Uveal Melanoma Cell Lines.....	51
3.1.2 Confirmation of Flow Cytometry Results for CD36 Expression by Western Blot.....	53
3.2 CD36 on its Effects on Migration and Invasion Capacity in Uveal Melanoma Cells.....	54

3.2.1 Tagging Mel270.....	54
3.2.2 siRNA mediated knockdown of CD36.....	54
3.2.3 Migration and Invasion Capacity of Uveal Melanoma Cells.....	55
3.3. <i>In vivo</i> Experiments to Determine the Role of CD36 through Liver Metastasis Model.	56
3.3.1 Generation of shRNA Stable Knockdown Cell Line with Tagged Mel270.....	56
3.3.2 Mouse Model of Uveal Melanoma Liver Metastasis.....	56
DISCUSSION.....	59
4.1 Future Use of the UMarkit Panel.....	59
4.2 CD36 and Post-translational Modifications.....	61
4.3 Animal Models of Uveal Melanoma.....	63
4.4 Quantifying Liver Metastases.....	66
CONCLUSION.....	68
REFERENCES.....	70
FIGURES.....	100

ABSTRACT (ENGLISH)

Uveal melanoma is the most common type of intraocular malignancy in adults. 50% of patients develop liver metastases and 80% will die within the first year. Early detection of this type of cancer is virtually impossible and there are currently no effective treatment methods. As uveal melanoma is a very heterogeneous cancer with tumor cells undergoing differentiation, we propose that these characteristics may explain the high metastatic potential and resistance to treatment that is frequently observed. To better characterize uveal melanoma cells, we developed a cytometry panel composed of 7 different markers associated with cell states and cancer progression and screened 11 uveal melanoma cell lines derived from primary or metastatic human tumors. These experiments allowed us to demonstrate that CD36 along with others had high variability in the positive signals detected depending on the cell line that was analyzed. CD36 is a receptor involved in lipid uptake but has also been identified in several cancer types as a poor prognostic marker for patients as it increases the metastatic potential of tumor cells. To better understand the role of *Cd36* in uveal melanoma, we suppressed its expression in uveal melanoma cell line using shRNA or siRNA to neutralize the mRNAs encoding the CD36 protein. We were able to demonstrate that the absence of *Cd36* decreases the migration capacity of tumor cells as well as their invasive potential. We are currently conducting in vivo experiments to validate our in vitro results. Considering our results and based on the current literature, we propose that CD36 expression could be one of the factors increasing the metastatic potential of uveal melanoma.

ABSTRACT (FRENCH)

Le mélanome uvéal est le type de cancer malin intra-oculaire le plus fréquent chez les adultes. 50 % des patients présentent des métastases au foie dont 80 % mourront au cours de la première année. La détection précoce de ce type de cancer est pratiquement impossible et il n'existe pas de méthodes ou de traitements efficaces actuellement. Le mélanome uvéal étant un cancer très hétérogène et dont les cellules tumorales subissent une différenciation importante, nous proposons que ces caractéristiques puissent expliquer le potentiel métastatique élevé et la résistance au traitement qui sont fréquemment observés. Dans le but de mieux caractériser les cellules de mélanome uvéal, nous avons mis au point un panel de cytométrie composé de 7 différents marqueurs que nous avons utilisé sur 10 lignées cellulaires de mélanome uvéal dérivées de tumeurs primaires ou métastatiques humaines. Ces expériences nous ont permis de mettre en évidence que l'expression de *CD36* était très hétérogène en fonction de la lignée cellulaire analysée. *CD36* est un récepteur impliqué dans l'absorption des lipides mais qui a aussi été identifié dans plusieurs types de cancer en tant que marqueur de mauvais pronostic pour les patients car augmentant le potentiel métastatique des cellules tumorales. Pour mieux comprendre le rôle de *CD36* dans le mélanome uvéal, nous avons supprimé son expression en utilisant des shRNA ou des siRNA pour neutraliser les ARNm codant pour la protéine *CD36*. Nous avons pu démontrer que l'absence de *CD36* diminue la capacité de migration des cellules tumorales ainsi que leur potentiel invasif. Nous procédons actuellement à des expériences in vivo afin de valider nos résultats in vitro. A la lumière de nos résultats et s'appuyant sur la littérature actuelle, nous proposons que l'expression de *CD36* pourrait être un des facteurs augmentant le potentiel métastatique du mélanome uvéal.

ACKNOWLEDGEMENTS

I would like to thank my supervisors Dr. Wilson H Miller Jr for his support with the valuable knowledge from the clinical perspective and Dr. Sonia del Rincon for her continuous trust and support to not only allow myself to do the research I aspire to do, but also for leading me to truly grow as a MSc trainee and as an individual. I would also like to thank all members of the Miller-del Rincon lab for their patience with my questions and for their support during my time as a MSc student at the lab. Extending from our lab, I would like to thank Dr. April Rose and her lab members for their general support as well as any feedback they had graciously offered. Specifically, I would like to emphasize the strong friendship that I have built with Mengqi Li and Jennifer Maxwell where they have whole-heartedly cheered me on during my research progress as well as my personal life. My project would not have been made possible without the help from the Flow Cytometry Facility, specifically Mr. Christian Young who was always welcoming and helpful even past the working hours. I would also like to thank Mr. Manuel Flores Molina whose door was always open for any questions which has allowed me to successfully carry out my project despite being a relatively novel field in the lab, as well as for all the career advice that he has provided me. Any *in vivo* experiment related works were truly made possible with the generous support from Ms. Veronique Michaud teaching me about IVIS imaging and mice handling as well as Raul Ernesto Flores Gonzalez from Miller-del Rincon lab who has trained me for splenic injections and have supported me with his tremendous patience. I would also like to thank my academic advisor Dr. Donna Senger and my committee members Dr. April Rose and Dr. Chantal Autexier for their valuable advice and guidance.

Most importantly, everything including moving to Montreal and living alone, starting, and completing my MSc all the while working part-time as a Clinical Affairs Specialist would not have

been made possible without the unconditional love and support from my mom, my dad, my brother, and my aunt. I cannot express enough how much I appreciate their time, patience, encouragements, and the emotional support that they have provided me with. I would also like to extend my gratitude to my manager at work who was always so understanding and supportive of both my education and my career. Lastly, I would like to thank my friends back home who have visited and allowed me to adjust to Montreal better, those that have always welcomed me back, as well as the new friends I have made here whom I had the joy of making great memories with.

CONTRIBUTION OF AUTHORS

Injections for *in vivo* experiment with shCTL and shCD36 knockdown cohort was done with Raul Ernesto Flores Gonzalez where half of the mice (4) were injected by Raul and the other half (4) were injected by myself.

All IHC staining were completed by Elizabeth Guettler.

All other data acquired in this thesis was gathered and analyzed exclusively by myself.

LIST OF FIGURES

Figure 1 Diagram of the Eye.

Figure 2 CD36 domains, post-modification sites, and its ligands.

Figure 3 Characterization of Uveal Melanoma Cell Lines with UMarkit.

Figure 4 Comparative CD36 Expression in Uveal Melanoma Cell Lines.

Figure 5 siRNA mediated *Cd36* Knockdown.

Figure 6 Depletion of *Cd36* leads to reduced migratory and invasive capacity in UM cell line.

Figure 7 *In vivo* liver metastasis experiments with Mel270 cells expressing shCTL or shCD36.

Supplementary Figure 1 Antibody Titration Visual Representation Graph.

Supplementary Figure 2 Explanatory diagrams for Scratch assay and Invasion assay.

Supplementary Figure 3 Wound Healing (Scratch) Assay and Invasion Assay with 92.1 and OMM2.5 UM Cell Line.

LIST OF TABLES

Table 1 Drugs Against CD36 and CD166 in Pre-clinical and Clinical Trials.

Table 2 Antibodies/Markers in the UMarkit Panel.

LIST OF ABBREVIATIONS

AGE	Advanced glycated end products
ALCAM	Activated leukocyte cell adhesion molecule
BITE	Bispecific T cell engager
CD166	Cluster of differentiation
CD271	Cluster of differentiation 271
CD36	Cluster of differentiation
CSC	Cancer stem cell
CTL	Cytolytic T lymphocytes
DMEM	Dulbecco's modified Eagle's medium
DPBS	Dulbecco's phosphate-buffered saline
ECM	Extracellular matrix
EMT	Epithelial to mesenchymal transition
FASN	Fatty acid synthase
FBS	Fetal bone serum
Gα_q	G-alpha protein Q
Gα_{11}	G-alpha protein 11
GDNF	Glial cell line derived factor
GEP	Gene expression profiling
GFRA2	GDNF family receptor alpha-2
GPCR	G-protein coupled receptor
Gp100	Glycoprotein 100
IGF-R1	Insulin growth factor receptor 1

IGF-1	Insulin growth factor 1
IgSF	Immunoglobulin superfamily
kDa	Kilodalton
LAG3	Lymphocyte-activation gene 3
LCFA	Long chain fatty acids
Luc	luciferase
MART-1	Melanoma Antigen Recognized by T-cell-1
MelanA	Melanoma Antigen
MHC	Major histocompatibility matrix
MITF	Melanocyte inducing transcription factor
NCG	NOD CRISPR prkdc Il2r Gamma
NCM	Normal choroidal melanocytes
NEAA	Non-essential amino acids
NGFR	Nerve Growth Factor Receptor
NRTN	Neurturin
ox-LDL	Oxidized low density lipoproteins
PAMPs	Pathogen associated molecular patterns
PFA	Paraformaldehyde
PI3K/AKT	Phosphoinositase-3-kinase/Ak strain transforming
PMEL	Premelanosome protein
PRR	Pattern recognition receptor
QoL	Quality of Life
RET	Rearranged during transfection

RPMI	Roswell Park Memorial Institute
SAB	Salyionolic acid beta
SDS	Sodium dodecyl sulfate
SSO	Sulfo-N-succinimydyl oleate
TBST	Tris buffered saline-Tween
VM	Vasculogenic mimicry
5-FU	5-Fluorouracil

LITERATURE REVIEW AND INTRODUCTION

1.1 The Physiology of the Eye

Vision is a critical component in human life that allows us to efficiently carry-out our daily activities. The human eye, also referred to as the “ocular globe”, takes in light from the environment and send signals to the brain through the optic nerve, ultimately allowing an individual to visualize their surroundings (*How the eyes work*, 2022). External muscles attached to the globe include the superior rectus, inferior rectus, medial rectus, lateral rectus, superior oblique, and the inferior oblique muscle which altogether allow movement of the eye for maximal central vision (Kels et al., 2015). This critical organ is composed of three primary layers around the vitreous cavity. The first layer being the outermost layer, commonly known as the “white” of the eye, is made up of the sclera and the cornea and its main functions include retaining structure and providing protection as shown in Figure 1 (Sridhar, 2018). The second middle layer known as the “uveal layer” consists of the iris, the ciliary body that produces the fluid in the eye and facilitates the re-shaping of the lens for accommodation during visualization (Yanoff & Duker, 2018), and the choroid which is a highly vascularized compartment and is the main regulator for blood flow in the eye and provides nutrients to the retina (Ehrlich et al., 2017; Boileau & Gilmour, 2012). Finally, the innermost layer is known as the retina with photoreceptor cells that convert light signals to visualize images. (Kels et al., 2015; K. H. Nguyen et al., 2020; Pradeep et al., 2022).

The eye colour is a distinct phenotype of an individual during their lifetime. The colours of the eye vary depending on the levels of pheomelanin and eumelanin produced by melanocytes. These melanocytes originate from the neural crest and are present in all components of the eye that make up the uveal layer. (Sitiwin et al., 2019). It is also important to

note that melanin found in the eyes have auxiliary functions such as protecting the eyes from light, acting as a metal chelator, as well as regulating oxidative stress (Sitiwin et al., 2019; Weidmann et al., 2017).

1.2 Uveal Melanoma

1.2.1 Disease Epidemiology

Uveal melanoma is the most commonly occurring intra-ocular malignant cancer type in adults with the incident rate of approximately 5 in every 1 million population (Kaliki & Shields, 2017; Singh et al., 2011). It occurs in the melanocytes of the choroid on the posterior side as well as the iris and the ciliary body on the anterior side of the uveal layer (Figure 1) with most of the reported cases occurring in the choroid (~90%) (Krantz et al., 2017). Amongst all ethnicities, the Caucasian, non-Hispanic white population has been identified to be the group that is most at risk making up approximately 97% of the total cases according to a study involving patient data from 1973 to 2008 (Hu et al., 2005; Kaliki & Shields, 2017; Singh et al., 2011). It remains unclear as to what leads to the development of uveal melanoma, however, several risk factors have been suggested from the past and existing cases. These factors include sex – with the male population having a 30% greater chance of developing uveal melanoma, older age – usually from 50-80 years of age with under 21 having lower chances of diagnosis and lower metastasis risk (Fry et al., 2018), fair skin colour, inability to tan, light coloured eyes such as blue or grey, and though rare, a germline mutation of *BAP1* loss which gives increases risk for metastasis relapse (Jager et al., 2020). Interestingly, geographic location also appears to be a risk factor as a study reports that uveal melanoma incidence risk increased with the increase in latitude in Europe (Krantz et al., 2017).

Despite being a relatively rare disease, approximately 50% of patients diagnosed with uveal melanoma develop metastasis to distant organs – predominantly to the liver (95%), followed by lungs (24%), the bones (16%), and the skin (11%) (Woodman, 2012). From the diagnosis with metastasis, uveal melanoma patients have a very poor one-year median survival of approximately 4 months with or without treatment (Gragoudas et al., 1991; Lane et al., 2018). Another study has highlighted the high mortality rate of 92% after 2 years with the diagnosis with metastasis and long-term survival past 5 years was only observed in approximately 1% of the total study cohort (Diener-West et al., 2005). With such statistics upon metastasis development, uveal melanoma patients are stratified into low (group 1A), intermediate (group 1B), and high (group 2) risk groups depending on the predicted patients' chances for developing metastasis in attempt to provide more prognostic information. The most commonly used prognostic testing in the clinic today is the gene expression profiling (GEP), also recognized as the DecisionDx-UM test (Harbour & Chen, 2013). With the additional information on tumor size and location, GEP has been considered to be more accurate than past prognostic methods such as cytogenetic testing for monosomy 3 for aggressive uveal melanoma (van Gils et al., 2008; Worley et al., 2007). However, due to the high variability in results depending on the physical location of the biopsy, this is yet to be standardized. Additionally with less than 5% of patients displaying detectable metastases at the time of initial diagnosis, early detection and diagnosis of uveal melanoma remains to be extremely difficult, which leaves patients with increased risk for cancer progression (Harbour & Chen, 2013; Stålhammar, 2020). Altogether, it is critical to be able to understand how the development of tumor cells in the uveal layer of the eye gets initiated and result in the progression to distant metastasis in almost half of the total patient population.

The predominant site of metastasis in uveal melanoma patients is the liver, however, it remains relatively unknown as to how the tumor cells travel and colonize primarily at the liver than at any other organs. So far, uveal melanoma cells are understood to be spreading through the blood from studies detecting cancerous molecules such as extracellular vesicles and circulating tumoral DNA in blood samples extracted from uveal melanoma patients. However, there is no clear relationship as to why the specific site of metastasis occurs at the liver. One of several proposed ideas is that the liver expresses a growth factor known as insulin growth factor 1 (IGF-1) and uveal melanoma cells express its receptor known as insulin growth factor receptor 1 (IGF-R1), attracting uveal melanoma cells specifically to the liver (Bustamante et al., 2021). A study has also reported increased metastasis related deaths due to increased levels of IGF-R1 expression by uveal melanoma patients (All-Ericsson et al., 2002). An interesting aspect about the IGF-proposed mechanism is that the activated MAPK pathway through the binding of the IGF-1 ligand to its receptor, is the same pathway to which uveal melanoma patients present resistance to MAPK- targeted therapy (Carvajal et al., 2014).

1.2.2 Cutaneous Melanoma versus Uveal Melanoma

Despite sharing a similar name, cutaneous melanoma and uveal melanoma are distinct from each other in terms of their mutation burden, risk factors, treatment options, and overall survival in patients. Cutaneous melanoma is often categorized into their genetic mutation subtypes which are *BRAF* mutant, *NRAS* mutant, *NF1* mutant, or triple-wild type (Akbani et al., 2015). Unlike cutaneous melanoma, around 90% of uveal melanoma patients usually harbour a *GNAQ* or a *GNA11* mutation on the G-protein alpha subunit in a mutually exclusive manner (Decatur et al., 2016). The *GNAQ* and *GNA11* encode for the G-alpha protein Q (G_{αq}) and G-

alpha protein 11 ($G_{\alpha 11}$) on the 7-transmembrane G-protein coupled receptor to activate pathways such as the MAPK, PI3K/AKT, and PKC (Shoushtari & Carvajal, 2014). This GDP to GTP hydrolysis-mediated activation of the receptor gets fixed in its constitutive activated state due to the mutations at the glutamine 209 (Q209) residue of the *GNAQ* and *GNAI1* (Shoushtari & Carvajal, 2014). These mutations alone remain insufficient to understand how uveal melanoma arise or to be able to determine patient prognosis. Secondary mutations in *BAP1*, *EIF1AX*, and/or *SF3B1* allow physicians to gain a better understanding on the type of uveal melanoma that the patient is diagnosed with, however this too, has not been very accurate in the clinics (Gallenga et al., 2022). Due to the identification of driver mutations and druggable targets for cutaneous melanoma, treatment options such as MEK inhibitors, *BRAF* inhibitors, and immunotherapy has led to improvements in patient survivals (Jenkins & Fisher, 2021). Moreover, as sun exposure appear to be the leading risk factor for developing cutaneous melanoma, preventative measures such as sun avoidance, wearing physical barriers such as sunglasses, and wearing sun protectants have been suggested. (Arisi et al., 2018). However, similar standardized treatments and preventative measures for uveal melanoma patients is yet to be discovered.

1.2.3 Treatment Options for Uveal Melanoma

Primary means of treatment options for uveal melanoma include enucleation, radiotherapy, and photodynamic therapy (J. Yang et al., 2018). In the past, enucleation has been the gold standard for treating uveal melanoma, but with advanced technology and with patients seeking to preserve the eye, small to medium sized tumors (size ranging from 1.00 mm to 8.00 mm in height or less than 16.0 mm in diameter) can be treated with radiotherapy to kill off cancerous cells through DNA damage of actively replicating cells (Reichstein & Brock, 2021).

There are four different types of radiotherapy available for uveal melanoma patients including plaque brachytherapy, proton beam therapy, along with gammaknife and cyberknife methods as a stereotactic radiosurgery treatment (Finger, 1997; Reichstein & Brock, 2021; Zemba et al., 2023).

Enucleation: Enucleation is a surgical approach to remove the entire eye which is usually the method of treatment with the presence of a big tumors that are greater than 8.00 mm in height or greater than 16.0 mm in diameter, significant vision loss, and the large extent of extraocular growth (PDQ Adult Treatment Editorial Board, 2002; Tataru & Pop, 2012; J. Yang et al., 2018). It has been understood that enucleation prevents metastasis and metastasis-related deaths only when the surgery is performed while the tumor is still small (1.00 mm – 3.00 mm in height or 5.00 mm – 16.00 mm in diameter) (PDQ Adult Treatment Editorial Board, 2022; B Damato, 2010). However, it remains a challenge to be able to detect uveal melanoma during its early stages as many of the cases remain asymptomatic (Krantz et al., 2017). Despite being such an invasive treatment method, the results are not as astonishing where multiple studies report that patients experience recurrence in the form of extrascleral extension, and that some even pass away within the first 5 years after surgery (Dogrusöz et al., 2020; Heng et al., 2022). In addition, a study by Damato et al. examining patients' quality of life (QoL) after enucleation highlights the significant psychological difficulties that they are faced with. Patients experience anxiety for metastasis and recurrence, visual difficulties while carrying out daily activities, have concerns about their visual appearance, and experience ocular discomforts as well as discharges, all leading up to higher likelihood to suffering depression or failing to maintain their emotional well-being (Damato et al., 2019).

Plaque Brachytherapy: Plaque brachytherapy has been the primary route for treatment other than enucleation and was developed due to the “Zimmerman hypothesis” during the 1970s. The hypothesis was that the development of metastasis in the liver may be due to the sudden increase in intraocular pressure after the optic nerve gets disconnected from the globe, leading to the spread of tumor cells into the systemic circulation, ultimately leading its way to the liver (Brewington et al., 2018). During this procedure, a gold plaque with radioactive materials is sutured on the eye over or near the tumor residing location in attempt to stop the growth of tumor cells through ionizing radiation (Peddada et al., 2019; Reichstein & Brock, 2021). Various types of radioactive compounds are available for treatment such as Iodine 125, Cobalt 60, Ruthenium 106, and Palladium 103 (Brewington et al., 2018; Carol L. Shields et al., 2000). After subsequent exposure with the chosen radioactive compound, the plaque is removed, and the patient is monitored for any recurrence or metastasis through ultrasound of the abdomen or liver biochemical tests (Bande Rodríguez et al., 2020). Plaque brachytherapy has shown improvement with patient survival and maintaining primary tumor (Jiang et al., 2020), however, this appears to be highly dependent on tumor size and the stage of uveal melanoma (Stålhammar, 2020). In addition, the anatomical placement capacity of the plaque has been the limiting factor in the extent of treatment efficacy (Peddada et al., 2019).

Proton beam therapy: This type of radiotherapy using protons as the charged particle, targets a specific area where the tumor is located. Protons are ejected at high speeds and are directed using tantalum clips which are sewn on patient’s episclera. This treatment approach targets specific regions and prevents the damaging of surrounding normal, non-cancerous cells with the large proton size and the narrow targeting range. But some disadvantages are that it requires strict restriction of any eye movements and the limited access to the proton accelerator

making this type of treatment very expensive (Finger, 1997; Gragoudas, 2006; Mishra & Daftari, 2016; Reichstein & Brock, 2021). Despite the mentioned disadvantages, proton beam radiotherapy remains the “gold standard” of the radiotherapy for treating primary uveal melanoma tumors due to its highest success rate without the need for secondary enucleation (Mishra & Daftari, 2016; Papakostas et al., 2017; Sikuade et al., 2015).

Stereotactic radiotherapy: Another type of radiotherapy that is performed on small to medium sized uveal melanoma tumors is the stereotactic radiotherapy. It is very similar to proton beam therapy except for the use of concentrated gamma or x-rays instead of protons. The radioactive compounds are emitted guided by a 3-dimensional (3D) image that is typically obtained using a CT scan rather than the invasive tantalum clips (Jaywant et al., 2003; Reichstein & Brock, 2021). “Gammaknife” and “CyberKnife” are the two different methods of stereotactic radiotherapy. The main difference between the two methods is that the “CyberKnife” approach is non-invasive and does not require the fixation of the skull using a device that is otherwise needed for “Gammaknife” (Özcan et al., 2020; Reichstein & Brock, 2021). Despite the high level of preservation rate of the eye at approximately 85% (Eibl-Lindner et al., 2016; Schmelter et al., 2022), local recurrence or metastasis and treatment-related adverse events such as radiation retinopathy, secondary glaucoma, loss of vision, and hemorrhage are still reported in a handful of patients (Eibl-Lindner et al., 2016; Finger, 1997; Modorati et al., 2020; Zemba et al., 2023).

MEK inhibitors: Uveal melanoma has a relatively low mutation burden making it a difficult tumor type to treat via druggable targets. As previously mentioned, majority of uveal melanoma patients harbour a *GNAQ* or a *GNA11* mutation in a mutually exclusive manner where the alpha subunit of the transmembrane G-protein coupled receptor (GPCR) that is responsible for the hydrolysis of GTP to GDP is mutated ultimately leading to the subsequent activation of

the MAPK pathway (Yongyun Li et al., 2020). This constitutive activation of the RAS-MEK-ERK pathway leads to the increased gene transcription and mRNA translation to support tumor cell survival and pro-oncogenic activities. To prevent this, researchers have introduced MEK inhibitors such as binimetinib, cobimetinib, trametinib, and seleumetinib that are clinically available to target the pathways downstream of tumors harbouring *GNAQ/GNA11* mutations. Unfortunately, various clinical trials proved none to minimal effects of these MEK inhibitors on the overall survival rate and the disease progression of uveal melanoma patients aside from also inducing treatment related adverse events (Carvajal et al., 2014, 2018; Steeb et al., 2018). As it will be discussed further below (section *1.3.3 Introduction to Cell States Markers*) many of the receptor markers associated with cell state and tumor progression in our novel flow-based analysis panel are also responsible for activating the MAPK pathway which we posit may be able to provide an explanation towards the treatment resistance that is observed in uveal melanoma patients.

Immunotherapy and Tebentafusp: Uveal melanoma patients, alike with other cancer patients have been trialed with immunotherapy using immune checkpoint inhibitors (CTLA-4 and PD-1). These immune checkpoint inhibitors allow persistent activation of cytotoxic T cells by preventing the binding of checkpoint proteins to its respective ligands and receptors (Wessely et al., 2020). CTLA-4 inhibitors, Ipilimumab and Tremelimumab have undergone clinical trials with uveal melanoma patients but have shown no effective progress as analyzed in the review article by Wessely and colleagues (Wessely et al., 2020). The median progression free survival was less than 2 years and as high as 52% of enrolled patients experienced adverse events. Similarly, Nivolumab and Pembrolizumab as PD-1 inhibition therapy showed poor outcomes in multiple clinical trials with uveal melanoma patients. Median overall survival was around 12

months and there was limited data available on progression free survival and adverse events due to the lack of information provided from the clinical trials (Wessely et al., 2020). Aside from these results, it is also important to take notice of the low response rates from these checkpoint inhibition therapies at 10% and 7% with CTLA-4 and PD-1 respectively in uveal melanoma patients (Bol et al., 2019). Such response rates could be supported by the single-cell RNA sequencing performed by Harbour's group where they saw less CTLA-4 and PD-1 expression in uveal melanoma patients. Instead, they reported there was predominant expression of lymphocyte-activation gene 3 (*LAG3*) (Durante et al., 2020). The group's sequencing results stay consistent with data from a study by Souri et al where they report the inverse correlation between *LAG3* and its ligand expression with patient prognosis (Souri et al., 2021). Recently, there has been a phase 2-3 double blind clinical trial with cutaneous melanoma patients for a *LAG3* blocking antibody known as relatlimab. Results showed that combined treatment with nivolumab and relatlimab showed better effect on patient prognosis than nivolumab treatment alone (Tawbi et al., 2022). Though this is yet to be trialed on uveal melanoma patients, such clinical trials provide evidence on the importance of *LAG3* as a target.

Another type of immunotherapy that has recently been approved by the FDA is commonly recognized with the name Tebentafusp and works to redirect T cells to melanoma cells. Tebentafusp is a bispecific protein that binds to CD3 on T cells via and simultaneously binds the glycoprotein 100 (*gp100*) presented on the surface of melanoma cells in patients specifically carrying the HLA-A*02:01 antigen (Hua et al., 2022; Winstead, 2021). Several clinical trials have confirmed higher 1-year overall survival rate with Tebentafusp treatment in patients with both treatment naïve and treatment-refractory metastasized uveal melanoma (Carvajal et al., 2022; Nathan et al., 2021). However, despite what appears to be an exciting

advancement for metastasizing uveal melanoma, there still remains multiple shortcomings to this type of immunotherapy with the main concern focused on the overall response rate. Moreover, Tebentafusp is only applicable to patients with a specific HLA antigen as mentioned above, and approximately 50% of the Caucasian, non-Hispanic population that make up majority of the total reported cases are eligible (B. E. Damato et al., 2019). This leaves a large gap between the two populations, and limitation persists even within the eligible population due to the overall response rate being very low at 5-9% (Carvajal et al., 2022; Hua et al., 2022; Middleton et al., 2020).

Uveal melanoma has a high metastatic potential and approximately 1% of the patient population have detectable metastasis at the time of diagnosis (Dogrusöz et al., 2020). Treatment options including enucleation, plaque brachytherapy, radiotherapy, MEK inhibitors, and immunotherapy have shown minimal effect on patients and metastasis is still observed even after treatment. Once metastasized, patients have a very low 1-year median survival of approximately 4 months (Lane et al., 2018; Rietschel et al., 2005). These outcomes highlight the critical need for us to identify additional druggable targets and treatment methods that can be standardized in majority of the uveal melanoma patients.

1.3 Phenotype Plasticity

1.3.1 Definition of Phenotypic Plasticity

For years, researchers have attempted to unravel the high metastatic potential of uveal melanoma especially with their detection rate being extremely low along with the reports on the occurrences of late metastases decades after resection (Kolandjian et al., 2013; Shields et al., 1985). One of the proposed mechanisms for approximately 50% of uveal melanoma patients

developing metastasis is high intratumor heterogeneity often observed as the result of individual tumor cells having the ability to switch from one cell state to another (de Lange et al., 2021; Folberg et al., 2006; Lin et al., 2021). Such phenomenon termed as “phenotype switching” is an adaptive feature and has been studied in the context of cancer progression, metastasis, and even the development of resistance to treatment options (Gupta et al., 2019). In the vertebrate eye, the cells of the pigmented regions – known as the iris and the retina – have been described to withhold the “unique ability to alter extensively their state of differentiation” according to a study that was published more than 4 decades ago (Okada, 1980). Moreover, it has been reported that the iris epithelium is capable of undergoing cell replication, de-differentiation, and re-differentiation studied in the context of post-lensectomy (Yamada et al., 1975). During the replication phase, cells appeared to undergo de-pigmentation and lose their given function as well as recruiting macrophages and neutrophils. Noting that it has been reported only a fraction of de-differentiated cells of the iris epithelium are re-differentiated into lens cells or iris epithelium, the phenotype plasticity portrayed by these cells suggest the possibility of inducing tumor cells (Yamada et al., 1975). To date, the most common example of phenotype switching in epithelial cancers is the epithelial-to-mesenchymal transition where cells lose their epithelial characteristics through events such as reduced cell polarity and cell to cell adhesion properties, eventually giving rise to the stem cell like phenotype (Bhatia et al., 2020). Transition into the mesenchymal cell state is often related with driving phenotypic plasticity in cancer cells where some population of tumor cells gain stem-cell like properties. In cutaneous melanoma, cell states also exist and have been characterized through their expression of specific cell surface receptors and associated transcription factors (Huang et al., 2021). More specifically, transcription factors appeared to induce differential gene expression leading to changes in phenotypes of cancer cells

observed with varying levels of genes expressions that are associated with tumor progression (Bhatia et al., 2020; Bi et al., 2020). According to prior literature, single cell RNA sequencing technologies have driven the identification of multiple cell states through the detection of receptors and their respective expression levels on individual cells that are predominantly expressed on a given tumor mass (Ennen et al., 2015; Tirosh et al., 2016). Identification of the different cell states that lead to tumor heterogeneity in cutaneous melanoma can act as a great tool to develop more effective and personalized therapy options for patients. Unfortunately, relative to other heterogeneous cancer types such as cutaneous melanoma and breast cancer, such cell state information remains elusive for uveal melanoma.

1.3.2 Phenotypic Plasticity in other Heterogeneous Cancer Types

When discussing phenotypic plasticity, cells' transition into stem cell state is an important hallmark to understand in terms of the cells' characteristics and their expected behavioral patterns especially in cancer. However, available reports and ongoing research confirm that cell states are not so distinct but rather very well-interconnected and progressive (Jia et al., 2017). Cell states have been associated with tumor initiation and progression, and researchers should pay close attention to the events that occur leading to these shifts in cell states. How cells undergo phenotype switching has been largely subdivided into 3 routes which include differentiation, de-differentiation, and trans-differentiation (Gupta et al., 2019). Cell differentiation is a well-known event where immature stem cells become a specific cell type and gain function in response to the different transcription factors leading up to differential gene expression (Musacchio & Helin, 2013). In contrast, de-differentiation refers to the opposite where specialized cells such as melanocytes lose their characteristics like pigmentation and

experience changes in their gene expression of specific markers such as upregulated *NGFR* or *Axl* and downregulated *MelanA* or *GP100* as well as gaining the potential to develop into any type of cells – including tumor cells (Y. J. Kim et al., 2021). Trans-differentiation of a cell occurs between a spectrum of cell states, and this may be induced by specific transcription factors and be detectable through the upregulation or downregulation of specific receptors as previously mentioned.

Some characteristics of stem cell states in cutaneous melanoma is that they are able to undergo self-renewal and differentiation, asymmetric division, show vascular mimicry, form melanospheres, and show positive expression for NGFR marker with a proposed detection for phenotype switching through a combined MITF and AXL expression levels (Fang et al., 2005; Girouard & Murphy, 2011; Huang et al., 2021; N. Nguyen et al., 2015). Melanoma stem cell-like state have been observed to play a role in tumor initiation, metastasis, and therapy resistance and depending on the phenotypic state of a given cell, the potential to fulfill these functions appear to be altered (Huang et al., 2021; N. Nguyen et al., 2015). Currently explored cell states of cutaneous melanoma include but are not limited to hyperdifferentiated state, melanocytic state, intermediate state, starved-like melanoma state, de-differentiated state, and neural crest stem cell-like state (Huang et al., 2021). Breast cancer is another heterogeneous cancer type that has been studied more with regards to the process of epithelial to mesenchymal transition (EMT). Some characteristics that define their stem cell like state are similar to that of cutaneous melanoma where cells show to undergo self-renewal process, differentiate into endothelial cells, produce tumorspheres, and carry out pro-angiogenic activities (Czerwinska et al., 2020; Kong et al., 2020; Murphy et al., 2014). However, markers of stem cells differed from cutaneous melanoma in that breast cancer stem cells were isolated through CD104 positive and CD44 high

expression (Kong et al., 2020). Currently distinguished cell states for breast cancer include highly plastic phenotype, epithelial phenotype, mesenchymal phenotype, and cancer stem cell phenotype – all showing different capacity towards tumor initiation, metastasis potential, and treatment resistance (Kong et al., 2020).

1.3.3 Introduction to Cell State Markers

As previously mentioned in section *1.2.1 Disease Epidemiology*, patients are stratified into different risk groups through the DecisionDx-UM gene expression profiling test. This test suggests that patients are subjected to different prognosis for uveal melanoma and that patients can be assigned to a risk group for developing metastasis depending on their results. However, a major shortcoming to this testing method is the use of fine needle aspiration biopsy as a method to collect samples. Uveal melanoma tumor mass is highly heterogeneous in that depending on the physical location of where the single bypass collection via needle biopsy takes place, the results may be highly variable (Stålhammar & Grossniklaus, 2021). Therefore, application of marker-based characterization of uveal melanoma tumors with markers associated with tumor progression may allow for the advancement towards accurate patient prognosis and early detection of metastasis. In chapter *2.4 Flow Cytometry* of this thesis, a flow cytometry-based assay, wherein we detect the expression of AXL, CD36, CD166, MelanA, NGFR, GFRA2, and GP100 has been described. In the next paragraphs, we explain these receptors in greater detail.

AXL: This receptor tyrosine kinase is broadly expressed in normal cells such as the bone marrow stroma cells, vascular smooth muscle cells, lens epithelial cells, retina, and renal cells (Axelrod & Pienta, 2014; Neubauer et al., 1994; The Human Protein Atlas). AXL has extracellular, transmembrane, and intracellular domains that work together to transduce signals

from the extracellular matrix into the cytoplasm once bound to its ligand, Gas6 or via the overexpression of AXL (Dagamajalu et al., 2021; Zhu et al., 2019). AXL activation results in activated downstream pathways including the MAPK pathway, PI3K/AKT pathway, and the JAK/STAT pathway (Axelrod & Pienta, 2014; Du et al., 2021; Zhu et al., 2019). Numerous studies suggest that through the activation of these aforementioned pathways, AXL contributes toward tumor progression through their regulation of cell to cell adhesion, tumor cell survival, migration, invasion, and drug resistance (Abu-Thuraia et al., 2020; Gay et al., 2017; Y Li et al., 2009; McCloskey et al., 1997; Taniguchi et al., 2019; Zhu et al., 2019). AXL appears to be not only a marker of the stem-cell like cell state but is also seen to be responsible for inducing this phenotype supported by studies where reduced metastasis has been observed with *Axl* knockdown in other cancer types (Gjerdrum et al., 2010; Rankin & Giaccia, 2016). In uveal melanoma, AXL expression has been shown to play a role in sustaining tumor cell survival specifically through the interaction between Gas6 and the AXL receptor ultimately allowing for cancer progression observed by liver metastasis for example (van Ginkel et al., 2004). AXL expression in the eye can only be detected in the retina (The Human Atlas).

Cluster of differentiation 36 (CD36): This is a scavenger receptor responsible for lipid uptake and is expressed on endothelial cells, monocytes, retinal pigment epithelium, hepatocytes, and adipocytes to name a few (Clemetson, 1997; Silverstein & Febbraio, 2009). CD36 is a transmembrane protein with its extracellular domain exposed to high levels of glycosylation (Isacke & Horton, 2000) and also interacting with numerous ligands such as thrombospondins, long chain fatty acids, collagens one(I) and four (IV), and retinal photoreceptor outer segments (Febbraio et al., 2001). Through the interaction with a diverse group of ligands, CD36 also plays a role in clearing apoptotic cells, regulating angiogenesis, transporting fatty acids as well as

being associated with the development of diseases such as atherosclerosis and various cancer types (Silverstein & Febbraio, 2009; Wang & Li, 2019). High expression of this receptor has been associated with poor prognosis in cancer patients where researchers reported positive correlation between tumor burden and metastasis risk and inverse correlation with patient survival (Hale et al., 2014b; Pan et al., 2019; Pascual et al., 2017; P. Yang et al., 2018). In cutaneous melanoma, increased CD36 expression has been associated with the starved-like melanoma cell state that showed higher tolerance to both nutrient starvation and therapy (Huang et al., 2021). CD36 expression is not detected in the uveal layer and any direct relationship between CD36 signaling and uveal melanoma is yet to be discovered. However, vasculogenic mimicry (VM) which is a process that aggressive tumor cells utilize to maintain survival by producing endothelial-like cells *de novo* has been first observed in uveal melanoma. There has been no further studies clarifying how this process arise in the context of uveal melanoma but a study by Martini and colleagues demonstrate that CD36 promotes the increased proximity between tumor endothelial cells and the tumor extracellular matrix (ECM) through its network with adhesion molecules (Martini et al., 2021; Wechman et al., 2020).

Cluster differentiation 166 (CD166): Also recognized as activated leukocyte cell adhesion molecule (ALCAM), CD166 is frequently expressed on the surfaces of many different cells including but not limited to pancreatic cells, epithelial cells, glial cells, blood cells, and immune cells (Kahlert et al., 2009; The Human Protein Atlas). It is a member of the immunoglobulin superfamily (IgSF) with five extracellular domains and the main function of CD166 is to act as a cell adhesion molecule through the binding to its receptor CD6 in a heterophilic manner or with another CD166 protein in a homophilic manner (Chappell et al., 2015; Dana, 2016). Previously, CD166 has been studied to be altering bone phenotype through

osteoblast differentiation and levels of hematopoietic stem cells. In continuum, this protein has been shown to be negatively correlated with patient survival as well as leading cancer progression by fostering cancer cells' ability to migrate and invade (Donizy et al., 2015; Hooker et al., 2015; Kahlert et al., 2009). Through knockdown experiments in ovarian cancer and pancreatic cancer, researchers showed that with depleted *Cd166* resulted in diminished cancer stem cell (CSC) characteristics in respective cell lines (Fujiwara et al., 2014; D. K. Kim et al., 2020). Clinically, CD166 expression level was monitored where they saw increased protein expression in primary tumors but a relatively reduced level in lymph node metastases, in which both resulted in poor patient prognosis (Donizy et al., 2015). CD166 is not known to be detected in the healthy uveal layer of the eye and the currently understood role of CD166 in uveal melanoma requires further validation, however, Djirackor et al. reported significantly higher CD166 positive population in tumor cells compared to normal choroidal melanocytes (NCM). They proposed its role as a CSC marker supported with increased migratory and melanosphere forming capacity which stayed consistent with the results from Jannie and colleagues where they reported the positive correlation between CD166 expression levels and the migratory capacity (Djirackor et al., 2019; Jannie et al., 2012).

Melanoma Antigen (MelanA): MelanA or also known as Melanoma Antigen Recognized by T cell-1 (MART-1) is a melanocyte differentiation marker and therefore, is only expressed on melanocytes present in areas such as the human skin and the retinal pigment epithelium of the eye (Coulie et al., 1994; De Mazière et al., 2002). It is a transmembrane protein that is expressed more intracellularly than on the plasma membrane (De Mazière et al., 2002). This protein has been studied in the context of immunotherapy due to its presentation to HLA-A* A201 cytolytic T lymphocytes (CTL) through the major histocompatibility matrix (MHC)

class 1 (Seiter et al., 2002). Not only is the protein expressed in normal melanocytes of the skin and the eye, but studies have confirmed their expression levels in cutaneous melanoma and uveal melanoma (Busam et al., 1998; Fan, 2011). MelanA expression levels in relevance to patient prognosis and cell states have been studied primarily in cutaneous melanoma in that there is an inverse relationship with tumor thickness and lower levels of MelanA by tumor cells portray a neural crest-like state (Berset et al., 2001; Su et al., 2017). Perhaps in a contrasting manner, in the context of uveal melanoma, a few studies report that MelanA is differentially expressed across cell lines and higher expression levels were seen in liver metastases (Fan, 2011; Hoefsmit et al., 2020).

Nerve Growth Factor Receptor (NGFR): Commonly recognized as cluster of differentiation 271 (CD271), this receptor is a transmembrane protein expressed on smooth muscle cells, melanocytes, mesenchymal cells, basal respiratory cells, and in the retina of the eye (The Human Protein Atlas; Tanaka, 2015). It acts as a receptor for a family of neurotrophin ligands at low affinity and has been shown to be involved with apoptotic events to induce Alzheimer's disease (Bruno et al., 2023). The relationship between NGFR and apoptosis has also been explored in cancer, but its roles appear to be both pro-tumorigenic and anti-tumorigenic. In colorectal cancer, NGFR mediated apoptosis led to increased sensitivity towards chemotherapy agent Fluorouracil (5-FU) but in lung cancer, colon cancer, liver cancer, neuroblastoma, osteosarcoma and skin cancer cell lines, apoptosis induced by reduced levels of NGFR lead to reduced survival or cancer cells as well as increased sensitivity towards chemotherapy (H. Chen et al., 2021; Zhou et al., 2016). Where in some cancers such as prostate and bladder cancers, NGFR act as a tumor suppressor, in cutaneous melanoma, breast cancers, and glioblastoma, it has been well established to drive tumor progression through greater proliferative capacity and

inhibiting the activity of the tumor suppressor p53, as well as initiating tumor development, (Bashir et al., 2022; Boiko et al., 2010; H. Chen et al., 2021; Redmer et al., 2014; Tsang et al., 2013; YANG et al., 2018; Zhou et al., 2016). Researchers suggest NGFR as a marker of stem cell state due to evidence such as mesenchymal cells expressing NGFR and studies confirming the receptor's pro-tumorigenic roles (Boiko et al., 2010; Redmer et al., 2014). Interestingly, tumor heterogeneity also appeared to be driven by CD271 where Redmer et al. confirmed varying levels of CD271 expressing cells having correlation to the rate of cell division (Redmer et al., 2014). Several studies have also confirmed the stem-cell like property that CD271 positive cells portray in uveal melanoma (Djirackor et al., 2019; Joshi et al., 2016; Valyi-Nagy et al., 2012). Levels of a known stem cell surface marker called CD166 was elevated along with NGFR expression. High levels of NGFR were also detected in cells participating in vascular mimicry in the uveal melanoma cells (Djirackor et al., 2019; Valyi-Nagy et al., 2012).

Glial cell line Derived Neurotrophic Factor (GDNF) Family Receptor Alpha-2

(GFRA2): This is a cell surface receptor that binds to glial GDNF and neurturin (NRTN) leading to the activation of the rearranged during transfection (RET) receptor for signaling (Jing et al., 1997; Takahashi, 2001). There are relatively limited studies available explaining the relationship between cancer progression with GFRA2, but Ishida et al. highlight its role in identifying cardiac progenitor cells as well as mediating cell differentiation in the heart and another study claiming the activation of the phosphoinositase-3-kinase/Ak strain transforming (PI3K/AKT) pathway via GFRA2 to induce neuroblastoma cell proliferation (Ishida et al., 2016; Zuoqing Li et al., 2019). According to Gu et al., increased GFRA2 expression was also observed in pancreatic tumors of bigger than or equal to 3.00 mm (Gu et al., 2016). In support with these previously mentioned phenotypes from cancer cells with GFRA2 expression, along with several studies in cutaneous

melanoma, this receptor appears to be a marker of the neural crest stem cell state as well as inducing intratumor heterogeneity through phenotype switching (Huang et al., 2021; Rambow et al., 2018). In a study by Rambow et al., it was observed that upon a combination therapy with BRAF and MEK inhibitors, GFRA2 expressing cells were subsequently elevated (Rambow et al., 2018). In addition, GFRA2 expression levels were observed to be negatively related to treatment response (Rambow et al., 2018).

Glycoprotein 100 (GP100): This protein is another melanocyte differentiation marker expressed in more diverse tissues groups but at low levels (Brouwenstijn et al., 1997; Seiter et al., 2002). As early as 1997, Brouwenstijn et al. observed GP100 expression in samples of lymph node, ovarium, retina, thyroid, liver, kidney, heart, and the oesophagus (Brouwenstijn et al., 1997). An alternate name for GP100 is premelanosome protein (PMEL) and is a transmembrane glycoprotein responsible for defining the structural organization of melanosomes leading to their maturation (*Pmel premelanosome protein [homo sapiens (human)]*, 2023). Expression levels of this protein has been associated with the differentiation status of cancer cells where high expression was indicative of a differentiated cell state apparent with a pigmented phenotype (Benboubker et al., 2022; Huang et al., 2021). Immunotherapeutic approaches have been designed with this marker in mind, because it was originally reported that melanoma infiltrating T lymphocytes recognized GP100 peptides presented by HLA-A*02:01 molecules (Kawakami & Rosenberg, 1997). Currently in uveal melanoma, GP100 is used as a bispecific T cell engager (BITE) for treatment with a newly approved drug called Tebentafusp (see section 1.2.3 *Treatment Options for Uveal Melanoma*).

1.4 CD36 in Cancer Progression

1.4.1 CD36 in Cells and Various Roles

CD36 is expressed on a wide variety of cells such as platelets, adipocytes, mammary epithelial, and even immune cells. With the molecular weight ranging from 53 to 88 kilodalton (kDa), this scavenger receptor is a transmembrane glycoprotein with two short cytoplasmic tails, two transmembrane domains, and a long extracellular domain that is exposed to high levels of post translational modifications (Figure 2) (Armesilla & Vega, 1994; R. Yang et al., 2022). To date, CD36 is susceptible to phosphorylation, ubiquitylation, palmitoylation, glycosylation, and acetylation where the extracellular domain has as much as 10 glycosylation sites, leading to alterations to its molecular weight (Tao et al., 1996; R. Yang et al., 2022). Post-translational modifications on CD36 has also been reported to affect where this protein is expressed amongst the cell surface, golgi apparatus, mitochondria, the endoplasmic reticulum, and endosomes (R. Yang et al., 2022).

Interestingly, CD36 has several ligands to which it binds to leading to the fulfillment of multiple roles in a wide range of differing cell types. The first group of ligands that commonly bind are lipid-related molecules such as long chain fatty acids (LCFA), oxidized low-density lipoproteins, and oxidized phospholipids (Kar et al., 2008). Upon binding these ligands, CD36 acts as a lipid transporter, lipolysis, induce pro-inflammatory response leading to diseases such as atherosclerosis and metabolic disorders, as well as carrying out functions such as phagocytosis and regulating fatty acid oxidation (Y. Chen et al., 2022; Ryeom et al., 1996; Silverstein & Febbraio, 2009; Wang & Li, 2019; Zhao et al., 2018). Another group of ligands that bind to CD36 are proteins including collagen, thrombospondin-I, amyloid beta, and advanced glycated end products (AGE) leading to the moderation of adhesive interactions between cell-cell and

cell-matrix, activate monocytes and platelets, prevent angiogenesis, and induce apoptosis (Asch et al., 1993; Dawson et al., 1997; Lehner & Quiroga, 2016; Silverstein & Febbraio, 2009; Susztak et al., 2005). Lastly, CD36 has also been studied in regards to its role in immunology as a pattern recognition receptor (PRR) on the surface of cells with a phagocytic function such as macrophages and monocytes as they are able to bind to the pathogen associated molecular patterns (PAMPs) on bacteria, fungi, and parasite infected human erythrocytes (Fraser et al., 2004; Silverstein & Febbraio, 2009; Wang & Li, 2019).

1.4.2 CD36 in Cancer

Glioblastoma, gastric cancer, human oral carcinoma, lung small cell carcinoma, and cervical cancer are just a few of the cancer types where CD36 overexpression was associated with tumor progression (Hale et al., 2014a; Pan et al., 2019; Pascual et al., 2017; P. Yang et al., 2018). From tumor initiation, tumor progression, development of metastasis, treatment resistance, and promoting phenotype switching, CD36 appears to act as a central regulator (Wang & Li, 2019). Amongst many of the previously mentioned functions of this surface receptor, lipid metabolism provides clues to be the promising pathway to investigate to unravel its pro-oncogenic role. The dysfunctional metabolic events led by CD36 with excessive fat supply can perhaps provide an explanation for the observed poor prognosis in breast cancer patients with *HER-2* gene that leads to the over-expression of the fatty acid synthase (*FASN*) (Feng et al., 2019; Pepino et al., 2014). Additionally, CD36 mediated uptake of a specific type of fatty acid known as palmitate acid has shown to increase migratory and invasive ability of gastric cancer cells (Pan et al., 2019). It is important to note however, that although we understand CD36 plays a role in fatty acid uptake to drive cancer, the mechanism behind how they get

transported intracellularly remains to be explored (Luo et al., 2021). CD36 is expressed in various regions of the human eye and multiple ocular-associated diseases have been associated with the CD36 receptor such as glaucoma and retinal and corneal neovascularization, however, a direct relationship with uveal melanoma progression with CD36 has not yet been established (R. Yang et al., 2022).

1.4.3 CD36 Inhibitors

The scavenger receptor's role as a driver of both tumor development and disease progression make it an attractive target to inhibit. Currently, there are various types of inhibitors available that work as a competitive or a non-competitive inhibitor of CD36. Sulfo-N-succinimidyl oleate (SSO) is a chemical inhibitor that works through competitive binding of the known ligands of this receptor (Kuda et al., 2013; Mansor et al., 2017). By inserting into the region at Lysine 164 which oxidized low density lipoproteins (ox-LDL) and long chain fatty acids (LCFA) bind to on CD36, sulfo-N-succinimidyl oleate (SSO) blocks CD36 signaling activity and lipid uptake through an irreversible inhibition (Kuda et al., 2013). Another inhibitor that works as an antagonist in inhibiting CD36 receptor is salvionolic acid beta (SAB) which works by preventing oxLDL uptake by CHO cells, THP-1 cells, and macrophages (Bao et al., 2012). Bao and colleagues have confirmed that introducing salvionolic acid beta reduced lipid uptake both *in vitro* and *in vivo* and reported reduced lipid accumulation in hyperlipidemic mouse models (Bao et al., 2012). Last group of inhibitors used to test CD36 roles in diseases are known as AP5055 and AP5258 which has been determined to prevent the binding of oxidized low-density lipoproteins (ox-LDL) and long chain fatty acids (LCFA) in a non-competitive manner (Geloan et al., 2012). Upon treating *Cd36*-expressing HEK293 cells and atherosclerotic

mice with AP5055 and AP5258, there was reduced foam cell formation along with reduced plasma triglyceride concentration (Geloan et al., 2012). Besides using drugs, another method of inhibiting CD36 in cancer models include the use of anti-CD36 monoclonal antibody (Martini et al., 2021).

As evident from inhibitors mentioned above, limiting the activity of CD36 appears to have a prophylactic effect through the interference in the process of lipid metabolism. Hence, there are many drugs for CD36 in clinical trials to prevent cancer progression as summarized in Table 1 (Wang & Li, 2019). Many of these inhibitors compete with the binding activity of thrombospondin-1 targeting the angiogenic activity that is also related to cancer progression. No direction relationship between these drugs and lipid uptake function of CD36 has been made, but ABT-510 which has entered phase 2 clinical trials showed weak levels of reduced myristate uptake which is a fatty acid playing a role in glycoprotein anchorage (Doering et al., 1993; Isenberg et al., 2008). However, due to side effects such as anemia, hemorrhage in the gastrointestinal tract, headache, dizziness, radiation pneumonitis and even death from bowel obstruction with perfusion was observed in clinical trials, leading to the termination of the trials (Ebbinghaus et al., 2007; Molckovsky & Siu, 2008). Due to these reasons and observed side effects in ongoing pre-clinical studies for potential target therapy against CD36, currently, there is yet to be an approved CD36 inhibiting drug used in the clinics (Table 1) (Wang & Li, 2019).

Table 1. Drugs Against CD36 and CD166 in Pre-clinical and Clinical Trials.

CD36	CD166
ABT-510	CX-2009
CVX-045	
ABT-526	
ABT-898	
CVX-022	
3TSR	
TAX2	
ELK-SAHPs	

1.5 Rationale, Objectives, and General Introduction to the Project

Uveal melanoma is a highly heterogeneous cancer type and intratumor heterogeneity has been linked to disease progression leading to metastasis and therapy resistance (Marusyk et al., 2020). Metastasis in uveal melanoma patients is a serious concern as less than 5% of the patients have detectable metastasis at the time of initial diagnosis and the median survival after diagnosis with metastasis only ranges between 4-6 months (Harbour & Chen, 2013; Lane et al., 2018; Rietschel et al., 2005). In other types of cancer such as cutaneous melanoma, various markers have been identified associated with metastasis risk and therapy resistance in relation to specific cell states. Therefore, I hypothesize that in uveal melanoma, there will be different cell states that co-exist to drive tumor heterogeneity and ultimately, metastasis. My project will first determine the extent of heterogeneity that can be observed from the uveal melanoma cell lines in the lab to

isolate a potential marker associated with metastasis development specifically in the context of uveal melanoma. Therefore, my aims are as following:

Aim 1: Characterize Uveal Melanoma Cell lines with markers related to cell states/disease progression.

Aim 2: Unravel a potential target mediating the high metastasis risk.

METHODS

2.1 Cells and reagents

Uveal melanoma cell lines (Mel270, 92.1, OMM2.5, MU2, MU2F, T108, T128, T142, T143, UM001, and H79) were kindly gifted by Dr. Solange Landreville (University of Laval, Quebec City). Mel270, 92.1, OMM2.5, MU2 and MU2F cells were cultured in Roswell Park Memorial Institute (RPMI) 1640 media (Wisent Bio Products) containing 10% fetal bovine serum (FBS) and 1% penicillin/streptomycin (Wisent). T108, T128, T142, T143, 293, and HEK293FT cells were cultured in Dulbecco's modified Eagle's medium (DMEM) (Wisent Bio Products) supplemented with 10% FBS and 1% penicillin/streptomycin. UM001 cells were cultured in RPMI 1640 media supplemented with 10% FBS, 1% penicillin/streptomycin, 2% GluataMax (Gibco), 1% HEPES (Wisent), and 1% non-essential amino acids (NEAA, Gibco). H79 cell line was grown in low-glucose DMEM supplemented with 10% FBS and 1% penicillin/streptomycin. Additional uveal melanoma cell lines (1088mel, 624.38mel, 397mel, and 1102mel) were kindly gifted by Dr Réjean Lapointe (University of Montreal, Montreal). All cell lines gifted by Dr Lapointe were cultured in RPMI 1640 media supplemented with 10% FBS and 1% penicillin/streptomycin.

Mel270 cells tagged with a luciferase (luc)-tdTomato (Mel270 luc-tdTomato/tagged cells) were used for both *in vitro* and *in vivo* assays. Briefly, second generation HIV-based lentiviral vectors were produced by co-transfecting HEK293FT cells with plasmids encoding the HIV-Rev (Addgene #12260), VSV-G (Addgene #12259), and the luc-tdTomato expression vector (Addgene #72486). Mel270 cells were then transduced by mixing the virus-containing supernatant, fresh media, and polybrene (8 μ g/mL). The cells were then subsequently sorted for tdTomato⁺ cells after 3 passages post transduction.

All cells were cultured in a humidified incubator at 37°C with 5% CO₂.

2.2 RNA interference

2.2.1 siRNA mediated CD36 knockdown

Pre-designed *CD36* siRNAs (duplex sequences shown below) were purchased from Integrated DNA Technologies (IDT; Ref #: 428499354 (siCD36 1) and 428499351 (siCD36 3)). Control siRNA (siCTL) was purchased from Qiagen (Cat No.: 1027280). All siRNAs were reconstituted and diluted in H₂O to a working concentration of 20µM, aliquoted, and stored at -80°C before use. For transient *Cd36* knockdown, Mel270 luc-tdTomato and 92.1 cells were seeded in 6-well plates at a concentration of 300,000 cells per well. For each well, siRNAs (1µL), Opti-MEM Reduced Serum Medium (500µL, Gibco), and Lipofectamine™ RNAiMAX Transfection Reagent (5µL, Invitrogen) were mixed by vortexing and were incubated in room temperature for 20 minutes. The mixture was then added to each well, followed by a media change 24 hours after transfection.

#428499354

```
5'- CAACCUAUUGGUCAAGCCAUCAGAA -3'
   ||||||||||||||||||||||||||||
3'- CAGUUGGAUAACCAGUUCGGUAGUCUU -3'
```

#428499351

```
5'- GGAUUAACCCAAAUGAAGAAGAAC -3'
   ||||||||||||||||||||||||||||
3'- UACCUAAUUUGGUUUACUUCUUCUUG -3'
```

2.2.2 shRNA mediated CD36 knockdown

Short hairpin RNA (shRNA)-mediated knockdown was achieved using lentiviruses produced with vectors from the McGill Genome Perturbation Centre (*Cd36*, TRCN0000056998

and TRCN0000057000) and the pLKO empty vector as control in the HEK293T cell line. Mel270 cells were infected in the presence of 4 µg/ml polybrene, and 3 days after viral infection, cells were treated and selected with 2.5 µg/ml puromycin and bulk-sorted for tdTomato⁺, *Cd36*⁻ cells.

2.3 Immunoblotting

Cell pellets were lysed using RIPA buffer (400mL double distilled water, 15mL sodium chloride 5M, 5mL of 10% sodium dodecyl sulfate (SDS), 2.5g sodium deoxycholate, 25mL TRIS 1M pH 7.4, and 5mL of NP40) complete with protease inhibitor and phosphatase inhibitor. Samples were sonicated at 50% amplitude for 4 seconds and were then centrifuged at maximum speed for 15 minutes at 4°C. Protein concentration of each sample was measured by Bradford assay. Samples were prepared at the desired concentration and mixed with 4X bromophenol blue dye at a ratio of 3:1. Proteins were separated on a 10% SDS-PAGE gel and were then transferred to a nitrocellulose membrane. The membrane was stained with Ponceaus S Staining solution and was then washed with Tris Buffered Saline-Tween (TBST) solution twice before blocking with 5% non-fat milk for 1 hour at room temperature. The membrane was then incubated in primary antibodies (diluted in 5% non-fat milk) at 4°C overnight. The next day, the membrane was washed with TBST (10 minutes per time, three times in total) and was then incubated in secondary antibody for 1 hour at room temperature. Membrane was again washed with TBST and was revealed using ECL Western Blotting Detection Reagent (Cytiva) or Immobilon Western Chemiluminescent HRP Substrate incubation (EMD Millipore). Antibodies used for immunoblotting include CD36 rabbit monoclonal antibody (EPR6573, Abcam #ab133625,

1:1000); GAPDH rabbit monoclonal antibody (D16H11, Cell Signaling Technologies #5174, 1:5000).

2.4 Flow Cytometry

2.4.1 Staining

Cells were trypsinized, then washed with 1X Dulbecco's phosphate-buffered saline (DPBS) and pipetted into a v-bottom 96-well plate at approximately 1 million cells per well. After centrifugation at 2000 rpm for 1 minute, supernatant was discarded, and cells were stained with the Live/Dead Fixable Aqua solution (Invitrogen, 1:100 in DPBS) at 4° for 30mins. After washing and discarding the supernatant, cells were blocked with a homemade Fc block buffer diluted in FACS buffer (500mL PBS, 1.6mL 20% NaN₃, 25mL FBS; filtered) at 1:10 on ice for 30 minutes. Cells were then stained with prediluted antibodies with conjugated fluorophores (Table 2) on ice for 30 minutes, washed once and was fixed with 4% paraformaldehyde (PFA) on ice for 30 minutes. Cells were washed once before getting resuspended in 300µL FACS buffer into polystyrene tubes (Corning, Cat#: CA60819-820).

2.4.2 Antibody Titration

Equal numbers of any combination of Mel270, 92.1, OMM2.5, MU2, MU2F, T108, T128, T142, T143, UM001, and H79 uveal melanoma cells (from Dr. Solange Landreville) were mixed for the titration of AXL, CD36, CD166, MelanA, NGFR, and GFRA2, whereas a complete mix of 1088mel, 624.38mel, 397mel, and 1102mel cells (from Dr. Réjean Lapointe) were used to titrate GP100. The mix of cells were pipetted into a v-bottom 96-well plate at approximately 2 million cells per well. After Live/Dead staining and Fc blocking, cells were

stained with each antibody which was serially diluted at 1:50, 1:100, 1:200, 1:400, and 1:800 dilutions in FACS buffer, with an unstained sample as the negative control (see section 2.4.1 *Staining* for detailed staining procedure). Optimal antibody dilution was defined based on visual separation of the negative and the positive populations (Supplementary Figure 1), along with the calculated separation index of each dilution.

2.4.3 Flow Cytometry Assays

For screening uveal melanoma cells with markers in the UMarkit panel, 130,000 of Mel270, 92.1, OMM2.5, MU2, MU2F, T108, T128, T142, T143, H79, and UM001 cells were seeded in a 15cm cell culture dish and were cultured for 96 hours. All cells were grown in their respective media and the media was changed once at 48 hours after seeding. Cells were then trypsinized, washed with 1X Dulbecco's phosphate-buffered saline (DPBS), and pipetted into a v-bottom 96-well plate at approximately 1 million cells per well. The staining process with prediluted antibodies of the UMarkit panel (Table 2) is as mentioned in section 2.4.1 *Staining*. Compensation controls were prepared with antibodies and their respective beads as summarized in Table 2 to avoid spectral overlap between colours. They were prepared by incubating 5 μ L of pre-diluted antibodies in approximately 100 μ L of respective beads in polystyrene tubes (Corning, Cat#: CA60819-820) on ice for 30 minutes. 2mL of FACS buffer was added to the stained beads and were spun down at 400g for 5 minutes. Supernatant was discarded and beads were resuspended in 300 μ L of FACS before running.

For Annexin/PI staining, 300,000 Mel270 tagged cells were seeded in a 6 well plate and were transfected with siCTL (control scramble sequence), siCD36 1, or siCD36 3. Media was changed once at the 24-hour timepoint post-transfection and at 48 hours, media and cells were

collected into a polystyrene tube from one well for each condition. Cells were centrifuged at 1700rpm for 3 minutes at 4°C. Supernatant was discarded, and cells were washed with 1 mL of DPBS before being centrifuged under the same conditions. Each tube of cells were stained for 15 minutes on ice with 20 μ L of staining mixture (10X binding buffer (BD BioSciences Cat#: 51-6612E), 180 μ L ddH₂O, 0.2 μ L Annexin V (Invitrogen Ref#: A23204), and 1 μ L PI (BD BioSciences Cat#: 51-66211E)).

All flow cytometry data were acquired on LSRFortessa or CantoII and were subsequently analyzed using FlowJo software.

Table 2. Antibodies/Markers in the UMarkit Panel.

Marker	Conjugated Fluorophore	Company	Beads
AXL	PE Cy7	eBiosciences	OneComp
CD36	PerCP-Cy5.5	BD Biosciences	OneComp
CD166	APC	BioLegend	OneComp
MelanA	APC Cy7	Novus Biologicals	OneComp
NGFR	BV421	BD Biosciences	UltraComp
GFRA2	AF488	Novus Biologicals	OneComp
GP100	CF594	Biotium	OneComp

2.5 Wound Healing Migration Assay

Cells were transfected with siRNAs as described in section 2.2.1 *siRNA mediated CD36 knockdown* and were grown until confluent approximately 24 hours after transfection. Scratch wounds were then created using a p10 pipette tip (Supplementary Figure 2A). Wells were washed once with PBS and fresh media was added. Images were taken immediately after using

an inverted microscope at 4X focus on different locations of the wound site (Supplementary figure 2A). After 24 hours, images were taken at the same locations. Images were analyzed with ImageJ software and percent wound closure was calculated with the following equation: $100 - [(width\ at\ 0\ hour) \div (width\ at\ 24\ hours) \times 100]$. All scratch assays were completed with technical triplicates and biological triplicates. Statistical analysis for scratch assays is specified in the figure legends.

2.6 Invasion Assay

Mel270 tagged and 92.1 cells were transfected as described in section 2.2.1 *siRNA mediated CD36 knockdown*. Mel270 tagged cells were cultured in serum-free media for approximately 16 hours before seeding. 92.1 cells did not undergo serum starvation. On the day of seeding, transwells (8.0 μ m, FALCON) were first coated with Matrigel at 300 μ g/ml for 30 mins at 37°C. Cells were then seeded in serum-free media at the concentration of 150,000 cells per well into the coated transwell inserts. Cells were allowed to migrate and invade to the bottom chamber containing media supplemented with 10% FBS as chemoattractant for 24 hours. Cells were fixed using 4% glutaraldehyde (Sigma) and stained with 0.5% crystal violet solution for 30 minutes. Non-migrated cells that remained on top of the transwell were manually removed using cotton tips (Supplementary Figure 2B). The remaining invaded cells were imaged using an inverted microscope at 10X magnification and were counted manually using the ImageJ software. All invasion assays were completed with technical replicates and biological triplicates. Statistical analysis for scratch assays is specified in the figure legends.

2.7 Proliferation Assay

Mel270 tagged cells and 92.1 cells were seeded in 6-well plates at 300,000 cells and 200,000 cells per well, respectively. Cells were trypsinized and counted using a hemocytometer at indicated time points (24 hours, 48 hours, and 72 hours).

2.8 RNA extraction and Quantitative real-time PCR

RNA was extracted from Mel270 tagged and 92.1 cell pellets with the E.Z.N.A.[®] Total RNA Kit 1 (omega BIO-TEK, SKU: R6834-01) following the manufacturer's instructions. Extracted RNA were quantified using the Nanodrop 1000 Spectrophotometer (ThermoFisher Scientific). cDNA was prepared from 1 μ g of the extracted RNA using the iScript[™] cDNA Synthesis Kit (BIO-RAD, Cat#: 1708891BUN). The target gene *CD36* and the housekeeping gene *HPRT1* were quantified using the Applied Biosystems 7500 Fast Real-Time PCR System with pre-designed gene probes (ThermoFisher Scientific, Cat#: 4331182 and 4333768F, respectively).

2.9 Splenic injection

4-6 weeks old NOD CRISPR *prkdc* *Il2r* Gamma (NCG) male mice were purchased from Charles River Laboratories. One day before the procedure, all mice were shaved and was given an ear tag for identification and approximately 1 hour before the procedure, all mice were given carprofen. Freshly trypsinized cells were washed and resuspended in DPBS at a concentration of 1.0 X 10⁷ cells per mL and were kept on ice before injection. All surgery tools were autoclaved before use. During the procedure, all mice were given isoflurane as anesthesia with oxygen (O₂). To access the spleen, a small incision was made on the skin just below the rib cage on the left

side of the mouse, followed by another incision on the muscle layer. Upon successful location of the spleen, connective tissues were removed using a cotton tip and the organ was “scooped out” using a curved tweezer. Splenic vein needed to be identified to observe the change in colour of the vein after injecting 1.0×10^6 cells into the spleen with a 26G 1mL needle. After allowing the blood to clot using a cotton tip, the spleen was put back into place and the muscle layer was closed using a 13mm 3/8c surgical suture. Approximately 10 μ L of lidocaine was given before closing the epidermal layer with surgical clips. Topical antibacterial cream was put around the surgical wound to prevent any infections from occurring. ~500 μ L of saline was given through subcutaneous injection before removing the mouse from anesthesia. Mice were put into their respective cages and into the 33°C incubators before being taken back to the sterilized animal room. At 24 hours and 48 hours post-injection, all mice that underwent surgery were given carprofen and saline. All procedures except the splenic injection took place under a ventilation hood to maintain a sterile environment.

2.10 Kinetic Curves for IVIS Imaging

After splenic injection of tumor cells, all mice in the same condition were injected with 200 μ L of D-luciferin via intraperitoneal (IP) injection. Images were taken using the IVIS machine every 3 minutes immediately after injection until a decline in signal emission was apparent. Luminescence signal from each image were graphed together from which the kinetic curve was generated. The timepoint at which maximum intensity is achieved was determined with the kinetic curve along with the percent total emission (photons/second) which was calculated by dividing all emission signals with the maximum emission.

2.11 Immunohistochemistry (IHC) Staining

Mouse livers were fixed in 10% formalin and were paraffine-embedded at the Research Pathology Facility at the Montreal Center for Experimental Therapeutics in Cancer (MCETC). Sections were deparaffinized and rehydrated before antigen retrieval. Antigen retrieval was performed by heating the sections with an antigen retrieval solution (50mL 10X TRIS EDTA pH9, 450mL double distilled water, 250 μ L Tween 20) in a pressure water bath to unmask the antigen epitope. The tissue sections were then stained with an antibody specific to human nucleolin (Abcam #ab136649, 1:100 dilution), using mouse brain as a negative control tissue. The tissue sections were then washed and incubated with HRP antibody. Antibody staining was visualized using Magenta Red (Dako) chromagen reagents and counter-stained with haematoxylin (Thermo Fisher Scientific). The slides were dehydrated and mounted with coverslips. All stained sections were imaged by ZEISS Axio Sca.Z1 to detect micrometastases and analysed using QuPath v0.2.3.

2.12 Statistical Analysis

All statistical analyses were performed using GraphPad Prism 9 Software. Figure legends specify the statistical analysis (Welch's t-test, one-way ANOVA) used for each assay and define error bars. P values less than 0.05 were considered significant.

RESULTS

3.1 Characterization of Uveal Melanoma Cell Lines

3.1.1 Flow Cytometry using a Novel “UMarkit” Panel shows High Heterogeneity Amongst Uveal Melanoma Cell Lines.

Uveal melanomas are highly heterogeneous as detected via single cell RNA sequencing in previous studies (Lin et al., 2021; Pandiani et al., 2021). To be able to assess if this heterogeneity is also detectable in our human uveal melanoma cell lines at the protein level, we have developed a novel multi-colour fluorescence activated cell sorting (FACS) panel consisting of seven different cell surface markers, which we have collectively termed as “UMarkit” (Table 2). Antibodies included in the UMarkit panel were against the following proteins: AXL, CD36, CD166, MelanA, NGFR, GFRA2, and GP100, and their general expression profiles and functions have been elaborated in section *1.3.3 Introduction to Cell State Markers*. With a mixture of several uveal melanoma cell lines as outlined in section *2.4.2 Antibody Titration*, successful antibody titration was achieved, giving us the optimized antibody dilutions to be used in the “UMarkit” panel (Table 2). Eleven different human cell lines derived from either a primary uveal melanoma or a uveal melanoma liver metastasis were characterized for the expression of the aforementioned proteins. Positive populations were identified with the gating strategy as depicted in Figure 3A and with the negative control of each antibody identified as the corresponding fluorescence *minus one antibody (FMO)* samples. The obtained results were quite fascinating in that we saw a great variability in the number of markers that were expressed by each cell line, along with the variability across the cell lines regarding the percentage of cells expressing each specific protein marker (Figure 3B). Through repeated screening, we were able to confirm the unique signatures of each cell line with the varying levels in the populations of

cells expressing each marker. Specifically, it was interesting to see AXL, a marker of stem-cell like phenotype with a role in sustaining tumor cell survival through its interaction with the *Gas6* ligand, was expressed only in the H79 cell line amongst the four liver metastasis derived cell lines (Figure 3B). Another interesting observation was that the cell line derived from the liver metastasis of the MU2 cell line annotated as MU2F, had similar percentage of cells with MelanA expression but once metastasized to the liver, there appeared to be an emergence of a fraction of cell population gaining CD166 expression as depicted in the bar graph for MU2F (Figure 3B). Across the panel of 11 different uveal melanoma cell lines, the melanocytic differentiation markers MelanA and GP100 remained largely undetected. However, it was noted that GP100 expression appeared to be correlated with the cells' pigmentation status in that increase in GP100 expression resulted in greater pigmentation (Figure 3C). Between T128, T142, and T143 cell lines, only three of the seven markers were detected, where we saw that the percentage of antibody positive cells were consistent. From the high level of similarity portrayed between these 3 cell lines, it was interesting to observe that only T128 had drastically over 10% of cells with NGFR expression unlike T142 or T143.

CD36 was detected in multiple uveal melanoma cell lines at varying levels. The majority of the Mel270, OMM2.5, and UM001 cells were CD36 positive whereas approximately half of the cells were positive for CD36 in 92.1, and a small population of approximately 1.00% was detected in H79 (Figures 3B and 4A). It is also important to point out that we have identified there to be a significant difference between the percentage of cells staining positive for CD36 expression from a given sample, compared to the average expression within the total CD36 positive cells gated out from each cell line. When we compared the mean fluorescence intensity (MFI) values of CD36 in Mel270 and 92.1, results showed that 92.1 had approximately 1.6-fold

more CD36 expression than Mel270. In line with this finding, the *Cd36* mRNA levels were higher in 92.1 than in Mel270 (Figure 4C). From these results, we can suggest that although Mel270 has more cells with CD36 expression, 92.1 cells appear to have higher expression for this surface receptor.

3.1.2 Confirmation of Flow Cytometry Results for CD36 Expression by Western Blot

Given the importance of CD36 in tumor progression (Pascual et al., 2017; Wang & Li, 2019), we wanted to confirm our flow cytometry data to ensure that the cell lines indeed were expressing CD36. We thus performed western blot analysis on a panel of uveal melanoma cell lysates probing for CD36 protein expression. The results with our UMarkit flow-based panel were highly replicated by western blot analysis in that we detected bands only in the cell lines that we have characterized cells to be positive for CD36 (Figure 4B). Moreover, the normal choroidal melanocytes did not show any expression for CD36 which stays consistent with the published literature that CD36 is only expressed in the retinal pigment epithelium of the eye (Silverstein & Febbraio, 2009). Mel270 and OMM2.5 cell lines profiled for CD36 expression with western blot analysis confirmed that the percentage of cells expressing CD36 is high, relative to the other cell lines that we have profiled. 92.1 and UM001 samples had bands of less intensity than those of Mel270 and OMM2.5. We made the additional observation that the CD36 bands detected were variable in molecular weight between the cell lines. With evidence from past literature and the nature of CD36 surface protein, we propose that this may be due to post-translational modifications that occur for CD36, such as glycosylation and phosphorylation (Luiken et al., 2016).

3.2 CD36 on its Effects on Migration and Invasion Capacity in Uveal Melanoma Cells

3.2.1 Tagging Mel270

Uveal melanoma metastasizes to the liver in approximately 50% of patients (B Damato, 2010; Rietschel et al., 2005; J. Yang et al., 2018), and splenic injection of tumor cells is used to model liver metastasis in mice (H. Yang et al., 2015). For any *in vivo* experiments, we wanted to be able to track uveal melanoma cells over time in the livers of mice while they are still alive. Therefore, we tagged our Mel270 parental cells with a vector expressing luciferase-tandem dimer Tomato (tdTomato). We had the alternative option to tag the Mel270 cell line with green fluorescence protein (GFP) fluorophore, however, GFP had a greater chance of overlapping with other colours in the UMarkit panel than the tdTomato (Table 2). This was something to consider as we would be able to then have the option to extract tumor lesions and characterize the liver-colonized tumor cells with the UMarkit panel. Mel270 was transduced with virus produced from the HEK293T cell line and was treated with puromycin before bulk sorting. Tagging of the cells was confirmed through luminescence and fluorescence with luciferase detected by the GloMax and tdTomato on the inverted microscope respectively (Figure 5A). We used this tagged version of the Mel270 cell line to perform all assays such as the wound closure assay, invasion assay as well as all *in vivo* studies.

3.2.2 siRNA Mediated Knockdown of CD36

To be able to unravel the role of CD36 in uveal melanoma and its role in the onset and development of liver metastasis, we depleted this receptor protein first in a cell line with the highest percentage of CD36 expressing cells, relative to all other markers. Mel270 was a great candidate in this aspect (Figures 3B, 4A, and 4B). Tagged-Mel270 cells were transfected with

control siRNA (negative control scrambled sequence) and two different CD36 siRNAs to induce a transient knockdown. Efficient knockdown of CD36 was confirmed through western blot analysis (Figure 5B). Next, we assessed whether the knockdown of CD36 had any effect on cell proliferation over three different time points at 24 hours, 48 hours, and 72 hours. Tagged Mel270 cells were plated and transfected with siRNAs and then fixed and stained with crystal violet, which revealed no significant difference in cell proliferation between the control siRNA and CD36 siRNA knockdown conditions (Figure 5C). We also assessed cell proliferation by counting the cells and once again there were no differences detected between both CD36 siRNAs and the scramble siRNA control conditions (Figure 5D). Lastly, to detect if any cell death occurs due to the siRNA knockdowns, we performed an apoptosis assay with Annexin V/propidium iodide (PI) staining and showed that the transfections of CTL or CD36 siRNAs did not lead to apoptotic cell death (Figure 5E). Therefore, we concluded that silencing of CD36 using siRNA did not affect the proliferation or apoptosis of Mel270 cells.

3.2.3 Migration and Invasion Capacity of Uveal Melanoma Cells

As previously mentioned in section *1.2.1 Disease Epidemiology*, metastasis risk is a critical component when treating uveal melanoma patients as there is very high metastatic potential at the rate of approximately 50% amongst all patients and the one-year survival rate is very poor (Rietschel et al., 2005). Therefore, to gain an understanding on the role of CD36 in characteristics associated with metastatic cells, we performed wound healing (scratch) assays and trans-well invasion assays in the context of the siRNA knockdown assay described in section *3.2.2 siRNA Mediated Knockdown of CD36*. As shown in Figure 6A, Mel270 tagged cells with CD36 knockdown had significantly less of its wound closed after 24 hours compared to the

control siRNA transfected cells, in the scratch assay. Next, using the boyden chamber invasion assay, the invasive capacity of the Mel270 tagged cells with CD36 expression knocked down invaded less, compared to the CTL siRNA knockdown conditions (Figure 6B). siCTL, siCD36 1, and siCD36 3 transfections were confirmed using flow cytometry (Figure 6C). These data collectively represent that *Cd36* may play a role in the migration and invasion of Mel270 uveal melanoma cells.

3.3 *In vivo* Experiments to Determine the Role of CD36 through Liver Metastasis Model

3.3.1 Generation of shRNA Stable Knockdown Cell Line with Tagged Mel270

siRNA mediated knockdown only results in a temporary knockdown of the target gene. However, as *in vivo* metastasis models require longer periods of time to allow for cells to reach distant organs, we produced a stable *Cd36* knockdown Mel270 *tagged* cell line using shRNA. Puromycin-resistant lentiviral control shRNA vector (pLKO) was used to generate a non-target (NT) *Mel270 tagged* cell line as a control, and two different shRNA sequences targeting CD36 were used to generate stable *Cd36* knockdown *Mel270 tagged* cell lines (for a brief schematic diagram of the protocol, please refer to Figure 7A). Stable knockdown of *Cd36* was confirmed through flow cytometry and western blot analysis where we verified that efficient silencing was achieved by one of the two CD36 shRNA constructs (Figure 7B).

3.3.2 Mouse Model of Uveal Melanoma Liver Metastasis

For us to next unravel the role of CD36 in uveal melanoma liver metastasis, we decided to perform splenic injections on NOD CRISPR Prkdc Il2r Gamma (NCG) male mice with the Mel270 cell lines. Splenic injection of tumor cells is a common method to induce liver metastasis

by injecting cancer cells into the spleen leading the cells to travel first through the splenic vein and into the portal vein to reach the liver. Prior to injecting the nontarget and stable *Cd36* knockdown cells, we first created a pilot cohort to see if metastasis to the liver can be achieved at all through the splenic injection of Mel270 tagged uveal melanoma tumor cells, as well as to determine the time point at which lesions on the surface of the livers can be detected but not overcrowded. After injection, approximate tumor burden was determined using *in vivo* imaging system (IVIS) detecting the luminescence emitted following intraperitoneal injection (IP) of D-luciferin. A kinetic curve was generated enabling us to determine the imaging timepoint to be 10 minutes post-injection with D-luciferin at which peak intensity will be achieved. All mice were imaged weekly until the first humane euthanization of mouse #116 at day 10 post-injection with the IVIS signal of 9.57×10^8 photons/s, but no surface tumor lesions on the liver, spleen, nor the lungs were visible (Figure 7D). However, IVIS imaging showed infiltration of tumor cells in the liver, residual tumor cells in the spleen from the injection (Figure 7D). The presence of Mel270 tagged uveal melanoma cell micrometastases in the liver were confirmed using human nucleolin immunohistochemistry (IHC) staining of liver sections, where only the human Mel270 tagged uveal melanoma cells stained positive for nucleolin in the mouse tissue (Figure 7D). On day 32 post tumor-cell injection, mice #118 and #120 showed 1.03×10^{11} photons/s and 2.77×10^{10} photons/s respectively on IVIS, and both animals were sacrificed with their liver, lungs, and spleen isolated. *Ex vivo* imaging of the liver showed that most of the tumor cells were residing in the liver than in the spleen or the lungs (Figure 7D). Tumor lesions on the surface of the liver and the spleen were visible with the naked eye at 32 days post tumor cell injection.

Next, to translate our *in vitro* studies where we revealed the significant effect of CD36 knockdown on migration and invasion (Figures 6A, 6B), *in vivo*, we injected 1.00×10^6 control

(shCTL) Mel270 tagged and stable *Cd36* knockdown (shCD36 knockdown) Mel270 tagged cells into the spleen of NCG mice. Based on the kinetic curve, optimal imaging time was calculated to be 9 minutes post-injection with D-luciferin for both control and knockdown conditions. Based on the results from the pilot cohort (Figure 7D), an *in vivo* experiment was designed (Figure 7C) and at day 24 post-injection of cells, the control group had an approximate average signal of 3.53×10^9 photons/s and the *Cd36* knockdown group had the approximate average signal of 1.81×10^{10} photons/s. Again, the liver, the lungs, and the spleen were extracted for *ex vivo* imaging that confirmed all the detected signal in the mice came predominantly from the liver, followed by the spleen (Figure 7E). Despite having higher luminescence signal emitted from the shCD36 knockdown group compared to the control group, we made the observation that livers of the mice in the shCD36 knockdown group had less liver surface lesions visible with the naked eye compared to that of the control group (Figure 7F), but this remains to be quantified. Based on this observation, work is ongoing to confirm the liver metastasis burden with human nucleolin immunohistochemistry staining on paraffin embedded sections of each liver from the study cohort.

DISCUSSIONS

Uveal melanoma is a complicated cancer type with patients showing poor prognosis upon diagnosis with metastasis (Lane et al., 2018). Despite treatment with enucleation, plaque brachytherapy, radiotherapy, and targeted therapy, progression to metastasis is seen in approximately 50% of the patient population. As of now, how metastases arise and why patients remain unresponsive to available therapy in uveal melanoma remains largely elusive. However, past literatures highlights the high levels of heterogeneity observed in uveal melanomas which has been further reported to be associated with tumor progression (de Lange et al., 2021; Diaz-Cano, 2012; Lin et al., 2021; Stålhammar & Grossniklaus, 2021). Heterogeneity can result from varying stages of de-differentiation in cells leading to a variety of “reversible” cell states known as phenotype plasticity. These different cell states have been studied in other heterogeneous cancer types such as cutaneous melanoma and different markers have been discovered denoting of a specific cell state. Therefore, in my thesis project, I designed a novel multiparameter flow-based assay to detect the expression of seven different cell surface markers, including AXL, CD36, CD166, MelanA, NGFR, GFRA2, and GP100, which we postulate are associated with uveal melanoma cell states in the context of metastasis and therapy resistance.

4.1 Future Use of the UMarkit Panel

The results from the screening of 11 different uveal melanoma cell lines supported prior literature in that we were able to confirm heterogeneity across and within different cell lines. There was a wide range in the total percentage of cells that were screened positive for any given specific marker of interest, as well as the variability in specific markers that were present in each of the different cell lines tested (Figure 3B). The expression of one cell surface marker known as

CD36 caught our attention due to its wide range in positive cell population across the uveal melanoma cell lines. Using western blot analysis for CD36, I was able to verify the accuracy of my flow cytometry assay as a method of detecting the specific uveal melanoma cell lines with their respective cell populations that were negative and positive for CD36 expression (Figure 4A, Figure 4B). CD36 was an excellent candidate for further interrogation, whereby we can study its role in uveal melanoma progression upon depletion or over-expression of *Cd36*. The candidacy of this receptor for study was further supported with the ongoing pre-clinical trials and clinical trials against CD36 (Table 1) (Wang & Li, 2019). This is a very important factor as ultimately; we hope to be able to translate our results and the screening tool into clinical practice.

Another interesting finding was that the expression of AXL and CD36 seemed to be inversely correlated. For example, in the uveal melanoma cell line H79 we detected a high number of AXL positive cells and a low number of cells positive for CD36. While in OMM2.5 and UM001 uveal melanoma cell lines there was a low percentage of AXL positive cells, whereas most of the cells were positive for CD36. It would be very interesting to see if there is any crosstalk between AXL and CD36 expression, such that the expression of one receptor may result in the repression of the other. Currently, work is ongoing in the lab on interrogating the pro-oncogenic role of *Axl* and with the results that are obtained, we will be able to further evaluate the relationship between AXL and CD36 on their involvement as cell state markers in relation to metastasis development. Moving forward, how the results from screening of the uveal melanoma cell lines using the UMarkit panel should be interpreted would need further investigation such as whether co-positivity amongst markers give a greater insight into cellular phenotypes (i.e., metastasis, therapy resistance). However, it is with no doubt that the results from this project provided more information on potential druggable targets for uveal melanoma

in which most appear to play a role in metastasis according to past literatures. With the new panel that we have developed, we are now able to use this tool to gather a more detailed database on uveal melanoma depending on the presence or absence of the marker of interest and at what levels of cells are positive which we hope will one day contribute to developing a standardized and an accessible prognostic and diagnostic tool in the clinics.

4.2 CD36 and Post-translational Modifications

As previously mentioned, we confirmed the flow cytometry data for the percentage of CD36 expressing cells with western blot analysis for CD36 (Figure 4B). The bands that appeared were largely detected just below the 75 kDa marker, but it was noted that in some cell lines the bands for CD36 appeared to have a slightly lower apparent molecular weight (Figure 4B). We propose that the difference in the migration of the CD36 protein is associated with its differential post-translation modifications in some cell lines versus others. CD36 has a long extracellular domain (Figure 2) with 10 different glycosylation sites which has been known to affect the apparent molecular weight of the receptor (Tao et al., 1996). Aside from glycosylation, CD36 can also be ubiquitylated, phosphorylated, acetylated, palmitoylated, and can also undergo O-GlcNAcylation (R. Yang et al., 2022). Several of these post-translational modifications such as ubiquitylation and phosphorylation have been reported to modulate CD36 trafficking to the cell surface rather than residing at the golgi apparatus, the mitochondria, or the endoplasmic reticulum as previously mentioned in section *1.4.1 CD36 in Cells and Various Roles* (R. Yang et al., 2022). Interestingly, the apparent molecular weights at which the CD36 bands appears at seem to correlate with the invasion capacity of the uveal melanoma cell lines. While performing invasion assays with additional cell lines, I observed that 92.1 and OMM2.5, with similar CD36

molecular weight detected (Supplementary Figure 3E), did not invade readily in the Matrigel coated trans-well assay. On the other hand, Mel270 cells, wherein the CD36 band was observed at a lower molecular weight than that of 92.1 and OMM2.5, invaded very well through the Matrigel coated trans-wells (Figure 4B and Supplementary Figure 3E). I indeed confirmed that the band I detected by western blot was CD36 in Mel270 and 92.1 cells, since knockdown of CD36 using siRNA or shRNA resulted in a loss of CD36 expression (Figures 5B, 7B and Supplementary Figure 3D). Along with these observations and with the knowledge that post-translational modifications also affect the binding stability of its ligands such as fatty acids associated with driving cancer progression, events of post-translational modifications appear to be an important factor when studying CD36 in tumor biology (Luo et al., 2021; Wang & Li, 2019). Future work in the lab will involve detecting, and inhibiting, these post-translational modifications on CD36, such as phosphorylation and glycosylation, to unravel their impact on the known roles of *Cd36*. We expect to reference from past literatures where they report phosphorylation of CD36 can be detected by performing immunoprecipitation or western blot with phospho-specific antibodies against the phosphorylation site of the CD36 extracellular domain threonine 92 (Thr92) (Chu & Silverstein, 2012; Ho et al., 2005). Similarly for CD36 glycosylation, past literatures use mass spectrometry or western blot analysis against CD36 antibody where they identify a CD36 band around 50kDa to be non-glycosylated versus the band appearing around 75kDa to be the glycosylated CD36 (Daquinag et al., 2021; Hoosdally et al., 2009). It will be interesting to see if blocking post translational modifications such as phosphorylation or glycosylation of CD36 by inhibiting enzymes that catalyze such reactions would be sufficient to restrict any metastasis related activities portrayed by CD36. Notably, Thr92 is phosphorylated by protein kinase C (PKC) which has been targeted in uveal melanoma

as a therapy option without success. Researchers have suggested there to be escape mechanisms associated with PKC inhibitors showing very low levels of response and effect in patients (Lietman & McKean, 2022; Park et al., 2022).

4.3 Animal Models of Uveal Melanoma

Currently there are no immunocompetent mouse models available to study uveal melanoma, thus we used the immunodeficient, NCG mouse model for our *in vivo* experiments. One limitation of this *in vivo* work with xenografts in NCG mice, is that it makes it difficult for us to investigate immune cell infiltration at the site of primary tumors or throughout the development of distant metastases. This can be a major drawback to our experiments when we study CD36 in relation to cancer as this well-known scavenger receptor is also expressed on macrophages. With our NCG mouse model, any results that we obtain must consider for the absence of functional T cells, B cells, and NK cells as well as for the reduced levels/function of macrophages and dendritic cells. Studies have demonstrated the relationship between CD36, macrophages, and liver metastasis where they describe there to be liver metastasis-associated macrophages in which higher levels of CD36 expression is observed and thereby, higher lipid metabolism is observed from these macrophages as well (P. Yang et al., 2022). With uveal melanoma patients being highly susceptible to developing liver metastasis, such shortcomings in animal models that serve to bridge between the lab and the clinic will lead to delays in providing new and effective treatment methods.

Despite the need to consider for the roles of immune cells as previously described, there are limited mouse models available to study the complete tumor microenvironment of uveal melanoma. Immunocompetent mouse models for uveal melanoma include the syngeneic

cutaneous melanoma mouse model where cutaneous melanoma cells from mice are injected into immunocompetent mice as only the cells from the same genetic background as the host can be accepted (Richards et al., 2020). However, the known mutational differences between cutaneous melanoma and uveal melanoma tell us that this model will not provide accurate representations. Another immunocompetent mouse model available to date is by genetically engineering uveal melanoma primary tumors by inducing *GNAQ* and *GNA11* mutations as well as sometimes introducing additional deletion of the *BAP1* gene (Richards et al., 2020). Engineering these transgenic mouse models are very time consuming with the high probability of not being able to achieve the primary tumor itself (Richards et al., 2020).

Where genetically engineered mouse models may provide information on the role of a specific gene in uveal melanoma, patient derived xenografts (PDX) may be a great option when exploring the general progression of uveal melanoma (Liu et al., 2023). PDX models are achieved by extracting tumor tissues from patients and implanting into study models such as mice (Abdolahi et al., 2022; Liu et al., 2023). PDX are available for uveal melanoma to represent the human disease which includes immunodeficient mouse models as well as zebrafish model. However, a major drawback to PDX is that only immunocompromised models are available which eliminates the engagement of immune cells during uveal melanoma progression.

Nonetheless, the information that can be obtained from immunocompromised mouse models are valuable. In this thesis, we can understand the role of CD36 in uveal melanoma metastasis development independent from any interventions that may result from the immune cells. By injecting stable control shRNA and *Cd36* shRNA knockdown Mel270 tagged cells via splenic injection, we were able to observe the effect of loss of *Cd36* specifically in tumor cells in mediating liver metastasis. One limitation of this *in vivo* study was that only 1 of the 2 shRNA

vectors we used to generate *Cd36* knockdown Mel270 tagged cells showed efficient knockdown (Figure 7B). Therefore, as there was no second shRNA mediated *Cd36* knockdown cells to verify the results we have obtained, results need to be interpreted with the consideration that validation is still required. However, works are ongoing in the lab with another *Cd36* shRNA vector to produce a second knockdown model in Mel270 tagged cell line to allow for this verification. Finally, upon generation of a future immunocompetent mouse model for uveal melanoma, the same experiment with NCG mice could be carried out with control cohort and *Cd36* knockdown cohort with liver metastasis achieved through splenic injections. If any differences in liver metastasis burden have changed compared to our current NCG mice experiment, amongst many possibilities, one area to explore may be the CD36 expressed on macrophages that are specifically associated with liver metastasis (P. Yang et al., 2022).

Another field of focus that immunocompetent mouse models for uveal melanoma can fulfill is to test the efficacy of immunotherapy. Although immunotherapies such as the immune checkpoint inhibitors targeting CTLA-4 and PD-1 have been approved for use for uveal melanoma patients, the response rate was just a mere 10% and 7% for CTLA-4 and PD-1, respectively (Bol et al., 2019). In fact, single cell RNA sequencing performed on uveal melanoma patient samples have revealed that compared to CTLA-4 or PD-1, LAG3 was more highly expressed (Durante et al., 2020). Another study by the same group has confirmed this and have added on that CD8⁺ T cells express more of the LAG3 receptor than CTLA-4 or PD-1 thereby suggesting the use of relatlimab may be more effective than anti-PD-1 or anti-CTLA-4 therapy alone (Lutzky et al., 2020). In addition, the newly approved drug called Tebentafusp as a form of BITE therapy is only applicable to patients with a specific HLA antigen which only accounts for approximately half of the Caucasian, non-Hispanic population (making up 98% of

all the uveal melanoma cases) (B. E. Damato et al., 2019; C. L. Shields et al., 2015). With mouse models that have functional T cells, B cells, macrophages and NK cells, it gives us the opportunity to identify if the response to immune targeted therapies could be augmented by combining it with a drug targeting CD36 for example. This aspect will be critical as any anti-cancer drugs developed against CD36 function will also affect the capacity at which immune cells expressing CD36 perform in the tumor microenvironment. Though the effects will vary depending on their reliance on CD36, this also appears to be a major area to consider when treating uveal melanoma patients as a study has already revealed the anti-tumor effect of CD36 depletion in CD8⁺ T cells as an example (Ma et al., 2021).

4.4 Quantifying Liver Metastasis

After injection with Mel270 tagged (luc-tdTomato) cells, with the use of IVIS imaging we detected luminescence signals from live mice. This gave us the approximate value of tumour cell burden in each mouse. However as noted in the *Results* section, though the *Cd36* knockdown cohort had greater signal detected than the control cohort, we saw that the luminescence signals detected by the imaging machine did not provide a completely accurate representation of the tumor burden visible on the surface of the liver upon necropsy (Figures 7E, 7F). We saw that despite higher luminescence signal, with the naked eye, the *Cd36* KD cohort appeared to have a “cleaner” liver surface compared to that of the control livers (Figure 7F). However, these observations need to be confirmed using traditional methods such as immunohistochemistry to robustly quantify liver metastasis allowing us to compare metastasis burden between the experimental conditions. Another field to explore from the data that I have acquired is to perhaps focus on the relationship between CD36 and colonization and subsequent outgrowth of uveal

melanoma cells at distant organs. CD36 positive cells are capable of initiating metastasis compared to cells with *Cd36* depletion (Zhuo Li & Kang, 2017). And with the splenic injection directing the cells from the spleen into the lungs rather than travelling from the primary tumor, we could investigate if the capacity of the cells to colonize at a secondary organ differs with *Cd36* knockdown. To further study colonization potential of uveal melanoma cells at distant organs upon *Cd36* knockdown, we can introduce another metastasis model of tail vein injection to investigate how much lung metastasis can be observed. The IVIS machine allows us to keep track of where the cells are and if successful splenic injection has been performed, however, from the results that we have obtained, it is suggestive that greater signal may not necessarily be indicative of more lesions (Figure 7F). Therefore, not only will it be important to understand the routes of metastasis to the liver in uveal melanoma as explained in section *1.2.1 Disease Epidemiology*, but it may be important to consider the extent as to how much the cells are able to not only travel to distant sites but to anchor and colonize.

CONCLUSION

In conclusion, uveal melanoma is a fatal cancer type where approximately half of the patients progress to metastasis and upon diagnosis with metastasis, it remains a challenge for patients to stay cancer-free despite available treatment options. My project has characterized 11 different uveal melanoma cell lines by developing a novel FACS-based panel consisting of several markers associated with metastasis and therapy resistance along with their role as a marker for a specific cell state. These cell lines had their own unique signature number of cells expressing a given marker from the panel. The information that we have gathered not only emphasizes the heterogeneity of uveal melanoma tumors as reported in literature, but also adds another layer of information with CD36 and its role in uveal melanoma specifically in the context of liver metastasis. High expression of this scavenger receptor has been associated with negative patient survival, increased metastasis risk, and increased tumor burden in other types of cancers. However, its roles in uveal melanoma besides driving vascular mimicry is yet to be explored in detail. Therefore, we performed a siRNA-mediated transient knockdown of *Cd36* and investigated whether this intervention had any effect on uveal melanoma cells' ability to migrate and invade *in vitro*. We were able to confirm that upon depletion of *Cd36*, the uveal melanoma cells' ability to migrate and invade was significantly repressed compared to the control condition. And from our western blot analysis for CD36 expression in uveal melanoma cell lines and invasion assay with 92.1 and OMM2.5 cell lines, we propose that there may be potential mechanisms to metastasis regulation by CD36 through its post-translational modifications such as glycosylation and phosphorylation.

To observe the effect of *Cd36* depletion in live animals, we generated an shRNA mediated Mel270 luc-tdTomato cell line. Interesting observation was made in that despite having

similar signal intensity detected by IVIS, shCD36 knockdown cohort mice appeared to have less surface lesions on the liver. To validate this observation, work is currently ongoing in the lab to complete human nucleolin IHC staining on paraffin embedded liver samples. Pilot study where mice were injected with Mel270 luc-tdTomato cells also showed lower levels of CD36 in tumors than in the surrounding liver cells. This result can be partially supported with past literatures reporting that liver cells express more CD36 through the rewiring of lipid metabolism during cancer progression. However, as there is a gap in knowledge looking at the relationship between CD36 expression in liver cells and CD36 expression in tumor cells, this can be an interesting avenue to explore.

This thesis along with many other published literatures highlight the crucial need for the advancement in understanding metastasis development in uveal melanoma patients. From the results that we have obtained, we propose CD36 as a promising study candidate especially so with the ongoing preclinical and clinical trials for drugs against this receptor (Table 1).

REFERENCES

- Abdolahi, S., Ghazvinian, Z., Muhammadnejad, S., Saleh, M., Asadzadeh Aghdaei, H., & Baghaei, K. (2022). Patient-derived xenograft (PDX) models, applications and challenges in cancer research. *Journal of Translational Medicine*, *20*(1), 206.
<https://doi.org/10.1186/s12967-022-03405-8>
- Abu-Thuraia, A., Goyette, M.-A., Boulais, J., Delliaux, C., Apcher, C., Schott, C., Chidiac, R., Bagci, H., Thibault, M.-P., Davidson, D., Ferron, M., Veillette, A., Daly, R. J., Gingras, A.-C., Gratton, J.-P., & Côté, J.-F. (2020). AXL confers cell migration and invasion by hijacking a PEAK1-regulated focal adhesion protein network. *Nature Communications*, *11*(1), 3586. <https://doi.org/10.1038/s41467-020-17415-x>
- Akbani, R., Akdemir, K. C., Aksoy, B. A., Albert, M., Ally, A., Amin, S. B., Arachchi, H., Arora, A., Auman, J. T., Ayala, B., Baboud, J., Balasundaram, M., Balu, S., Barnabas, N., Bartlett, J., Bartlett, P., Bastian, B. C., Baylin, S. B., Behera, M., ... Zou, L. (2015). Genomic Classification of Cutaneous Melanoma. *Cell*, *161*(7), 1681–1696.
<https://doi.org/10.1016/j.cell.2015.05.044>
- All-Ericsson, C., Girnita, L., Seregard, S., Bartolazzi, A., Jager, M. J., & Larsson, O. (2002). Insulin-like growth factor-1 receptor in uveal melanoma: a predictor for metastatic disease and a potential therapeutic target. *Investigative Ophthalmology & Visual Science*, *43*(1), 1–8.
- Arisi, M., Zane, C., Caravello, S., Rovati, C., Zanca, A., Venturini, M., & Calzavara-Pinton, P. (2018). Sun Exposure and Melanoma, Certainties and Weaknesses of the Present Knowledge. *Frontiers in Medicine*, *5*. <https://doi.org/10.3389/fmed.2018.00235>
- Armesilla, A. L., & Vega, M. A. (1994). Structural organization of the gene for human CD36

- glycoprotein. *The Journal of Biological Chemistry*, 269(29), 18985–18991.
- Asch, A. S., Liu, I., Briccetti, F. M., Barnwell, J. W., Kwakye-Berko, F., Dokun, A., Goldberger, J., & Pernambuco, M. (1993). Analysis of CD36 Binding Domains: Ligand Specificity Controlled by Dephosphorylation of an Ectodomain. *Science*, 262(5138), 1436–1440.
<https://doi.org/10.1126/science.7504322>
- Axelrod, H., & Pienta, K. J. (2014). Axl as a mediator of cellular growth and survival. *Oncotarget*, 5(19), 8818–8852. <https://doi.org/10.18632/oncotarget.2422>
- Bande Rodríguez, M. F., Fernandez Marta, B., Lago Baameiro, N., Santiago-Varela, M., Silva-Rodríguez, P., Blanco-Teijeiro, M. J., Pardo Perez, M., & Piñeiro Ces, A. (2020). Blood Biomarkers of Uveal Melanoma: Current Perspectives. *Clinical Ophthalmology*, Volume 14, 157–169. <https://doi.org/10.2147/OPHTH.S199064>
- Bao, Y., Wang, L., Xu, Y., Yang, Y., Wang, L., Si, S., Cho, S., & Hong, B. (2012). Salvianolic acid B inhibits macrophage uptake of modified low density lipoprotein (mLDL) in a scavenger receptor CD36-dependent manner. *Atherosclerosis*, 223(1), 152–159.
<https://doi.org/10.1016/j.atherosclerosis.2012.05.006>
- Bashir, N., Ishfaq, M., Mazhar, K., Khan, J. S., & Shahid, R. (2022). Upregulation of CD271 transcriptome in breast cancer promotes cell survival via NFκB pathway. *Molecular Biology Reports*, 49(1), 487–495. <https://doi.org/10.1007/s11033-021-06900-1>
- Benboubker, V., Boivin, F., Dalle, S., & Caramel, J. (2022). Cancer Cell Phenotype Plasticity as a Driver of Immune Escape in Melanoma. *Frontiers in Immunology*, 13.
<https://doi.org/10.3389/fimmu.2022.873116>
- Berset, M., Cerottini, J.-P., Guggisberg, D., Romero, P., Burri, F., Rimoldi, D., & Panizzon, R. G. (2001). Expression of melan-a/MART-1 antigen as a prognostic factor in primary

- cutaneous melanoma. *International Journal of Cancer*, 95(1), 73–77.
[https://doi.org/10.1002/1097-0215\(20010120\)95:1<73::AID-IJC1013>3.0.CO;2-S](https://doi.org/10.1002/1097-0215(20010120)95:1<73::AID-IJC1013>3.0.CO;2-S)
- Bhatia, S., Wang, P., Toh, A., & Thompson, E. W. (2020). New Insights Into the Role of Phenotypic Plasticity and EMT in Driving Cancer Progression. *Frontiers in Molecular Biosciences*, 7. <https://doi.org/10.3389/fmolb.2020.00071>
- Bi, M., Zhang, Z., Jiang, Y.-Z., Xue, P., Wang, H., Lai, Z., Fu, X., De Angelis, C., Gong, Y., Gao, Z., Ruan, J., Jin, V. X., Marangoni, E., Montaudon, E., Glass, C. K., Li, W., Huang, T. H.-M., Shao, Z.-M., Schiff, R., ... Liu, Z. (2020). Enhancer reprogramming driven by high-order assemblies of transcription factors promotes phenotypic plasticity and breast cancer endocrine resistance. *Nature Cell Biology*, 22(6), 701–715. <https://doi.org/10.1038/s41556-020-0514-z>
- Boiko, A. D., Razorenova, O. V., van de Rijn, M., Swetter, S. M., Johnson, D. L., Ly, D. P., Butler, P. D., Yang, G. P., Joshua, B., Kaplan, M. J., Longaker, M. T., & Weissman, I. L. (2010). Human melanoma-initiating cells express neural crest nerve growth factor receptor CD271. *Nature*, 466(7302), 133–137. <https://doi.org/10.1038/nature09161>
- Bol, Ellebaek, Hoejberg, Bagger, Larsen, Klausen, Køhler, Schmidt, Bastholt, Kiilgaard, Donia, & Svane. (2019). Real-World Impact of Immune Checkpoint Inhibitors in Metastatic Uveal Melanoma. *Cancers*, 11(10), 1489. <https://doi.org/10.3390/cancers11101489>
- Brewington, B. Y., Shao, Y. F., Davidorf, F. H., & Cebulla, C. M. (2018). Brachytherapy for patients with uveal melanoma: historical perspectives and future treatment directions. *Clinical Ophthalmology, Volume 12*, 925–934. <https://doi.org/10.2147/OPHTH.S129645>
- Brouwenstijn, N., Slager, E., Bakker, A., Schreurs, M., Van der Spek, C., Adema, G., Schrier, P., & Figdor, C. (1997). Transcription of the gene encoding melanoma-associated antigen

gp100 in tissues and cell lines other than those of the melanocytic lineage. *British Journal of Cancer*, 76(12), 1562–1566. <https://doi.org/10.1038/bjc.1997.597>

Bruno, F., Abondio, P., Montesanto, A., Luiselli, D., Bruni, A. C., & Maletta, R. (2023). The Nerve Growth Factor Receptor (NGFR/p75NTR): A Major Player in Alzheimer's Disease. *International Journal of Molecular Sciences*, 24(4), 3200. <https://doi.org/10.3390/ijms24043200>

Busam, K. J., Chen, Y.-T., Old, L. J., Stockert, E., Iversen, K., Coplan, K. A., Rosai, J., Barnhill, R. L., & Jungbluth, A. A. (1998). Expression of Melan-A (MART1) in Benign Melanocytic Nevi and Primary Cutaneous Malignant Melanoma. *The American Journal of Surgical Pathology*, 22(8), 976–982. <https://doi.org/10.1097/00000478-199808000-00007>

Bustamante, P., Piquet, L., Landreville, S., & Burnier, J. V. (2021). Uveal melanoma pathobiology: Metastasis to the liver. *Seminars in Cancer Biology*, 71, 65–85. <https://doi.org/10.1016/j.semcancer.2020.05.003>

Carvajal, R. D., Butler, M. O., Shoushtari, A. N., Hassel, J. C., Ikeguchi, A., Hernandez-Aya, L., Nathan, P., Hamid, O., Piulats, J. M., Rioth, M., Johnson, D. B., Luke, J. J., Espinosa, E., Leyvraz, S., Collins, L., Goodall, H. M., Ranade, K., Holland, C., Abdullah, S. E., ... Sato, T. (2022). Clinical and molecular response to tebentafusp in previously treated patients with metastatic uveal melanoma: a phase 2 trial. *Nature Medicine*, 28(11), 2364–2373. <https://doi.org/10.1038/s41591-022-02015-7>

Carvajal, R. D., Piperno-Neumann, S., Kapiteijn, E., Chapman, P. B., Frank, S., Joshua, A. M., Piulats, J. M., Wolter, P., Cocquyt, V., Chmielowski, B., Evans, T. R. J., Gastaud, L., Linette, G., Berking, C., Schachter, J., Rodrigues, M. J., Shoushtari, A. N., Clemett, D., Ghiorghiu, D., ... Nathan, P. (2018). Selumetinib in Combination With Dacarbazine in

Patients With Metastatic Uveal Melanoma: A Phase III, Multicenter, Randomized Trial (SUMIT). *Journal of Clinical Oncology*, 36(12), 1232–1239.

<https://doi.org/10.1200/JCO.2017.74.1090>

Carvajal, R. D., Sosman, J. A., Quevedo, J. F., Milhem, M. M., Joshua, A. M., Kudchadkar, R.

R., Linette, G. P., Gajewski, T. F., Lutzky, J., Lawson, D. H., Lao, C. D., Flynn, P. J.,

Albertini, M. R., Sato, T., Lewis, K., Doyle, A., Ancell, K., Panageas, K. S., Bluth, M., ...

Schwartz, G. K. (2014). Effect of Selumetinib vs Chemotherapy on Progression-Free Survival in Uveal Melanoma. *JAMA*, 311(23), 2397.

<https://doi.org/10.1001/jama.2014.6096>

Chappell, P. E., Garner, L. I., Yan, J., Metcalfe, C., Hatherley, D., Johnson, S., Robinson, C. V,

Lea, S. M., & Brown, M. H. (2015). Structures of CD6 and Its Ligand CD166 Give Insight into Their Interaction. *Structure*, 23(8), 1426–1436.

<https://doi.org/10.1016/j.str.2015.05.019>

Chen, H., Huang, J., Chen, C., Jiang, Y., Feng, X., Liao, Y., & Yang, Z. (2021). NGFR Increases

the Chemosensitivity of Colorectal Cancer Cells by Enhancing the Apoptotic and

Autophagic Effects of 5-fluorouracil via the Activation of S100A9. *Frontiers in Oncology*,

11. <https://doi.org/10.3389/fonc.2021.652081>

Chen, Y., Zhang, J., Cui, W., & Silverstein, R. L. (2022). CD36, a signaling receptor and fatty

acid transporter that regulates immune cell metabolism and fate. *Journal of Experimental*

Medicine, 219(6). <https://doi.org/10.1084/jem.20211314>

Chu, L.-Y., & Silverstein, R. L. (2012). CD36 Ectodomain Phosphorylation Blocks

Thrombospondin-1 Binding. *Arteriosclerosis, Thrombosis, and Vascular Biology*, 32(3),

760–767. <https://doi.org/10.1161/ATVBAHA.111.242511>

- Clemetson, K. J. (1997). *Blood glycoproteins**~~~~~This chapter is dedicated to Prof. R. U. Lemieux who played a major role in awakening a whole generation to the importance of carbohydrate structure in biology. (pp. 173–201). [https://doi.org/10.1016/S0167-7306\(08\)60622-5](https://doi.org/10.1016/S0167-7306(08)60622-5)
- Coulie, P. G., Brichard, V., Van Pel, A., Wölfel, T., Schneider, J., Traversari, C., Mattei, S., De Plaen, E., Lurquin, C., Szikora, J. P., Renauld, J. C., & Boon, T. (1994). A new gene coding for a differentiation antigen recognized by autologous cytolytic T lymphocytes on HLA-A2 melanomas. *Journal of Experimental Medicine*, *180*(1), 35–42. <https://doi.org/10.1084/jem.180.1.35>
- Czerwinska, P., Jaworska, A. M., Włodarczyk, N. A., & Mackiewicz, A. A. (2020). Melanoma Stem Cell-Like Phenotype and Significant Suppression of Immune Response within a Tumor Are Regulated by TRIM28 Protein. *Cancers*, *12*(10), 2998. <https://doi.org/10.3390/cancers12102998>
- Dagamajalu, S., Rex, D. A. B., Palollathil, A., Shetty, R., Bhat, G., Cheung, L. W. T., & Prasad, T. S. K. (2021). A pathway map of AXL receptor-mediated signaling network. *Journal of Cell Communication and Signaling*, *15*(1), 143–148. <https://doi.org/10.1007/s12079-020-00580-5>
- Damato, B. E., Dukes, J., Goodall, H., & Carvajal, R. D. (2019). Tebentafusp: T Cell Redirection for the Treatment of Metastatic Uveal Melanoma. *Cancers*, *11*(7), 971. <https://doi.org/10.3390/cancers11070971>
- Damato, B. (2010). Does ocular treatment of uveal melanoma influence survival? *British Journal of Cancer*, *103*(3), 285–290. <https://doi.org/10.1038/sj.bjc.6605765>
- Damato, Bertil, Hope-Stone, L., Cooper, B., Brown, S., Heimann, H., & Dunn, L. (2019).

- Patient-Reported Outcomes and Quality of Life after Treatment for Choroidal Melanoma. *Ocular Oncology and Pathology*, 5(6), 402–411. <https://doi.org/10.1159/000496927>
- Dana, H. (2016). CD166 as a Stem Cell Marker? A Potential Target for Therapy Colorectal Cancer? *Journal of Stem Cell Research & Therapeutics*, 1(6). <https://doi.org/10.15406/jsrt.2016.01.00041>
- Daquinag, A. C., Gao, Z., Fussell, C., Immaraj, L., Pasqualini, R., Arap, W., Akimzhanov, A. M., Febbraio, M., & Kolonin, M. G. (2021). Fatty acid mobilization from adipose tissue is mediated by CD36 posttranslational modifications and intracellular trafficking. *JCI Insight*, 6(17). <https://doi.org/10.1172/jci.insight.147057>
- Dawson, D. W., Pearce, S. F. A., Zhong, R., Silverstein, R. L., Frazier, W. A., & Bouck, N. P. (1997). CD36 Mediates the In Vitro Inhibitory Effects of Thrombospondin-1 on Endothelial Cells. *Journal of Cell Biology*, 138(3), 707–717. <https://doi.org/10.1083/jcb.138.3.707>
- de Lange, M. J., Nell, R. J., & van der Velden, P. A. (2021). Scientific and clinical implications of genetic and cellular heterogeneity in uveal melanoma. *Molecular Biomedicine*, 2(1), 25. <https://doi.org/10.1186/s43556-021-00048-x>
- De Mazière, A. M., Muehlethaler, K., Van Donselaar, E., Salvi, S., Davoust, J., Cerottini, J.-C., Lévy, F., Slot, J. W., & Rimoldi, D. (2002). The Melanocytic Protein Melan-A/MART-1 Has a Subcellular Localization Distinct from Typical Melanosomal Proteins. *Traffic*, 3(9), 678–693. <https://doi.org/10.1034/j.1600-0854.2002.30909.x>
- Decatur, C. L., Ong, E., Garg, N., Anbunathan, H., Bowcock, A. M., Field, M. G., & Harbour, J. W. (2016). Driver Mutations in Uveal Melanoma. *JAMA Ophthalmology*, 134(7), 728. <https://doi.org/10.1001/jamaophthalmol.2016.0903>
- Diaz-Cano, S. J. (2012). Tumor Heterogeneity: Mechanisms and Bases for a Reliable

- Application of Molecular Marker Design. *International Journal of Molecular Sciences*, 13(2), 1951–2011. <https://doi.org/10.3390/ijms13021951>
- Diener-West, M., Reynolds, S. M., Agugliaro, D. J., Caldwell, R., Cumming, K., Earle, J. D., Hawkins, B. S., Hayman, J. A., Jaiyesimi, I., Jampol, L. M., Kirkwood, J. M., Koh, W. J., Robertson, D. M., Shaw, J. M., Straatsma, B. R., & Thoma, J. (2005). Development of metastatic disease after enrollment in the COMS trials for treatment of choroidal melanoma: Collaborative Ocular Melanoma Study Group Report No. 26. *Archives of Ophthalmology*. <https://doi.org/10.1001/archopht.123.12.1639>
- Djirackor, L., Kalirai, H., Coupland, S. E., & Petrovski, G. (2019). CD166^{high} Uveal Melanoma Cells Represent a Subpopulation With Enhanced Migratory Capacity. *Investigative Ophthalmology & Visual Science*, 60(7), 2696. <https://doi.org/10.1167/iovs.18-26431>
- Doering, T. L., Pessin, M. S., Hoff, E. F., Hart, G. W., Raben, D. M., & Englund, P. T. (1993). Trypanosome metabolism of myristate, the fatty acid required for the variant surface glycoprotein membrane anchor. *The Journal of Biological Chemistry*, 268(13), 9215–9222.
- Dogrusöz, M., Brouwer, N. J., de Geus, S. J. R., Ly, L. V., Böhringer, S., van Duinen, S. G., Kroes, W. G. M., van der Velden, P. A., Haasnoot, G. W., Marinkovic, M., Luyten, G. P. M., Kivelä, T. T., & Jager, M. J. (2020). Prognostic Factors Five Years After Enucleation for Uveal Melanoma. *Investigative Ophthalmology & Visual Science*, 61(3), 31. <https://doi.org/10.1167/iovs.61.3.31>
- Donizy, P., Zietek, M., Halon, A., Leskiewicz, M., Kozyra, C., & Matkowski, R. (2015). Prognostic significance of ALCAM (CD166/MEMD) expression in cutaneous melanoma patients. *Diagnostic Pathology*, 10(1), 86. <https://doi.org/10.1186/s13000-015-0331-z>
- Du, W., Phinney, N. Z., Huang, H., Wang, Z., Westcott, J., Toombs, J. E., Zhang, Y., Beg, M. S.,

- Wilkie, T. M., Lorens, J. B., & Brekken, R. A. (2021). AXL Is a Key Factor for Cell Plasticity and Promotes Metastasis in Pancreatic Cancer. *Molecular Cancer Research*, *19*(8), 1412–1421. <https://doi.org/10.1158/1541-7786.MCR-20-0860>
- Durante, M. A., Rodriguez, D. A., Kurtenbach, S., Kuznetsov, J. N., Sanchez, M. I., Decatur, C. L., Snyder, H., Feun, L. G., Livingstone, A. S., & Harbour, J. W. (2020). Single-cell analysis reveals new evolutionary complexity in uveal melanoma. *Nature Communications*, *11*(1), 496. <https://doi.org/10.1038/s41467-019-14256-1>
- Ebbinghaus, S., Hussain, M., Tannir, N., Gordon, M., Desai, A. A., Knight, R. A., Humerickhouse, R. A., Qian, J., Gordon, G. B., & Figlin, R. (2007). Phase 2 Study of ABT-510 in Patients with Previously Untreated Advanced Renal Cell Carcinoma. *Clinical Cancer Research*, *13*(22), 6689–6695. <https://doi.org/10.1158/1078-0432.CCR-07-1477>
- Eibl-Lindner, K., Fürweger, C., Nentwich, M., Foerster, P., Wowra, B., Schaller, U., & Muacevic, A. (2016). Robotic radiosurgery for the treatment of medium and large uveal melanoma. *Melanoma Research*, *26*(1), 51–57. <https://doi.org/10.1097/CMR.0000000000000199>
- Ennen, M., Keime, C., Kobi, D., Mengus, G., Lipsker, D., Thibault-Carpentier, C., & Davidson, I. (2015). Single-cell gene expression signatures reveal melanoma cell heterogeneity. *Oncogene*, *34*(25), 3251–3263. <https://doi.org/10.1038/onc.2014.262>
- Fan, X. (2011). Differential expression of Mart-1 in human uveal melanoma cells. *Molecular Medicine Reports*. <https://doi.org/10.3892/mmr.2011.504>
- Fang, D., Nguyen, T. K., Leishear, K., Finko, R., Kulp, A. N., Hotz, S., Van Belle, P. A., Xu, X., Elder, D. E., & Herlyn, M. (2005). A Tumorigenic Subpopulation with Stem Cell Properties in Melanomas. *Cancer Research*, *65*(20), 9328–9337. <https://doi.org/10.1158/0008->

5472.CAN-05-1343

- Febbraio, M., Hajjar, D. P., & Silverstein, R. L. (2001). CD36: a class B scavenger receptor involved in angiogenesis, atherosclerosis, inflammation, and lipid metabolism. *Journal of Clinical Investigation*, *108*(6), 785–791. <https://doi.org/10.1172/JCI14006>
- Feng, W. W., Wilkins, O., Bang, S., Ung, M., Li, J., An, J., del Genio, C., Canfield, K., DiRenzo, J., Wells, W., Gaur, A., Robey, R. B., Guo, J. Y., Powles, R. L., Sotiriou, C., Pusztai, L., Febbraio, M., Cheng, C., Kinlaw, W. B., & Kurokawa, M. (2019). CD36-Mediated Metabolic Rewiring of Breast Cancer Cells Promotes Resistance to HER2-Targeted Therapies. *Cell Reports*, *29*(11), 3405-3420.e5. <https://doi.org/10.1016/j.celrep.2019.11.008>
- Finger, P. T. (1997). Radiation therapy for choroidal melanoma. *Survey of Ophthalmology*, *42*(3), 215–232. [https://doi.org/10.1016/S0039-6257\(97\)00088-X](https://doi.org/10.1016/S0039-6257(97)00088-X)
- Folberg, R., Arbieva, Z., Moses, J., Hayee, A., Sandal, T., Kadkol, S., Lin, A. Y., Valyi-Nagy, K., Setty, S., Leach, L., Chévez-Barrios, P., Larsen, P., Majumdar, D., Pe'er, J., & Maniotis, A. J. (2006). Tumor Cell Plasticity in Uveal Melanoma. *The American Journal of Pathology*, *169*(4), 1376–1389. <https://doi.org/10.2353/ajpath.2006.060223>
- Fraser, I. P., Stuart, L., & Ezekowitz, R. A. B. (2004). TLR-independent pattern recognition receptors and anti-inflammatory mechanisms. *Journal of Endotoxin Research*, *10*(2), 120–124. <https://doi.org/10.1179/096805104225004013>
- Fry, M. V, Augsburger, J. J., Hall, J., & Corrêa, Z. M. (2018). Posterior uveal melanoma in adolescents and children: current perspectives. *Clinical Ophthalmology, Volume 12*, 2205–2212. <https://doi.org/10.2147/OPHTH.S142984>
- Fujiwara, K., Ohuchida, K., Sada, M., Horioka, K., Ulrich, C. D., Shindo, K., Ohtsuka, T., Takahata, S., Mizumoto, K., Oda, Y., & Tanaka, M. (2014). CD166/ALCAM Expression Is

- Characteristic of Tumorigenicity and Invasive and Migratory Activities of Pancreatic Cancer Cells. *PLoS ONE*, 9(9), e107247. <https://doi.org/10.1371/journal.pone.0107247>
- Gallenga, C. E., Franco, E., Adamo, G. G., Violanti, S. S., Tassinari, P., Tognon, M., & Perri, P. (2022). Genetic Basis and Molecular Mechanisms of Uveal Melanoma Metastasis: A Focus on Prognosis. *Frontiers in Oncology*, 12. <https://doi.org/10.3389/fonc.2022.828112>
- Gay, C. M., Balaji, K., & Byers, L. A. (2017). Giving AXL the axe: targeting AXL in human malignancy. *British Journal of Cancer*, 116(4), 415–423. <https://doi.org/10.1038/bjc.2016.428>
- Geloen, A., Helin, L., Geeraert, B., Malaud, E., Holvoet, P., & Marguerie, G. (2012). CD36 Inhibitors Reduce Postprandial Hypertriglyceridemia and Protect against Diabetic Dyslipidemia and Atherosclerosis. *PLoS ONE*, 7(5), e37633. <https://doi.org/10.1371/journal.pone.0037633>
- Girouard, S. D., & Murphy, G. F. (2011). Melanoma stem cells: not rare, but well done. *Laboratory Investigation*, 91(5), 647–664. <https://doi.org/10.1038/labinvest.2011.50>
- Gjerdrum, C., Tiron, C., Høiby, T., Stefansson, I., Haugen, H., Sandal, T., Collett, K., Li, S., McCormack, E., Gjertsen, B. T., Micklem, D. R., Akslen, L. A., Glackin, C., & Lorens, J. B. (2010). Axl is an essential epithelial-to-mesenchymal transition-induced regulator of breast cancer metastasis and patient survival. *Proceedings of the National Academy of Sciences*, 107(3), 1124–1129. <https://doi.org/10.1073/pnas.0909333107>
- Gragoudas, E. S. (2006). Proton Beam Irradiation of Uveal Melanomas: The First 30 Years The Weisenfeld Lecture. *Investigative Ophthalmology & Visual Science*, 47(11), 4666. <https://doi.org/10.1167/iovs.06-0659>
- Gragoudas, E. S., Egan, K. M., Seddon, J. M., Glynn, R. J., Walsh, S. M., Finn, S. M.,

- Munzenrider, J. E., & Spar, M. D. (1991). Survival of Patients with Metastases from Uveal Melanoma. *Ophthalmology*, 98(3). [https://doi.org/10.1016/S0161-6420\(91\)32285-1](https://doi.org/10.1016/S0161-6420(91)32285-1)
- Gu, J., Wang, D., Zhang, J., Zhu, Y., Li, Y., Chen, H., Shi, M., Wang, X., Shen, B., Deng, X., Zhan, Q., Wei, G., & Peng, C. (2016). GFR α 2 prompts cell growth and chemoresistance through down-regulating tumor suppressor gene PTEN via Mir-17-5p in pancreatic cancer. *Cancer Letters*, 380(2), 434–441. <https://doi.org/10.1016/j.canlet.2016.06.016>
- Gupta, P. B., Pastushenko, I., Skibinski, A., Blanpain, C., & Kuperwasser, C. (2019). Phenotypic Plasticity: Driver of Cancer Initiation, Progression, and Therapy Resistance. *Cell Stem Cell*, 24(1), 65–78. <https://doi.org/10.1016/j.stem.2018.11.011>
- Hale, J. S., Otvos, B., Sinyuk, M., Alvarado, A. G., Hitomi, M., Stoltz, K., Wu, Q., Flavahan, W., Levison, B., Johansen, M. L., Schmitt, D., Neltner, J. M., Huang, P., Ren, B., Sloan, A. E., Silverstein, R. L., Gladson, C. L., DiDonato, J. A., Brown, J. M., ... Lathia, J. D. (2014a). Cancer Stem Cell-Specific Scavenger Receptor CD36 Drives Glioblastoma Progression. *Stem Cells*, 32(7), 1746–1758. <https://doi.org/10.1002/stem.1716>
- Hale, J. S., Otvos, B., Sinyuk, M., Alvarado, A. G., Hitomi, M., Stoltz, K., Wu, Q., Flavahan, W., Levison, B., Johansen, M. L., Schmitt, D., Neltner, J. M., Huang, P., Ren, B., Sloan, A. E., Silverstein, R. L., Gladson, C. L., DiDonato, J. A., Brown, J. M., ... Lathia, J. D. (2014b). Cancer Stem Cell-Specific Scavenger Receptor CD36 Drives Glioblastoma Progression. *Stem Cells*, 32(7), 1746–1758. <https://doi.org/10.1002/stem.1716>
- Harbour, J. W., & Chen, R. (2013). The DecisionDx-UM Gene Expression Profile Test Provides Risk Stratification and Individualized Patient Care in Uveal Melanoma. *PLoS Currents*, APR 2013. <https://doi.org/10.1371/currents.eogt.af8ba80fc776c8f1ce8f5dc485d4a618>
- Heng, J. S., Perzia, B. M., Sinard, J. H., & Pointdujour-Lim, R. (2022). Local recurrence of uveal

- melanoma and concomitant brain metastases associated with an activating telomerase promoter mutation seven years after secondary enucleation. *American Journal of Ophthalmology Case Reports*, 27, 101607. <https://doi.org/10.1016/j.ajoc.2022.101607>
- Ho, M., Hoang, H. L., Lee, K. M., Liu, N., MacRae, T., Montes, L., Flatt, C. L., Yipp, B. G., Berger, B. J., Looareesuwan, S., & Robbins, S. M. (2005). Ectophosphorylation of CD36 Regulates Cytoadherence of *Plasmodium falciparum* to Microvascular Endothelium under Flow Conditions. *Infection and Immunity*, 73(12), 8179–8187. <https://doi.org/10.1128/IAI.73.12.8179-8187.2005>
- Hoefsmit, E. P., Rozeman, E. A., Van, T. M., Dimitriadis, P., Krijgsman, O., Conway, J. W., Pires da Silva, I., van der Wal, J. E., Ketelaars, S. L. C., Bresser, K., Broeks, A., Kerkhoven, R. M., Reeves, J. W., Warren, S., Kvistborg, P., Scolyer, R. A., Kapiteijn, E. W., Peeper, D. S., Long, G. V, ... Blank, C. U. (2020). Comprehensive analysis of cutaneous and uveal melanoma liver metastases. *Journal for ImmunoTherapy of Cancer*, 8(2), e001501. <https://doi.org/10.1136/jitc-2020-001501>
- Hooker, R. A., Chitteti, B. R., Egan, P. H., Cheng, Y. H., Himes, E. R., Meijome, T., Srour, E. F., Fuchs, R. K., & Kacena, M. A. (2015). Activated leukocyte cell adhesion molecule (ALCAM or CD166) modulates bone phenotype and hematopoiesis. *Journal of Musculoskeletal & Neuronal Interactions*, 15(1), 83–94.
- Hoosdally, S. J., Andress, E. J., Wooding, C., Martin, C. A., & Linton, K. J. (2009). The Human Scavenger Receptor CD36. *Journal of Biological Chemistry*, 284(24), 16277–16288. <https://doi.org/10.1074/jbc.M109.007849>
- Hu, D. N., Yu, G. P., McCormick, S. A., Schneider, S., & Finger, P. T. (2005). Population-based incidence of uveal melanoma in various races and ethnic groups. *American Journal of*

- Ophthalmology*, 140(4). <https://doi.org/10.1016/j.ajo.2005.05.034>
- Hua, P. G., Carlson, D. D., & R. Starr, P. B. J. (2022). Tebentafusp-tebn: A Novel Bispecific T-Cell Engager for Metastatic Uveal Melanoma. *Journal of the Advanced Practitioner in Oncology*, 13(7), 717–723. <https://doi.org/10.6004/jadpro.2022.13.7.8>
- Huang, F., Santinon, F., Flores González, R. E., & del Rincón, S. V. (2021). Melanoma Plasticity: Promoter of Metastasis and Resistance to Therapy. *Frontiers in Oncology*, 11. <https://doi.org/10.3389/fonc.2021.756001>
- Isacke, C. M., & Horton, M. A. (2000). CD36. In *The Adhesion Molecule FactsBook* (pp. 244–246). Elsevier. <https://doi.org/10.1016/B978-012356505-1/50084-8>
- Isenberg, J. S., Yu, C., & Roberts, D. D. (2008). Differential effects of ABT-510 and a CD36-binding peptide derived from the type 1 repeats of thrombospondin-1 on fatty acid uptake, nitric oxide signaling, and caspase activation in vascular cells. *Biochemical Pharmacology*, 75(4), 875–882. <https://doi.org/10.1016/j.bcp.2007.10.025>
- Ishida, H., Saba, R., Kokkinopoulos, I., Hashimoto, M., Yamaguchi, O., Nowotschin, S., Shiraishi, M., Ruchaya, P., Miller, D., Harmer, S., Poliandri, A., Kogaki, S., Sakata, Y., Dunkel, L., Tinker, A., Hadjantonakis, A.-K., Sawa, Y., Sasaki, H., Ozono, K., ... Yashiro, K. (2016). GFRA2 Identifies Cardiac Progenitors and Mediates Cardiomyocyte Differentiation in a RET-Independent Signaling Pathway. *Cell Reports*, 16(4), 1026–1038. <https://doi.org/10.1016/j.celrep.2016.06.050>
- Jager, M. J., Shields, C. L., Cebulla, C. M., Abdel-Rahman, M. H., Grossniklaus, H. E., Stern, M.-H., Carvajal, R. D., Belfort, R. N., Jia, R., Shields, J. A., & Damato, B. E. (2020). Uveal melanoma. *Nature Reviews Disease Primers*, 6(1), 24. <https://doi.org/10.1038/s41572-020-0158-0>

- Jannie, K. M., Stipp, C. S., & Weiner, J. A. (2012). ALCAM Regulates Motility, Invasiveness, and Adherens Junction Formation in Uveal Melanoma Cells. *PLoS ONE*, 7(6), e39330. <https://doi.org/10.1371/journal.pone.0039330>
- Jaywant, S. M., Osei, E. K., & Ladak, S. (2003). Stereotactic radiotherapy in the treatment of ocular melanoma: A noninvasive eye fixation aid and tracking system. *Journal of Applied Clinical Medical Physics*, 4(2), 156–161. <https://doi.org/10.1120/jacmp.v4i2.2531>
- Jenkins, R. W., & Fisher, D. E. (2021). Treatment of Advanced Melanoma in 2020 and Beyond. *Journal of Investigative Dermatology*, 141(1), 23–31. <https://doi.org/10.1016/j.jid.2020.03.943>
- Jia, D., Jolly, M. K., Kulkarni, P., & Levine, H. (2017). Phenotypic Plasticity and Cell Fate Decisions in Cancer: Insights from Dynamical Systems Theory. *Cancers*, 9(12), 70. <https://doi.org/10.3390/cancers9070070>
- Jiang, P., Purtskhvanidze, K., Kandzia, G., Neumann, D., Luetzen, U., Siebert, F.-A., Roider, J., & Dunst, J. (2020). 106Ruthenium eye plaque brachytherapy in the management of medium sized uveal melanoma. *Radiation Oncology*, 15(1), 183. <https://doi.org/10.1186/s13014-020-01621-4>
- Jing, S., Yu, Y., Fang, M., Hu, Z., Holst, P. L., Boone, T., Delaney, J., Schultz, H., Zhou, R., & Fox, G. M. (1997). GFR α -2 and GFR α -3 Are Two New Receptors for Ligands of the GDNF Family. *Journal of Biological Chemistry*, 272(52), 33111–33117. <https://doi.org/10.1074/jbc.272.52.33111>
- Joshi, P., Kooshki, M., Aldrich, W., Varghai, D., Zborowski, M., Singh, A. D., & Triozzi, P. L. (2016). Expression of natural killer cell regulatory microRNA by uveal melanoma cancer stem cells. *Clinical & Experimental Metastasis*, 33(8), 829–838.

<https://doi.org/10.1007/s10585-016-9815-9>

- Kahlert, C., Weber, H., Mogler, C., Bergmann, F., Schirmacher, P., Kenngott, H. G., Mattered, U., Mollberg, N., Rahbari, N. N., Hinz, U., Koch, M., Aigner, M., & Weitz, J. (2009). Increased expression of ALCAM/CD166 in pancreatic cancer is an independent prognostic marker for poor survival and early tumour relapse. *British Journal of Cancer*, *101*(3), 457–464. <https://doi.org/10.1038/sj.bjc.6605136>
- Kaliki, S., & Shields, C. L. (2017). Uveal melanoma: Relatively rare but deadly cancer. In *Eye (Basingstoke)* (Vol. 31, Issue 2). <https://doi.org/10.1038/eye.2016.275>
- Kar, N. S., Ashraf, M. Z., Valiyaveetil, M., & Podrez, E. A. (2008). Mapping and characterization of the binding site for specific oxidized phospholipids and oxidized low density lipoprotein of scavenger receptor CD36. *The Journal of Biological Chemistry*, *283*(13), 8765–8771. <https://doi.org/10.1074/jbc.M709195200>
- Karunakaran, U., Elumalai, S., Moon, J.-S., & Won, K.-C. (2021). CD36 Signal Transduction in Metabolic Diseases: Novel Insights and Therapeutic Targeting. *Cells*, *10*(7), 1833. <https://doi.org/10.3390/cells10071833>
- Kawakami, Y., & Rosenberg, S. A. (1997). Immunobiology of Human Melanoma Antigens MART-1 and gp100 and their Use for Immuno-Gene Therapy. *International Reviews of Immunology*, *14*(2–3), 173–192. <https://doi.org/10.3109/08830189709116851>
- Kels, B. D., Grzybowski, A., & Grant-Kels, J. M. (2015). Human ocular anatomy. *Clinics in Dermatology*, *33*(2). <https://doi.org/10.1016/j.clindermatol.2014.10.006>
- Kim, D. K., Ham, M. H., Lee, S. Y., Shin, M. J., Kim, Y. E., Song, P., Suh, D.-S., & Kim, J. H. (2020). CD166 promotes the cancer stem-like properties of primary epithelial ovarian cancer cells. *BMB Reports*, *53*(12), 622–627.

<https://doi.org/10.5483/BMBRep.2020.53.12.102>

- Kim, Y. J., Sheu, K. M., Tsoi, J., Abril-Rodriguez, G., Medina, E., Grasso, C. S., Torrejon, D. Y., Champhekar, A. S., Litchfield, K., Swanton, C., Speiser, D. E., Scumpia, P. O., Hoffmann, A., Graeber, T. G., Puig-Saus, C., & Ribas, A. (2021). Melanoma dedifferentiation induced by IFN- γ epigenetic remodeling in response to anti-PD-1 therapy. *Journal of Clinical Investigation*, *131*(12). <https://doi.org/10.1172/JCI145859>
- Kolandjian, N. A., Wei, C., Patel, S. P., Richard, J. L., Dett, T., Papadopoulos, N. E., & Bedikian, A. Y. (2013). Delayed Systemic Recurrence of Uveal Melanoma. *American Journal of Clinical Oncology*, *36*(5), 443–449. <https://doi.org/10.1097/COC.0b013e3182546a6b>
- Kong, D., Hughes, C. J., & Ford, H. L. (2020). Cellular Plasticity in Breast Cancer Progression and Therapy. *Frontiers in Molecular Biosciences*, *7*. <https://doi.org/10.3389/fmolb.2020.00072>
- Krantz, B. A., Dave, N., Komatsubara, K. M., Marr, B. P., & Carvajal, R. D. (2017). Uveal melanoma: epidemiology, etiology, and treatment of primary disease. *Clinical Ophthalmology*, *Volume 11*, 279–289. <https://doi.org/10.2147/OPHTH.S89591>
- Kuda, O., Pietka, T. A., Demianova, Z., Kudova, E., Cvacka, J., Kopecky, J., & Abumrad, N. A. (2013). Sulfo-N-succinimidyl Oleate (SSO) Inhibits Fatty Acid Uptake and Signaling for Intracellular Calcium via Binding CD36 Lysine 164. *Journal of Biological Chemistry*, *288*(22), 15547–15555. <https://doi.org/10.1074/jbc.M113.473298>
- Lane, A. M., Kim, I. K., & Gragoudas, E. S. (2018). Survival rates in patients after treatment for metastasis from uveal melanoma. *JAMA Ophthalmology*, *136*(9). <https://doi.org/10.1001/jamaophthalmol.2018.2466>

- Lehner, R., & Quiroga, A. D. (2016). Fatty Acid Handling in Mammalian Cells. In *Biochemistry of Lipids, Lipoproteins and Membranes* (pp. 149–184). Elsevier.
<https://doi.org/10.1016/B978-0-444-63438-2.00005-5>
- Li, Y, Ye, X., Tan, C., Hongo, J.-A., Zha, J., Liu, J., Kallop, D., Ludlam, M. J. C., & Pei, L. (2009). Axl as a potential therapeutic target in cancer: role of Axl in tumor growth, metastasis and angiogenesis. *Oncogene*, 28(39), 3442–3455.
<https://doi.org/10.1038/onc.2009.212>
- Li, Yongyun, Shi, J., Yang, J., Ge, S., Zhang, J., Jia, R., & Fan, X. (2020). Uveal melanoma: progress in molecular biology and therapeutics. *Therapeutic Advances in Medical Oncology*, 12, 175883592096585. <https://doi.org/10.1177/1758835920965852>
- Li, Zhuo, & Kang, Y. (2017). Lipid Metabolism Fuels Cancer’s Spread. *Cell Metabolism*, 25(2), 228–230. <https://doi.org/10.1016/j.cmet.2017.01.016>
- Li, Zuoqing, Xie, J., Fei, Y., Gao, P., Xie, Q., Gao, W., & Xu, Z. (2019). GDNF family receptor alpha 2 promotes neuroblastoma cell proliferation by interacting with PTEN. *Biochemical and Biophysical Research Communications*, 510(3), 339–344.
<https://doi.org/10.1016/j.bbrc.2018.12.169>
- Lietman, C. D., & McKean, M. (2022). Targeting GNAQ/11 through PKC inhibition in uveal melanoma. *Cancer Gene Therapy*, 29(12), 1809–1813. <https://doi.org/10.1038/s41417-022-00437-6>
- Lin, W., Beasley, A. B., Ardakani, N. M., Denisenko, E., Calapre, L., Jones, M., Wood, B. A., Warburton, L., Forrest, A. R. R., & Gray, E. S. (2021). Intra- and intertumoral heterogeneity of liver metastases in a patient with uveal melanoma revealed by single-cell RNA sequencing. *Molecular Case Studies*, 7(5), a006111. <https://doi.org/10.1101/mcs.a006111>

- Liu, Y., Wu, W., Cai, C., Zhang, H., Shen, H., & Han, Y. (2023). Patient-derived xenograft models in cancer therapy: technologies and applications. *Signal Transduction and Targeted Therapy*, 8(1), 160. <https://doi.org/10.1038/s41392-023-01419-2>
- Luiken, J. J. F. P., Chanda, D., Nabben, M., Neumann, D., & Glatz, J. F. C. (2016). Post-translational modifications of CD36 (SR-B2): Implications for regulation of myocellular fatty acid uptake. *Biochimica et Biophysica Acta (BBA) - Molecular Basis of Disease*, 1862(12), 2253–2258. <https://doi.org/10.1016/j.bbadis.2016.09.004>
- Luo, X., Zheng, E., Wei, L., Zeng, H., Qin, H., Zhang, X., Liao, M., Chen, L., Zhao, L., Ruan, X. Z., Yang, P., & Chen, Y. (2021). The fatty acid receptor CD36 promotes HCC progression through activating Src/PI3K/AKT axis-dependent aerobic glycolysis. *Cell Death & Disease*, 12(4), 328. <https://doi.org/10.1038/s41419-021-03596-w>
- Lutzky, J., Lutzky, J., Feun, L., & Harbour, W. (2020). 430 A phase II study of nivolumab + BMS-986016 (relatlimab) in patients with metastatic uveal melanoma(UM) (CA224–094). *Regular and Young Investigator Award Abstracts*, A261.2-A262. <https://doi.org/10.1136/jitc-2020-SITC2020.0430>
- Ma, X., Xiao, L., Liu, L., Ye, L., Su, P., Bi, E., Wang, Q., Yang, M., Qian, J., & Yi, Q. (2021). CD36-mediated ferroptosis dampens intratumoral CD8⁺ T cell effector function and impairs their antitumor ability. *Cell Metabolism*, 33(5), 1001-1012.e5. <https://doi.org/10.1016/j.cmet.2021.02.015>
- Mansor, L. S., Sousa Fialho, M. da L., Yea, G., Coumans, W. A., West, J. A., Kerr, M., Carr, C. A., Luiken, J. J. F. P., Glatz, J. F. C., Evans, R. D., Griffin, J. L., Tyler, D. J., Clarke, K., & Heather, L. C. (2017). Inhibition of sarcolemmal FAT/CD36 by sulfo-N-succinimidyl oleate rapidly corrects metabolism and restores function in the diabetic heart following

hypoxia/reoxygenation. *Cardiovascular Research*, 113(7), 737–748.

<https://doi.org/10.1093/cvr/cvx045>

Martini, C., DeNichilo, M., King, D. P., Cockshell, M. P., Ebert, B., Dale, B., Ebert, L. M., Woods, A., & Bonder, C. S. (2021). CD36 promotes vasculogenic mimicry in melanoma by mediating adhesion to the extracellular matrix. *BMC Cancer*, 21(1), 765.

<https://doi.org/10.1186/s12885-021-08482-4>

Marusyk, A., Janiszewska, M., & Polyak, K. (2020). Intratumor Heterogeneity: The Rosetta Stone of Therapy Resistance. *Cancer Cell*, 37(4), 471–484.

<https://doi.org/10.1016/j.ccell.2020.03.007>

McCloskey, P., Fridell, Y.-W., Attar, E., Villa, J., Jin, Y., Varnum, B., & Liu, E. T. (1997). GAS6 Mediates Adhesion of Cells Expressing the Receptor Tyrosine Kinase Axl. *Journal of Biological Chemistry*, 272(37), 23285–23291. <https://doi.org/10.1074/jbc.272.37.23285>

Middleton, M. R., McAlpine, C., Woodcock, V. K., Corrie, P., Infante, J. R., Steven, N. M., Evans, T. R. J., Anthoney, A., Shoushtari, A. N., Hamid, O., Gupta, A., Vardeu, A., Leach, E., Naidoo, R., Stanhope, S., Lewis, S., Hurst, J., O’Kelly, I., & Sznol, M. (2020).

Tebentafusp, A TCR/Anti-CD3 Bispecific Fusion Protein Targeting gp100, Potently Activated Antitumor Immune Responses in Patients with Metastatic Melanoma. *Clinical Cancer Research*, 26(22), 5869–5878. <https://doi.org/10.1158/1078-0432.CCR-20-1247>

Mishra, K. K., & Daftari, I. K. (2016). Proton therapy for the management of uveal melanoma and other ocular tumors. *Chinese Clinical Oncology*, 5(4), 50.

<https://doi.org/10.21037/cco.2016.07.06>

Modorati, G. M., Dagan, R., Mikkelsen, L. H., Andreasen, S., Ferlito, A., & Bandello, F. (2020). Gamma Knife Radiosurgery for Uveal Melanoma: A Retrospective Review of Clinical

- Complications in a Tertiary Referral Center. *Ocular Oncology and Pathology*, 6(2), 115–122. <https://doi.org/10.1159/000501971>
- Molckovsky, A., & Siu, L. L. (2008). First-in-class, first-in-human phase I results of targeted agents: Highlights of the 2008 American Society of Clinical Oncology meeting. *Journal of Hematology & Oncology*, 1(1), 20. <https://doi.org/10.1186/1756-8722-1-20>
- Murphy, G. F., Wilson, B. J., Girouard, S. D., Frank, N. Y., & Frank, M. H. (2014). Stem cells and targeted approaches to melanoma cure. *Molecular Aspects of Medicine*, 39, 33–49. <https://doi.org/10.1016/j.mam.2013.10.003>
- Musacchio, A., & Helin, K. (2013). Cell cycle, differentiation and disease. *Current Opinion in Cell Biology*, 25(6), 673–675. <https://doi.org/10.1016/j.ceb.2013.09.003>
- Nathan, P., Hassel, J. C., Rutkowski, P., Baurain, J.-F., Butler, M. O., Schlaak, M., Sullivan, R. J., Ochsenreither, S., Dummer, R., Kirkwood, J. M., Joshua, A. M., Sacco, J. J., Shoushtari, A. N., Orloff, M., Piulats, J. M., Milhem, M., Salama, A. K. S., Curti, B., Demidov, L., ... Piperno-Neumann, S. (2021). Overall Survival Benefit with Tebentafusp in Metastatic Uveal Melanoma. *New England Journal of Medicine*, 385(13), 1196–1206. <https://doi.org/10.1056/NEJMoa2103485>
- Neubauer, A., Fiebeler, A., Graham, D. K., O'Bryan, J. P., Schmidt, C. A., Barckow, P., Serke, S., Siegert, W., Snodgrass, H. R., & Huhn, D. (1994). Expression of axl, a transforming receptor tyrosine kinase, in normal and malignant hematopoiesis. *Blood*, 84(6), 1931–1941.
- Nguyen, K. H., Patel, B. C., & Tadi, P. (2020). Anatomy, Head and Neck, Eye Retina. In *StatPearls*.
- Nguyen, N., Coutts, K. L., Luo, Y., & Fujita, M. (2015). Understanding melanoma stem cells. *Melanoma Management*, 2(2), 179–188. <https://doi.org/10.2217/mmt.15.4>

- Okada, T. S. (1980). *chapter 11 Cellular Metaplasia or Transdifferentiation as a Model for Retinal Cell Differentiation* (pp. 349–380). [https://doi.org/10.1016/S0070-2153\(08\)60162-3](https://doi.org/10.1016/S0070-2153(08)60162-3)
- Özcan, G., Gündüz, A. K., Mirzayev, İ., Oysul, K., & Uysal, H. (2020). Early Results of Stereotactic Radiosurgery in Uveal Melanoma and Risk Factors for Radiation Retinopathy. *Turkish Journal of Ophthalmology*, *50*(3), 156–162. <https://doi.org/10.4274/tjo.galenos.2019.78370>
- Pan, J., Fan, Z., Wang, Z., Dai, Q., Xiang, Z., Yuan, F., Yan, M., Zhu, Z., Liu, B., & Li, C. (2019). CD36 mediates palmitate acid-induced metastasis of gastric cancer via AKT/GSK-3 β / β -catenin pathway. *Journal of Experimental & Clinical Cancer Research*, *38*(1), 52. <https://doi.org/10.1186/s13046-019-1049-7>
- Pandiani, C., Strub, T., Nottet, N., Cheli, Y., Gambi, G., Bille, K., Husser, C., Dalmaso, M., Béranger, G., Lassalle, S., Magnone, V., Pédeutour, F., Irondelle, M., Maschi, C., Nahon-Estève, S., Martel, A., Caujolle, J.-P., Hofman, P., LeBrigand, K., ... Bertolotto, C. (2021). Single-cell RNA sequencing reveals intratumoral heterogeneity in primary uveal melanomas and identifies HES6 as a driver of the metastatic disease. *Cell Death & Differentiation*, *28*(6), 1990–2000. <https://doi.org/10.1038/s41418-020-00730-7>
- Papakostas, T. D., Lane, A. M., Morrison, M., Gragoudas, E. S., & Kim, I. K. (2017). Long-term Outcomes After Proton Beam Irradiation in Patients With Large Choroidal Melanomas. *JAMA Ophthalmology*, *135*(11), 1191. <https://doi.org/10.1001/jamaophthalmol.2017.3805>
- Park, J. J., Stewart, A., Irvine, M., Pedersen, B., Ming, Z., Carlino, M. S., Diefenbach, R. J., & Rizos, H. (2022). Protein kinase inhibitor responses in uveal melanoma reflects a diminished dependency on PKC-MAPK signaling. *Cancer Gene Therapy*, *29*(10), 1384–1393. <https://doi.org/10.1038/s41417-022-00457-2>

- Pascual, G., Avgustinova, A., Mejetta, S., Martín, M., Castellanos, A., Attolini, C. S.-O., Berenguer, A., Prats, N., Toll, A., Hueto, J. A., Bescós, C., Di Croce, L., & Benitah, S. A. (2017). Targeting metastasis-initiating cells through the fatty acid receptor CD36. *Nature*, *541*(7635), 41–45. <https://doi.org/10.1038/nature20791>
- PDQ Adult Treatment Editorial Board. (2002). *Intraocular (Uveal) Melanoma Treatment (PDQ®): Health Professional Version*.
- Peddada, K., Sangani, R., Menon, H., & Verma, V. (2019). Complications and adverse events of plaque brachytherapy for ocular melanoma. *Journal of Contemporary Brachytherapy*, *11*(4), 392–397. <https://doi.org/10.5114/jcb.2019.87407>
- Pepino, M. Y., Kuda, O., Samovski, D., & Abumrad, N. A. (2014). Structure-Function of CD36 and Importance of Fatty Acid Signal Transduction in Fat Metabolism. *Annual Review of Nutrition*, *34*(1), 281–303. <https://doi.org/10.1146/annurev-nutr-071812-161220>
- Pradeep, T., Mehra, D., & Le, P. H. (2022). Histology, Eye. *StatPearls*.
- Rambow, F., Rogiers, A., Marin-Bejar, O., Aibar, S., Femel, J., Dewaele, M., Karras, P., Brown, D., Chang, Y. H., Debiec-Rychter, M., Adriaens, C., Radaelli, E., Wolter, P., Bechter, O., Dummer, R., Levesque, M., Piris, A., Frederick, D. T., Boland, G., ... Marine, J.-C. (2018). Toward Minimal Residual Disease-Directed Therapy in Melanoma. *Cell*, *174*(4), 843-855.e19. <https://doi.org/10.1016/j.cell.2018.06.025>
- Rankin, E., & Giaccia, A. (2016). The Receptor Tyrosine Kinase AXL in Cancer Progression. *Cancers*, *8*(11), 103. <https://doi.org/10.3390/cancers8110103>
- Redmer, T., Welte, Y., Behrens, D., Fichtner, I., Przybilla, D., Wruck, W., Yaspo, M.-L., Lehrach, H., Schäfer, R., & Regenbrecht, C. R. A. (2014). The Nerve Growth Factor Receptor CD271 Is Crucial to Maintain Tumorigenicity and Stem-Like Properties of

- Melanoma Cells. *PLoS ONE*, 9(5), e92596. <https://doi.org/10.1371/journal.pone.0092596>
- Reichstein, D. A., & Brock, A. L. (2021). Radiation therapy for uveal melanoma: a review of treatment methods available in 2021. *Current Opinion in Ophthalmology*, 32(3), 183–190. <https://doi.org/10.1097/ICU.0000000000000761>
- Richards, J. R., Yoo, J. H., Shin, D., & Odelberg, S. J. (2020). Mouse models of uveal melanoma: Strengths, weaknesses, and future directions. *Pigment Cell & Melanoma Research*, 33(2), 264–278. <https://doi.org/10.1111/pcmr.12853>
- Rietschel, P., Panageas, K. S., Hanlon, C., Patel, A., Abramson, D. H., & Chapman, P. B. (2005). Variates of survival in metastatic uveal melanoma. *Journal of Clinical Oncology : Official Journal of the American Society of Clinical Oncology*, 23(31), 8076–8080. <https://doi.org/10.1200/JCO.2005.02.6534>
- Ryeom, S. W., Sparrow, J. R., & Silverstein, R. L. (1996). CD36 participates in the phagocytosis of rod outer segments by retinal pigment epithelium. *Journal of Cell Science*, 109(2), 387–395. <https://doi.org/10.1242/jcs.109.2.387>
- Schmelter, V., Schneider, F., Guenther, S. R., Fuerweger, C., Muacevic, A., Priglinger, S. G., Liegl, R., & Foerster, P. (2022). Local Recurrence in Choroidal Melanomas following Robotic-Assisted Radiosurgery (CyberKnife). *Ocular Oncology and Pathology*, 8(4–6), 221–229. <https://doi.org/10.1159/000527915>
- Seiter, S., Monsurro, V., Nielsen, M.-B., Wang, E., Provenzano, M., Wunderlich, J. R., Rosenberg, S. A., & Marincola, F. M. (2002). Frequency of MART-1/MelanA and gp100/PMel17-specific T cells in tumor metastases and cultured tumor-infiltrating lymphocytes. *Journal of Immunotherapy (Hagerstown, Md. : 1997)*, 25(3), 252–263. <https://doi.org/10.1097/01.CJI.0000015209.05216.79>

- Shields, C. L., Kaliki, S., Cohen, M. N., Shields, P. W., Furuta, M., & Shields, J. A. (2015). Prognosis of uveal melanoma based on race in 8100 patients: The 2015 Doyne Lecture. *Eye (Basingstoke)*, 29(8). <https://doi.org/10.1038/eye.2015.51>
- Shields, Carol L., Shields, J. A., Cater, J., Gündüz, K., Miyamoto, C., Micaily, B., & Brady, L. W. (2000). Plaque Radiotherapy for Uveal Melanoma Long-term Visual Outcome in 1106 Consecutive Patients. *Archives of Ophthalmology*, 118(9), 1219. <https://doi.org/10.1001/archopht.118.9.1219>
- Shields, J. A., Augsburger, J. J., Donoso, L. A., Bernardino, V. B., & Portenar, M. (1985). Hepatic Metastasis and Orbital Recurrence of Uveal Melanoma After 42 Years. *American Journal of Ophthalmology*, 100(5), 666–668. [https://doi.org/10.1016/0002-9394\(85\)90621-X](https://doi.org/10.1016/0002-9394(85)90621-X)
- Shoushtari, A. N., & Carvajal, R. D. (2014). GNAQ and GNA11 mutations in uveal melanoma. *Melanoma Research*, 24(6), 525–534. <https://doi.org/10.1097/CMR.000000000000121>
- Sikuade, M. J., Salvi, S., Rundle, P. A., Errington, D. G., Kacperek, A., & Rennie, I. G. (2015). Outcomes of treatment with stereotactic radiosurgery or proton beam therapy for choroidal melanoma. *Eye*, 29(9), 1194–1198. <https://doi.org/10.1038/eye.2015.109>
- Silverstein, R. L., & Febbraio, M. (2009). CD36, a Scavenger Receptor Involved in Immunity, Metabolism, Angiogenesis, and Behavior. *Science Signaling*, 2(72). <https://doi.org/10.1126/scisignal.272re3>
- Singh, A. D., Turell, M. E., & Topham, A. K. (2011). Uveal melanoma: Trends in incidence, treatment, and survival. *Ophthalmology*, 118(9). <https://doi.org/10.1016/j.ophtha.2011.01.040>
- Sitiwin, E., Madigan, M. C., Gratton, E., Cherepanoff, S., Conway, R. M., Whan, R., &

- Macmillan, A. (2019). Shedding light on melanins within in situ human eye melanocytes using 2-photon microscopy profiling techniques. *Scientific Reports*, 9(1).
<https://doi.org/10.1038/s41598-019-54871-y>
- Souri, Z., Wierenga, A. P. A., Kroes, W. G. M., van der Velden, P. A., Verdijk, R. M., Eikmans, M., Luyten, G. P. M., & Jager, M. J. (2021). LAG3 and Its Ligands Show Increased Expression in High-Risk Uveal Melanoma. *Cancers*, 13(17), 4445.
<https://doi.org/10.3390/cancers13174445>
- Sridhar, M. S. (2018). Anatomy of cornea and ocular surface. In *Indian Journal of Ophthalmology* (Vol. 66, Issue 2). https://doi.org/10.4103/ijo.IJO_646_17
- Stålhammar, G. (2020). Forty-year prognosis after plaque brachytherapy of uveal melanoma. *Scientific Reports*, 10(1), 11297. <https://doi.org/10.1038/s41598-020-68232-7>
- Stålhammar, G., & Grossniklaus, H. E. (2021). Intratumor Heterogeneity in Uveal Melanoma BAP-1 Expression. *Cancers*, 13(5), 1143. <https://doi.org/10.3390/cancers13051143>
- Steeb, T., Wessely, A., Ruzicka, T., Heppt, M. V., & Berking, C. (2018). How to MEK the best of uveal melanoma: A systematic review on the efficacy and safety of MEK inhibitors in metastatic or unresectable uveal melanoma. *European Journal of Cancer*, 103, 41–51.
<https://doi.org/10.1016/j.ejca.2018.08.005>
- Su, Y., Wei, W., Robert, L., Xue, M., Tsoi, J., Garcia-Diaz, A., Homet Moreno, B., Kim, J., Ng, R. H., Lee, J. W., Koya, R. C., Comin-Anduix, B., Graeber, T. G., Ribas, A., & Heath, J. R. (2017). Single-cell analysis resolves the cell state transition and signaling dynamics associated with melanoma drug-induced resistance. *Proceedings of the National Academy of Sciences*, 114(52), 13679–13684. <https://doi.org/10.1073/pnas.1712064115>
- Susztak, K., Ciccone, E., McCue, P., Sharma, K., & Böttinger, E. P. (2005). Multiple Metabolic

- Hits Converge on CD36 as Novel Mediator of Tubular Epithelial Apoptosis in Diabetic Nephropathy. *PLoS Medicine*, 2(2), e45. <https://doi.org/10.1371/journal.pmed.0020045>
- Takahashi, M. (2001). The GDNF/RET signaling pathway and human diseases. *Cytokine & Growth Factor Reviews*, 12(4), 361–373. [https://doi.org/10.1016/S1359-6101\(01\)00012-0](https://doi.org/10.1016/S1359-6101(01)00012-0)
- Taniguchi, H., Yamada, T., Wang, R., Tanimura, K., Adachi, Y., Nishiyama, A., Tanimoto, A., Takeuchi, S., Araujo, L. H., Boroni, M., Yoshimura, A., Shiotsu, S., Matsumoto, I., Watanabe, S., Kikuchi, T., Miura, S., Tanaka, H., Kitazaki, T., Yamaguchi, H., ... Yano, S. (2019). AXL confers intrinsic resistance to osimertinib and advances the emergence of tolerant cells. *Nature Communications*, 10(1), 259. <https://doi.org/10.1038/s41467-018-08074-0>
- Tao, N., Wagner, S. J., & Lublin, D. M. (1996). CD36 Is Palmitoylated on Both N- and C-terminal Cytoplasmic Tails. *Journal of Biological Chemistry*, 271(37), 22315–22320. <https://doi.org/10.1074/jbc.271.37.22315>
- Tataru, C. P., & Pop, M. D. (2012). Enucleation in malignant choroidal melanoma - results in 15 years of using a new material in the prosthesis of the orbital cavity. *Journal of Medicine and Life*, 5(2), 185–188.
- Tawbi, H. A., Schadendorf, D., Lipson, E. J., Ascierto, P. A., Matamala, L., Castillo Gutiérrez, E., Rutkowski, P., Gogas, H. J., Lao, C. D., De Menezes, J. J., Dalle, S., Arance, A., Grob, J.-J., Srivastava, S., Abaskharoun, M., Hamilton, M., Keidel, S., Simonsen, K. L., Sobiesk, A. M., ... Long, G. V. (2022). Relatlimab and Nivolumab versus Nivolumab in Untreated Advanced Melanoma. *New England Journal of Medicine*, 386(1), 24–34. <https://doi.org/10.1056/NEJMoa2109970>
- Tirosh, I., Izar, B., Prakadan, S. M., Wadsworth, M. H., Treacy, D., Trombetta, J. J., Rotem, A.,

- Rodman, C., Lian, C., Murphy, G., Fallahi-Sichani, M., Dutton-Regester, K., Lin, J.-R., Cohen, O., Shah, P., Lu, D., Genshaft, A. S., Hughes, T. K., Ziegler, C. G. K., ... Garraway, L. A. (2016). Dissecting the multicellular ecosystem of metastatic melanoma by single-cell RNA-seq. *Science*, *352*(6282), 189–196. <https://doi.org/10.1126/science.aad0501>
- Tsang, J. Y. S., Wong, K. H. Y., Lai, M. W. H., Lacambra, M. D., Ko, C.-W., Chan, S. K., Lam, C. C. F., Yu, A. M. C., Tan, P.-H., & Tse, G. M. (2013). Nerve growth factor receptor (NGFR): a potential marker for specific molecular subtypes of breast cancer. *Journal of Clinical Pathology*, *66*(4), 291–296. <https://doi.org/10.1136/jclinpath-2012-201027>
- Valyi-Nagy, K., Kormos, B., Ali, M., Shukla, D., & Valyi-Nagy, T. (2012). Stem cell marker CD271 is expressed by vasculogenic mimicry-forming uveal melanoma cells in three-dimensional cultures. *Molecular Vision*, *18*, 588–592.
- van Gils, W., Lodder, E. M., Mensink, H. W., Kilic, E., Naus, N. C., Bru"ggewirth, H. T., van IJcken, W., Paridaens, D., Luyten, G. P., & de Klein, A. (2008). Gene Expression Profiling in Uveal Melanoma: Two Regions on 3p Related to Prognosis. *Investigative Ophthalmology & Visual Science*, *49*(10), 4254. <https://doi.org/10.1167/iovs.08-2033>
- van Ginkel, P. R., Gee, R. L., Shearer, R. L., Subramanian, L., Walker, T. M., Albert, D. M., Meisner, L. F., Varnum, B. C., & Polans, A. S. (2004). Expression of the Receptor Tyrosine Kinase Axl Promotes Ocular Melanoma Cell Survival. *Cancer Research*, *64*(1), 128–134. <https://doi.org/10.1158/0008-5472.CAN-03-0245>
- Wang, J., & Li, Y. (2019). CD36 tango in cancer: signaling pathways and functions. *Theranostics*, *9*(17), 4893–4908. <https://doi.org/10.7150/thno.36037>
- Wechman, S. L., Emdad, L., Sarkar, D., Das, S. K., & Fisher, P. B. (2020). *Vascular mimicry: Triggers, molecular interactions and in vivo models* (pp. 27–67).

<https://doi.org/10.1016/bs.acr.2020.06.001>

Weidmann, C., Pomerleau, J., Trudel-Vandal, L., & Landreville, S. (2017). Differential responses of choroidal melanocytes and uveal melanoma cells to low oxygen conditions. *Molecular Vision*, 23.

Wessely, A., Steeb, T., Erdmann, M., Heinzerling, L., Vera, J., Schlaak, M., Berking, C., & Heppt, M. V. (2020). The Role of Immune Checkpoint Blockade in Uveal Melanoma. *International Journal of Molecular Sciences*, 21(3), 879.

<https://doi.org/10.3390/ijms21030879>

Woodman, S. E. (2012). Metastatic uveal melanoma: Biology and emerging treatments. In *Cancer Journal* (Vol. 18, Issue 2). <https://doi.org/10.1097/PPO.0b013e31824bd256>

Worley, L. A., Onken, M. D., Person, E., Robirds, D., Branson, J., Char, D. H., Perry, A., & Harbour, J. W. (2007). Transcriptomic versus Chromosomal Prognostic Markers and Clinical Outcome in Uveal Melanoma. *Clinical Cancer Research*, 13(5), 1466–1471. <https://doi.org/10.1158/1078-0432.CCR-06-2401>

Wu, Y., Liu, Y., Li, X., Kebebe, D., Zhang, B., Ren, J., Lu, J., Li, J., Du, S., & Liu, Z. (2019). Research progress of in-situ gelling ophthalmic drug delivery system. *Asian Journal of Pharmaceutical Sciences*, 14(1), 1–15. <https://doi.org/10.1016/j.ajps.2018.04.008>

Yamada, T., Roesel, M. E., & Beauchamp, J. J. (1975). Cell cycle parameters in dedifferentiating iris epithelial cells. *Development*, 34(2), 497–510. <https://doi.org/10.1242/dev.34.2.497>

Yang, H., Cao, J., & Grossniklaus, H. E. (2015). Uveal Melanoma Metastasis Models. *Ocular Oncology and Pathology*, 1(3), 151–160. <https://doi.org/10.1159/000370153>

Yang, J., Manson, D. K., Marr, B. P., & Carvajal, R. D. (2018). Treatment of uveal melanoma: where are we now? *Therapeutic Advances in Medical Oncology*, 10, 175883401875717.

<https://doi.org/10.1177/1758834018757175>

- Yang, P., Qin, H., Li, Y., Xiao, A., Zheng, E., Zeng, H., Su, C., Luo, X., Lu, Q., Liao, M., Zhao, L., Wei, L., Varghese, Z., Moorhead, J. F., Chen, Y., & Ruan, X. Z. (2022). CD36-mediated metabolic crosstalk between tumor cells and macrophages affects liver metastasis. *Nature Communications*, *13*(1), 5782. <https://doi.org/10.1038/s41467-022-33349-y>
- Yang, P., Su, C., Luo, X., Zeng, H., Zhao, L., Wei, L., Zhang, X., Varghese, Z., Moorhead, J. F., Chen, Y., & Ruan, X. Z. (2018). Dietary oleic acid-induced CD36 promotes cervical cancer cell growth and metastasis via up-regulation Src/ERK pathway. *Cancer Letters*, *438*, 76–85. <https://doi.org/10.1016/j.canlet.2018.09.006>
- Yang, R., Liu, Q., & Zhang, M. (2022). The Past and Present Lives of the Intraocular Transmembrane Protein CD36. *Cells*, *12*(1), 171. <https://doi.org/10.3390/cells12010171>
- YANG, W.-H., CHENG, C.-Y., CHEN, M.-F., & WANG, T.-C. (2018). Cell Subpopulations Overexpressing p75NTR Have Tumor-initiating Properties in the C6 Glioma Cell Line. *Anticancer Research*, *38*(9), 5183–5192. <https://doi.org/10.21873/anticancer.12841>
- Zemba, M., Dumitrescu, O.-M., Gheorghe, A. G., Radu, M., Ionescu, M. A., Vatafu, A., & Dinu, V. (2023). Ocular Complications of Radiotherapy in Uveal Melanoma. *Cancers*, *15*(2), 333. <https://doi.org/10.3390/cancers15020333>
- Zhao, L., Varghese, Z., Moorhead, J. F., Chen, Y., & Ruan, X. Z. (2018). CD36 and lipid metabolism in the evolution of atherosclerosis. *British Medical Bulletin*, *126*(1), 101–112. <https://doi.org/10.1093/bmb/ldy006>
- Zhou, X., Hao, Q., Liao, P., Luo, S., Zhang, M., Hu, G., Liu, H., Zhang, Y., Cao, B., Baddoo, M., Flemington, E. K., Zeng, S. X., & Lu, H. (2016). Nerve growth factor receptor negates the tumor suppressor p53 as a feedback regulator. *ELife*, *5*.

<https://doi.org/10.7554/eLife.15099>

Zhu, C., Wei, Y., & Wei, X. (2019). AXL receptor tyrosine kinase as a promising anti-cancer approach: functions, molecular mechanisms and clinical applications. *Molecular Cancer*, 18(1), 153. <https://doi.org/10.1186/s12943-019-1090-3>

FIGURES

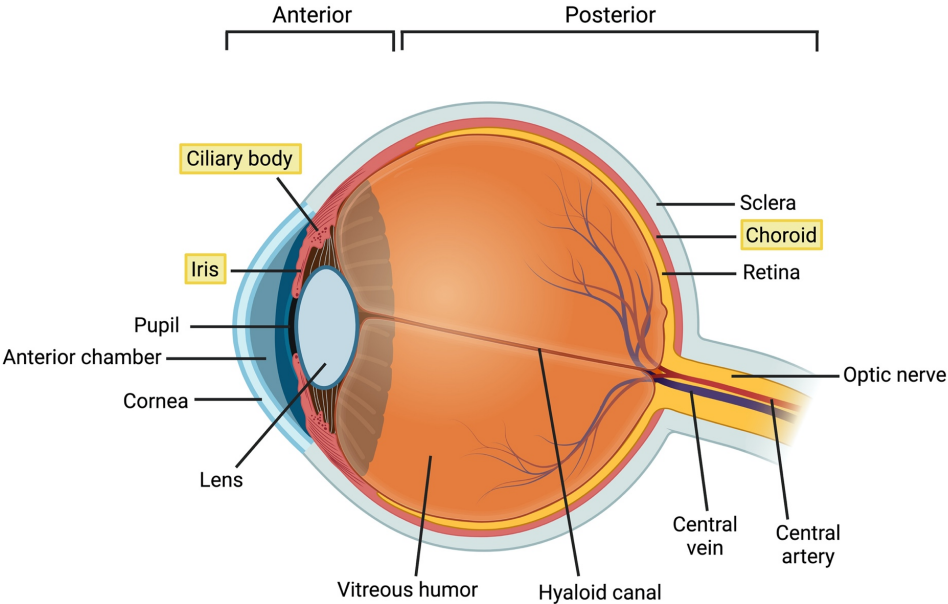


Figure 1 Diagram of the Eye. A simple diagram of the Eye (globe) indicating the anterior and the posterior regions of the organ with ciliary body, iris, and choroid highlighted as these are main areas where uveal melanoma occurs. Generated with Biorender.com. Adapted from (Wu et al., 2019).

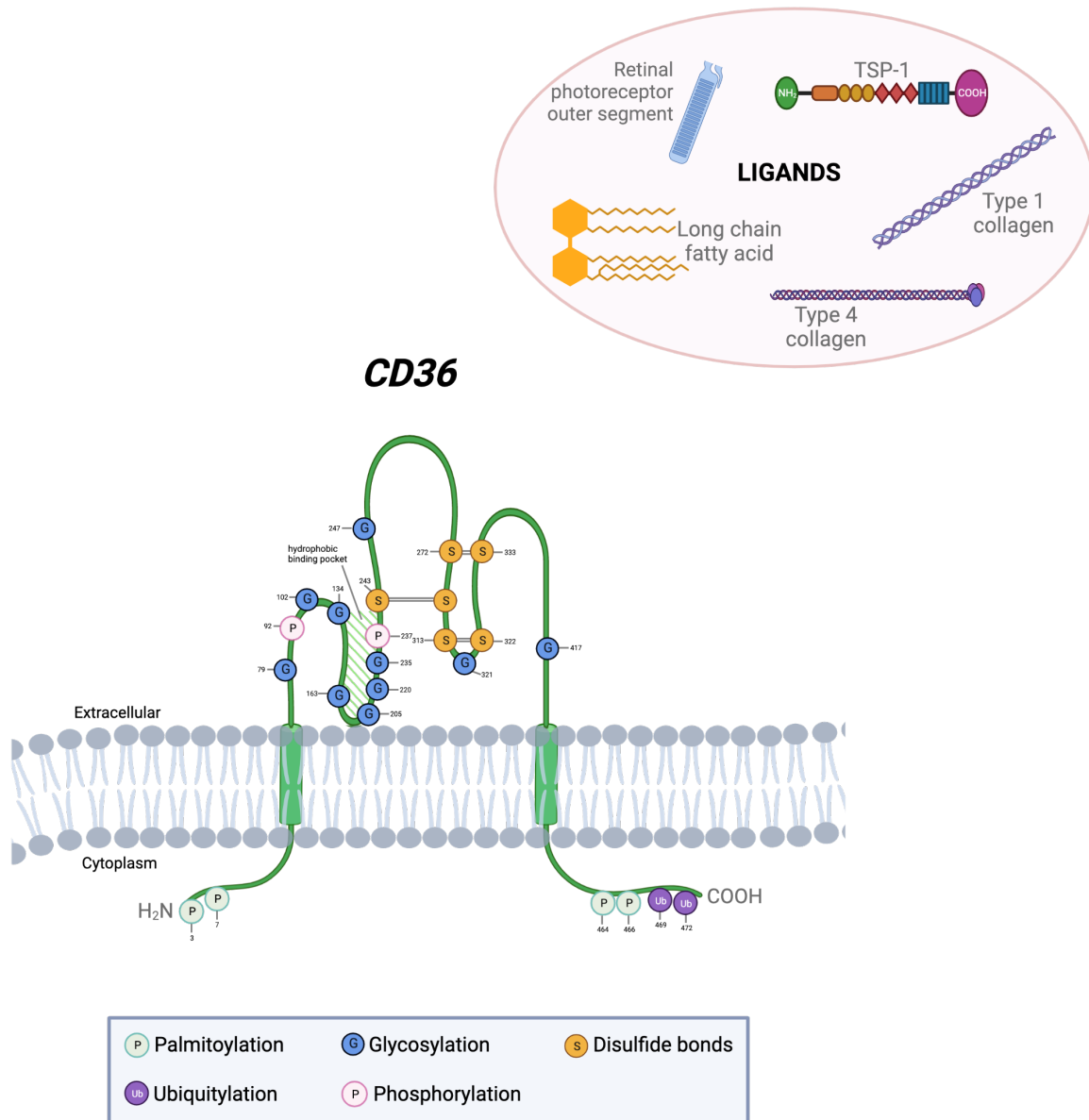


Figure 2 CD36 domains, post-modification sites, and its ligands. Diagram of CD36 transmembrane receptor with intracellular domains and a long extracellular domain with many sites for post-translational modifications. Some of its ligands include thrombospondin-1 (TSP-1), retinal photoreceptor outer segment, long chain fatty acids, Type 1 and Type 4 collagens. Generated with Biorender.com. Adapted from (Karunakaran et al., 2021).

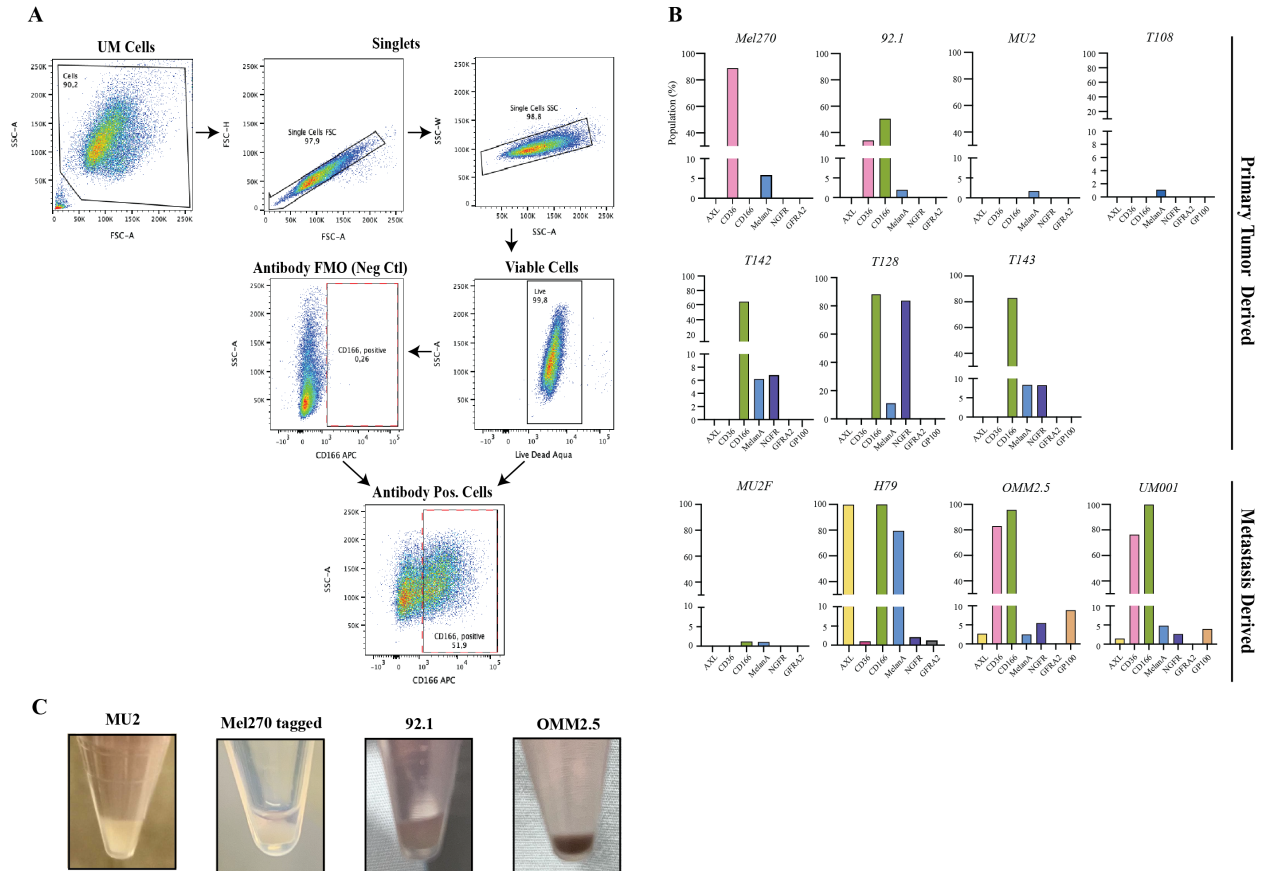


Figure 3 Characterization of Uveal Melanoma Cell Lines with UMarkit. A Gating strategy explaining how uveal melanoma cells were gated following acquisition by flow cytometry. Singlets were selected for followed by isolation of viable cells. Each antibody used in the flow panel had a negative control annotated as “FMO sample” to be able to create a gate for identifying cells with the specific marker of interest. Shown is CD166 as one example of an antibody in the flow panel. **B** Summary of uveal melanoma cell lines derived from a primary tumor or the liver metastasis. The bar graphs show the percentage of the total cells staining positive for each specific protein. **C**) Comparative images of cell pellets for MU2, Mel270 luc-tdTomato (tagged), 92.1, and OMM2.5 cell lines for their pigmentation status.

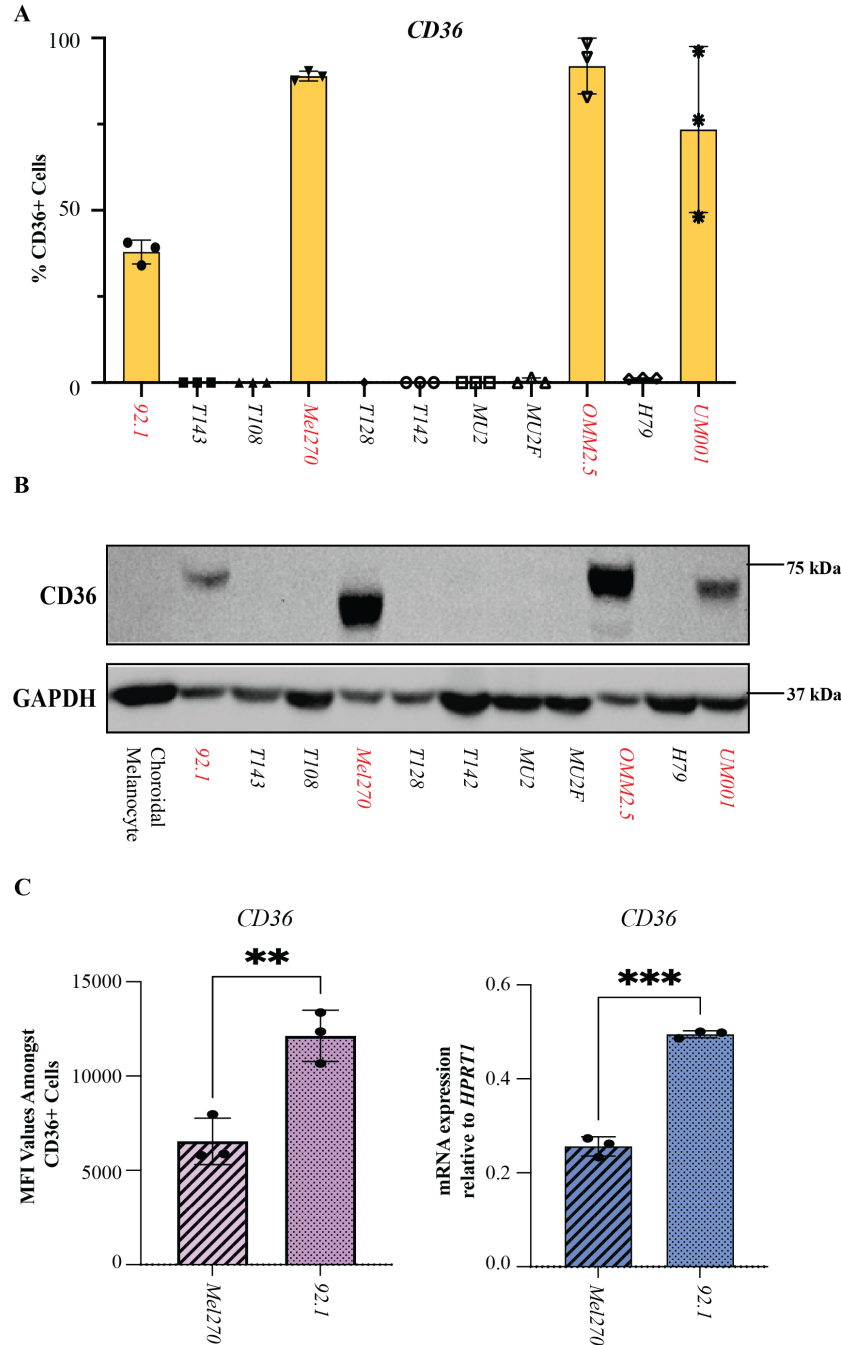


Figure 4 Comparative CD36 Expression in Uveal Melanoma Cell Lines. **A** Each dot represents one sample (n=3). Bars end at the mean of each cohort; error bars, SD. Bar graph representing the percentage of CD36 positive cells in eleven different uveal melanoma cell lines. **B** Western blot analysis of choroidal melanocyte and uveal melanoma cell lysates to detect CD36 protein levels. GAPDH is used as a loading control. **C** Each dot represents one sample (Mel270 n=3, 92.1 n=3) (ns $P \geq 0.05$, * $P \leq 0.05$, ** $P \leq 0.01$, *** $P \leq 0.001$; Welch's t-test) **Left:** MFI values from flow cytometry analyses comparing average CD36 signals emitted from the CD36+ population. **Right:** Relative *Cd36* mRNA levels for Mel270 cells and 92.1 cells analyzed with qPCR.

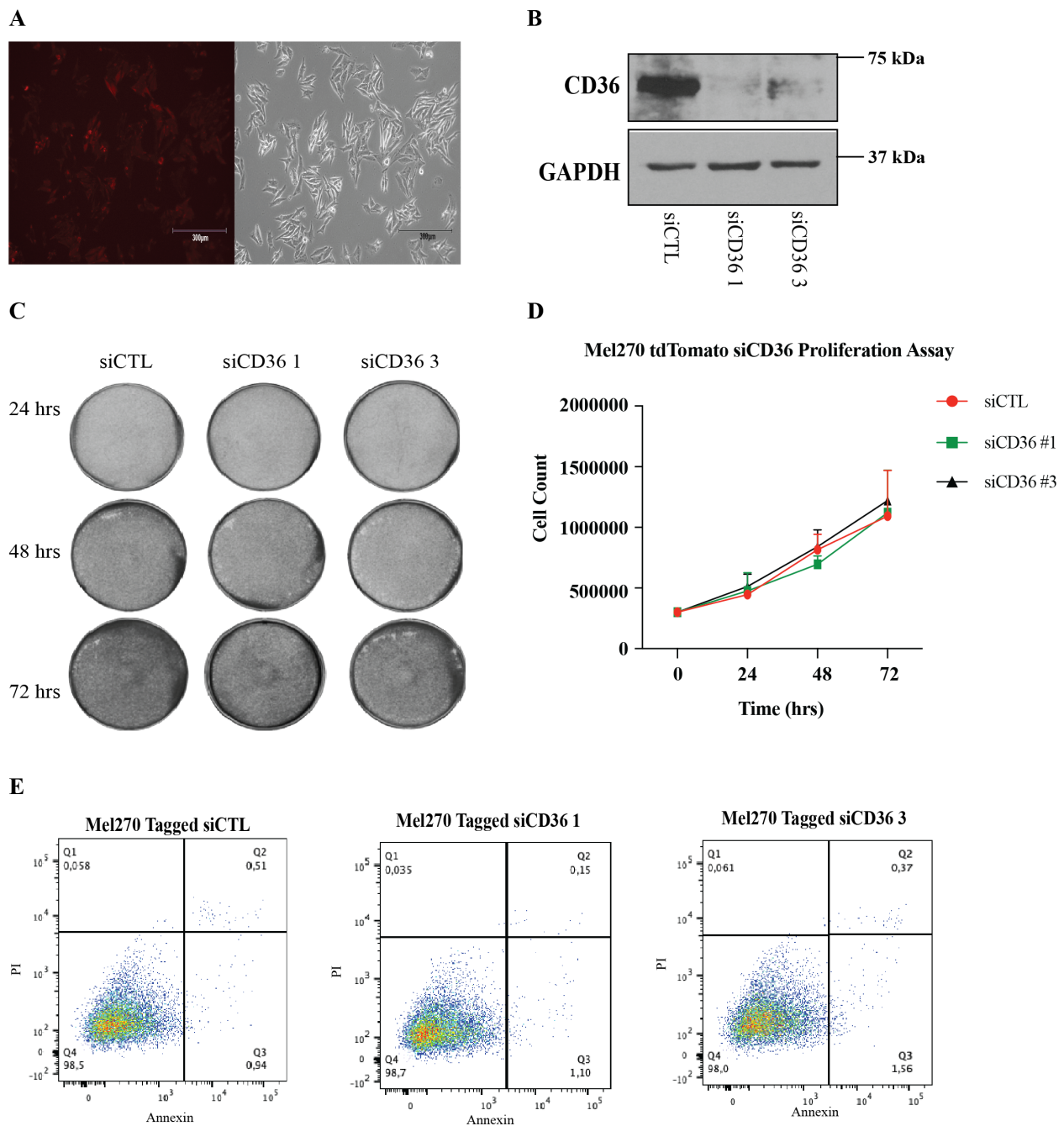


Figure 5 siRNA mediated *Cd36* Knockdown. **A** Confirmation of tagging of Mel270 cells. **Right:** Brightfield image of Mel270 luc-tdTomato (tagged) cells under 10X magnification under the inverted microscope. **Left:** GFP image of Mel270 luc-tdTomato (tagged) cells under 10X magnification. **B** Western blot analysis to confirm *CD36* knockdown after transfecting cells with siRNA: scrambled control (siCTL), siCD36 1, and siCD36 3. **C** Proliferation assay in 6 well plates between 3 different conditions (siCTL, siCD36 1, siCD36 3) across 3 different time points (24 hours, 48 hours, 72 hours). **D** Line graph of cell counts on a proliferation assay with 3 different conditions (siCTL, siCD36 1, siCD36 3) on 3 different time points (24 hours, 48 hours,

72 hours). Each dot represents n=3 where no * represent ns analyzed through one-way ANOVA (ns $P \geq 0.05$). **E** Apoptosis assay with Annexin V and PI staining 48 hours after transfecting cells with siCTL, siCD36 1 or siCD36 3. Low cell percentage in quadrants 1,2, and 3 represent low percentage of cells that have undergone both early and late apoptotic events.

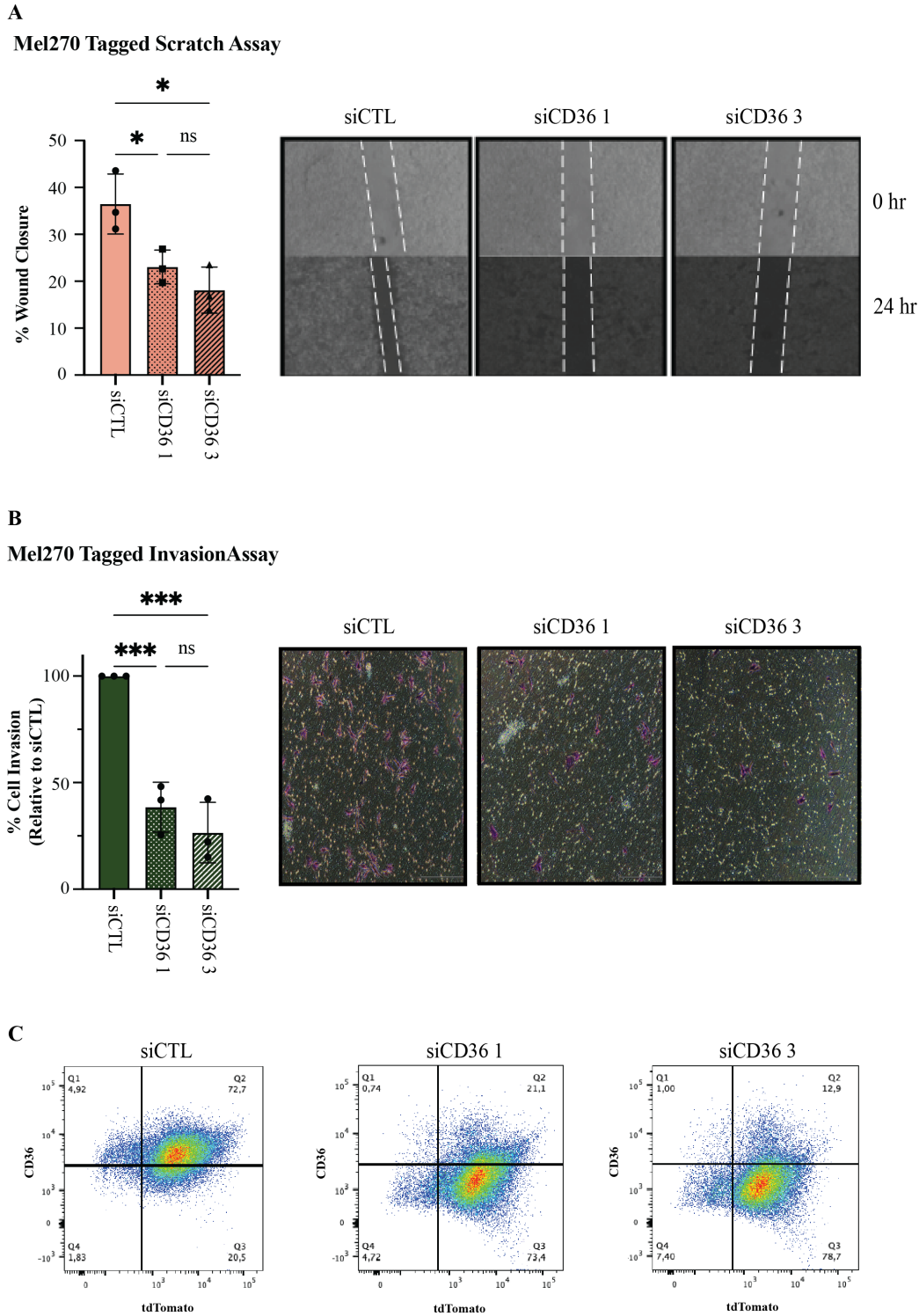
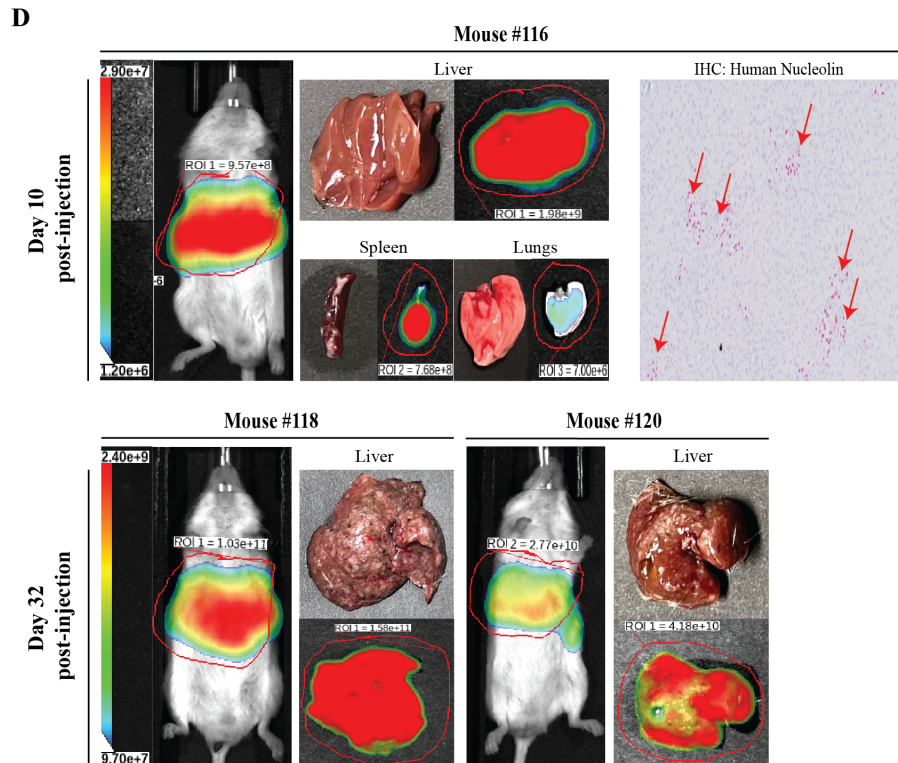
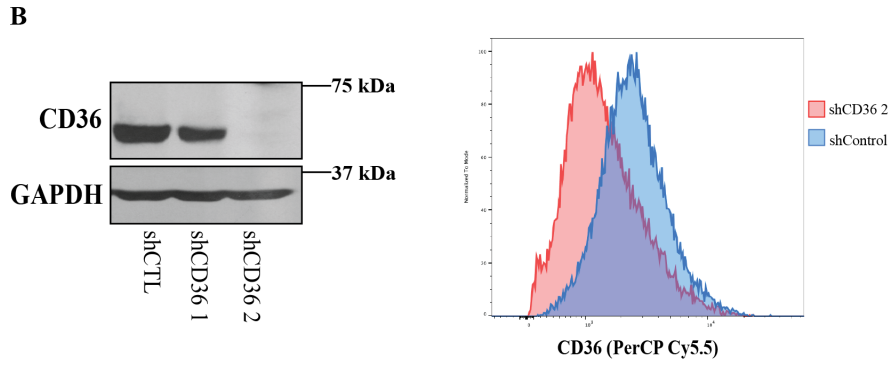
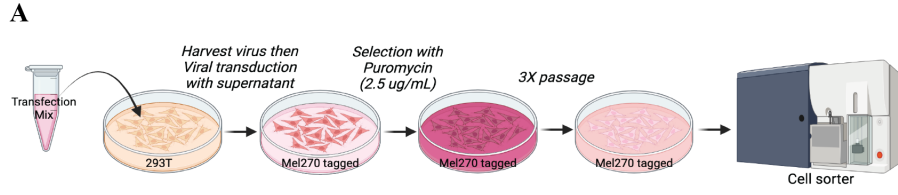


Figure 6 Depletion of *Cd36* leads to reduced migratory and invasive capacity in UM cell line. A Left: Bar graph for wound healing (scratch) assay with Mel270 luc-tdTomato (tagged) cells depicting respective percent wound closure for each condition. **Right:** Representative images for wound closure at 0-hour post-scratch and 24 hours post-scratch for siCTL, siCD36 1, and siCD36 3 transfected samples. **B Left:** Bar graph for invasion assay with Mel270 luc-

tdTomato (tagged) cells relative to the control condition. **Right:** Representative images showing crystal-violet stained cells (purple) that have invaded through Matrigel-coated transwell in each condition. **C** Flow cytometry confirmation of *Cd36* knockdown whilst retaining signal for tdTomato in Mel270 luc-tdTomato (tagged) cells used for all scratch assays and invasion assays. Reduced cell percentage in quadrant 2 in siCD36 1 and siCD36 3 sample shows depletion in *Cd36* whilst maintaining tdTomato signal on the x-axis. Top of bar graph represents average of group; error bars, SD. Each dot represents 1 assay completed with 3 technical replicates (siCTL, siCD36 1, siCD36 3, n=3) (ns $P \geq 0.05$, * $P \leq 0.05$, ** $P \leq 0.01$, *** $P \leq 0.001$; One-way ANOVA).



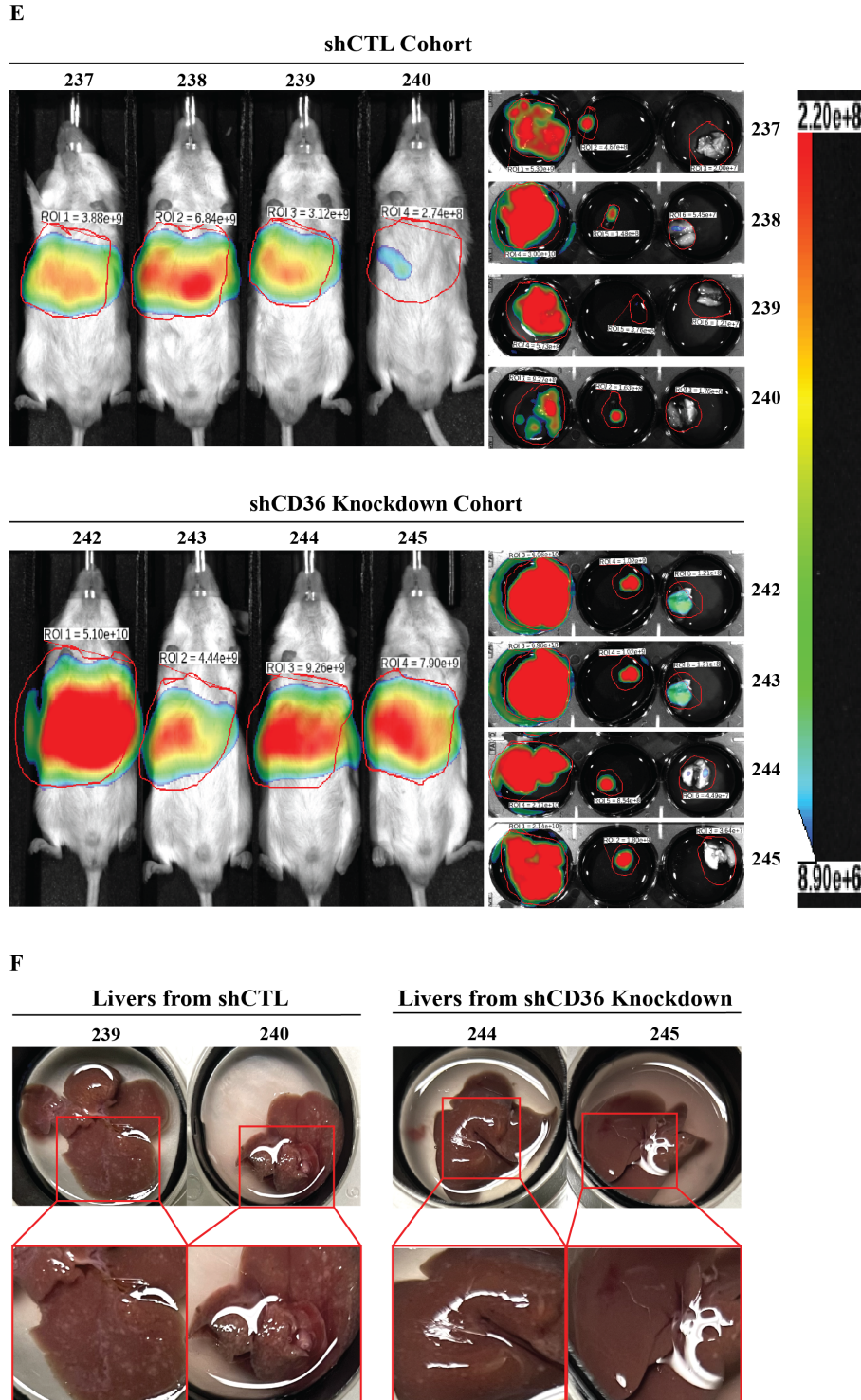
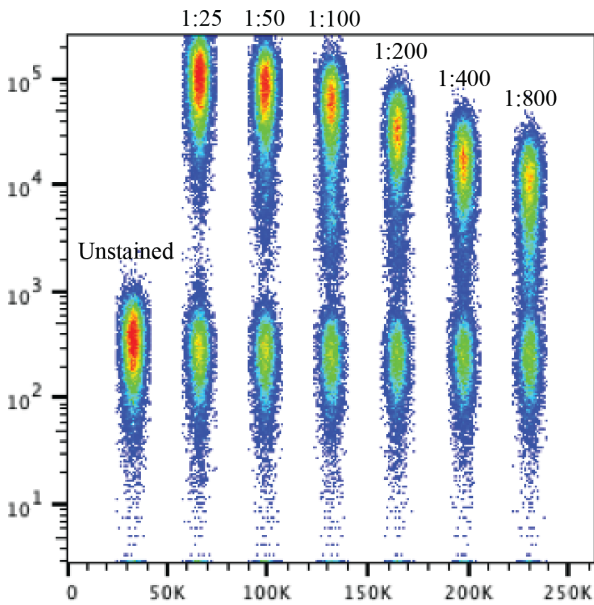


Figure 7 *In vivo* liver metastasis experiments with Mel270 cells expressing shCTL or shCD36. **A** Schematic diagram for the generation of shRNA mediated *Cd36* knockdown Mel270 tagged cells. Generated with Biorender.com. **B Left:** Western blot analysis confirming the efficiency of *Cd36* knockdown in the Mel270 tagged cell line. Results confirm there is efficient knockdown only with the shCD36 2 vector compared to the shCTL. **Right:** histogram from a flow cytometry analysis to confirm *Cd36* knockdown from shCD36 2 vector (red) compared to

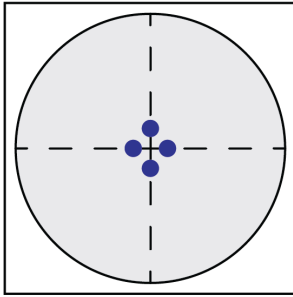
the shCTL (blue). **C** Schematic diagram describing the timeline of the *in vivo* experiments from splenic injection to euthanize the animal to IHC staining to detect human nucleolin and *CD36*. Within the 24 days from injection of tumor cells to euthanization, IVIS images were taken weekly to track tumor cell burden and to confirm injections have achieved successful liver colonization. **D** Mice injected with 1.0×10^6 Mel270 luc-tdTomato cells. **Top:** Signal emitted (9.57×10^8 photons/s) from mouse #116 from the pilot cohort at Day 10 post injection. Surface lesions on the liver were not detectable, nor on the spleen or lungs. However, ex vivo imaging confirmed presence of tumor cells on all three organs. IHC staining for human nucleolin on paraffin embedded liver sample confirmed micro-metastases at Day 10 post injection. **Bottom:** Signal emitted from mouse #118 (1.03×10^{11} photons/s) and #120 (2.77×10^{10} photons/s) from the pilot cohort at day 32 post-injection. Surface lesions on both livers are detectable but appear to be too overcrowded to allow for any comparisons of tumor number to be made between livers. **E** Summary of the study cohort on day 32 post-injection comparing the effect of shCD36 depletion on liver metastasis burden by injecting mice with 1.0×10^6 of either Mel270 luc-tdTomato shCTL cells or Mel270 td-Tomato shCD36 knockdown cells. IVIS images of the mice and organs (from left: liver, spleen lungs) for shCTL and shCD36 knockdown cohort show higher signal emitted by the shCD36 knockdown group than the shCTL cohort. **F** Comparative images of the livers from mice #239 and #240 from the shCTL cohort and the livers from mice #244 and #245 from the shCD36 knockdown cohort. Despite the shCD36 knockdown cohort having slightly higher signal emitted (#244: 9.26×10^9 photons/s; #245: 7.90×10^9 photons/s) than the shCTL cohort (#239: 3.12×10^9 photons/s; #240: 2.74×10^8 photons/s), there appeared to reduced surface liver lesions when visualized by the naked eye.

Antibody Titration Concatenated Graph

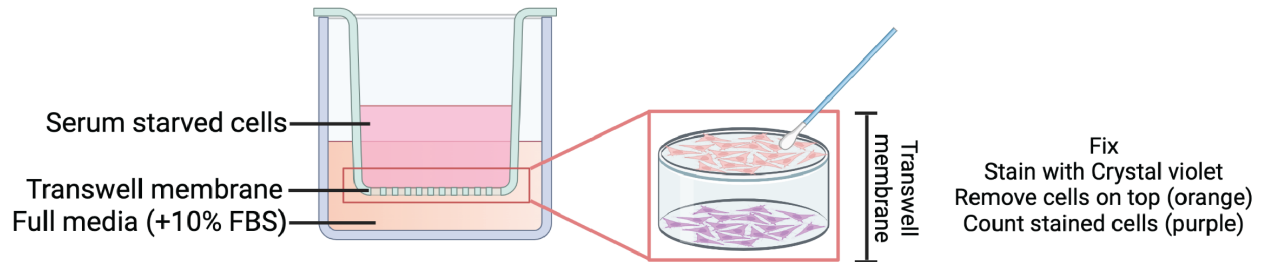


Supplementary Figure 1 Antibody Titration Visual Representation Graph. Example of a concatenated graph for antibody titration with all the dilutions of the antibody. This graph was produced for each antibody in the UMarkit panel to determine the ideal dilution to identify positive populations.

A



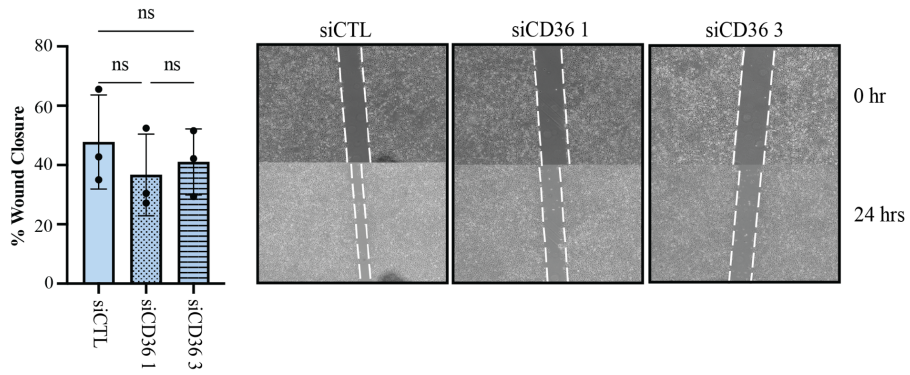
B



Supplementary Figure 2 Explanatory diagrams for Scratch assay and Invasion assay. A Diagram of a single well in a 6-well plate where dotted lines indicate where the scratch was made using a p10 pipette tip for wound healing (scratch) assays. Images were taken at the blue dots. **B** Illustration of an invasion assay using transwell and the location of the non-invaded (orange cells) cells and the invaded cells (purple cells). Using a cotton tip, non-invaded (orange cells) were swabbed off after fixing with 4% glutaraldehyde solution and staining with crystal violet solution.

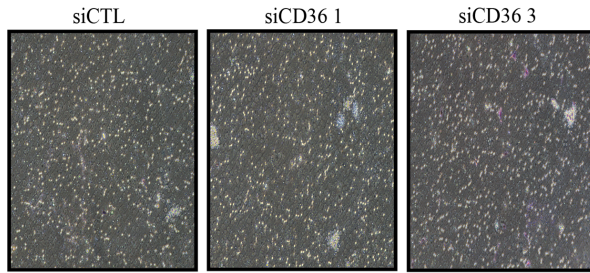
A

92.1 Scratch Assay

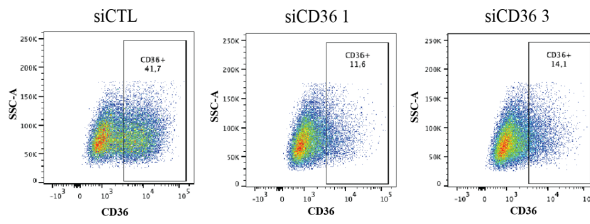


B

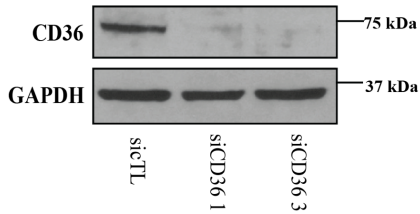
92.1 Invasion Assay



C

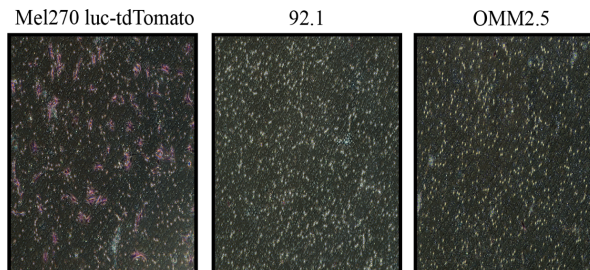


D



E

UM Cell Lines Invasion Assays



Supplementary Figure 3 Wound Healing (Scratch) Assay and Invasion Assay with 92.1 UM Cell Line. **A Left:** Bar graph representing the % wound closed with 92.1 cells in each condition (siCTL, siCD36 1, siCD36 3). Each dot represents 1 assay completed with 3 technical replicates (siCTL, siCD36 1, siCD36 3, n=3) (ns $P \geq 0.05$; One-way ANOVA) and end of bar represents average of the cohort; error bar, SD. Results do not show any significant difference between control condition and *Cd36* depletion condition. **Right:** Representative images of the scratch assay at 0 hr and 24 hours post-scratch. **B** Representative images of the results at 24 hours after seeding of the invasion assay with 92.1 cells under three conditions (siCTL, siCD36 1, siCD36 3). Invaded cells were very minimal, and no trends were discovered. **C** Flow cytometry confirmation of *Cd36* knockdown in 92.1 cells used for the scratch assays and invasion assays. Reduced cell percentage in the gate for siCD36 1 and siCD36 3 transfected samples indicate depletion of *Cd36* compared to the siCTL transfected samples. **D** Western blot analysis to confirm *Cd36* knockdown after transfecting cells with siRNA: scrambled control (siCTL), siCD36 1, and siCD36 3 in 92.1 cell line. **E** Representative images of invasion assay results for uveal melanoma cell lines Mel270 luc-tdTomato, 92.1, and OMM2.5. Cells have not been transfected with any siRNAs.